

Title of thesis:

A Novel SNR Estimation Technique for OFDM Systems

I, SHAHID MANZOOR

hereby allow my thesis to be placed at the Information Resource Center (IRC) of Universiti Teknologi PETRONAS (UTP) with the following conditions:

1. The thesis becomes the property of UTP.
2. The IRC of UTP may make copies of the thesis for academic purposes only.
3. This thesis is classified as

Confidential

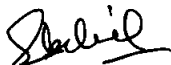
Non-confidential

If this thesis is confidential, please state the reason:

The contents of the thesis will remain confidential for _____ years.

Remarks on disclosure:

Endorsed by



Signature of Author



Signature of Supervisor

Permanent Address: House # CB-51/01 P.O.Box 26 Area
P.O.F Wah Cantt .Tehsil Taxila,
47030, Pakistan

Name of Supervisor
Assoc. Prof. Dr. Varun Jeoti

Date: 04/09/2008

Date: 5th Spt '08

UNIVERSITI TEKNOLOGI PETRONAS

A Novel SNR Estimation Technique for OFDM Systems

By

Shahid Manzoor

A THESIS

SUBMITTED TO THE POSTGRADUATE STUDIES PROGRAMME
AS A REQUIREMENT FOR THE
DEGREE OF MASTERS OF SCIENCE IN ELECTRICAL AND ELECTRONIC
ENGINEERING

Electrical and Electronic Engineering

BANDAR SERI ISKANDAR,
PERAK

July, 2008

DECLARATION

I hereby declare that the thesis is based on my original work except for quotations and citations which have been duly acknowledged. I also declare that it has not been previously or concurrently submitted for any other degree at UTP or other institutions.

Signature: 

Name : Shahid Manzoor

Date : 04/09/2008

ACKNOWLEDGEMENT

All praises be to Allah, the most gracious and most merciful, who provided me the courage and strength that enabled me to complete this work. I pray to Him to include me among those who are rewarded for just seeking knowledge.

I would like to express my gratitude and thanks to all people who encouraged and helped me throughout this research work.

First of all, I would like to acknowledge the immense contributions, guidance and encouragement from my supervisor Assoc. Prof. Dr. Varun Jeoti. He has been a mentor and also friend to me. Throughout the whole duration of this work, I have learnt much from him, not only in terms of technical knowledge but also the finer points of being a better researcher. Without his guidance, this work would not have yielded such positive results and published at international levels. Indeed his dedication is such that it surpasses boundaries of office hours as evident by the hours of personal time that he has spent with me in discussions of the research work.

I would also like to thank Dr. Nidal Kamel (Seniour Lecturer, Universiti Teknologi PETRONAS, Malaysia) for his helpful discussions, reviews and comments on our proposed schemes. He is an expert in the field of SNR estimation but yet he displayed such willingness to help a beginner like me and answered my questions throughout my research work.

The help of Micheal Drieberg is also gratefully acknowledged. He enabled me to understand the OFDM systems better. He was very helpful in answering many of the questions that I had concerning some aspects of the research work.

I am grateful to the fellow postgraduate students and undergraduate students in UTP that have been through the thick and thin with me throughout the duration of my pursuit for

this Master degree. They have been constant sources of encouragement and companionship in times when the going was getting very tough. Their friendships are likened to rare gems.

I would like to pay the most sincere thanks to my parents, whose teaching, encouragement and education, enabled me to pursue achievement in research. My sincere thanks to my elder brothers Mr. Rana Sajid Manzoor and Mr. Rana Majid Manzoor, from whom I got instructions on each and every step of my life, whenever I got struck. Without their care and faith, I would never be able to stand where I am today. I would also like to thank my sisters, my special lady and my friends (Nauroze, Asif, Imran, Shahzad, Sakandar, Mansoor and Mr. and Mrs. Ayyaz Muhammad) for their continuous support, encouragement and prayers during my pursuit of this master degree.

DEDICATION

To my beloved parents

ABSTRACT

Orthogonal Frequency Division Multiplexing (OFDM) systems have received a lot of attention because of their robust performance in frequency dispersive channels. Further performance improvement is achieved by employing more sophisticated receiver techniques that often require the knowledge of signal-to-noise ratio (SNR) - broadly defined as the ratio of the desired signal power to the unwanted noise power. For example, noise variance and, hence, signal to noise ratio (SNR) estimates of the received signal are very important for the channel quality control in communication systems. Similarly, in advanced communication systems, SNR estimation is used for adaptive algorithms for modulation, power control and coding.

The objective of the work undertaken in this thesis is to design a front-end noise power estimator and, thence, SNR estimator. The proposed SNR estimator utilizes the OFDM preamble signal – the preamble used for synchronization. The estimation is achieved by auto correlating the preamble and it is deployed right at the front-end of the receiver. Noise power and, hence, signal power is estimated from the correlation results. The technique is also extended to obtaining noise power estimates of colored noise using wavelet-packet based filter bank analysis of the noise.

In order to benchmark the proposed noise power and SNR estimation technique, a complete end-to-end fixed-broadband-wireless-access-system (IEEE 802.16d) simulation has been developed and the results are compared with other works reported in the literature. The simulations are conducted in both frequency non-dispersive and dispersive channels with real additive white Gaussian noise (AWGN) and also colored noise. It is observed that the proposed estimator gives better SNR estimates. The proposed estimator is also checked with WiMAX systems (IEEE802.16d, 2004) using SUI multipath channels and with Wi-Fi systems (IEEE802.11a) with indoor channel models. The estimator performs SNR estimation at front-end of the receiver unlike all other estimators which perform SNR estimation at back-end of the receiver. Furthermore, the proposed estimator has relatively low computational complexity; for it makes use of only one

OFDM preamble signal to find the SNR estimates. The criteria of good SNR estimator are accuracy of estimates, low complexity and easy to implement. The results show that the proposed estimator fulfills these criteria successfully.

TABLE OF CONTENT

Status of Thesis.....	i
Approval Page	ii
Title Page	iii
Declaration.....	iv
Acknowledgement.....	v
Dedication.....	vii
Abstract.....	viii
Table of Contents	x
List of Tables	xv
List of Figures.....	xvi
List of Abbreviations	xix
CHAPTER 1: INTRODUCTION.....	1
1.1 Motivation.....	1
1.2 Types of SNR Estimators.....	3
1.3 SNR Estimation Problem Statement.....	4
1.4 Objectives of Research.....	5
1.5 Contribution Of This Thesis.....	6
1.6 Organization of Thesis.....	6
CHAPTER 2: BACKGROUND.....	8
2.1 Introduction.....	8
2.2 Wireless Channel.....	8
2.3 OFDM.....	12
2.3.1 OFDM Principles.....	16
2.4 Literature Review.....	19
2.4.1 Overview of SNR Estimation.....	19

2.5 SNR Estimation in OFDM Systems.....	23
2.6 Previous SNR Estimation Algorithms for OFDM Systems.....	25
2.6.1 Reddy SNR Estimation.....	25
2.6.1.1 Estimation of Noise Power and Signal Power.....	27
2.6.1.2 Signal Power Estimation.....	27
2.6.1.3 Noise Power Estimation in Sub-bands.....	28
2.6.1.4 Signal Power Estimation in Sub-band.....	29
2.6.1.5 SNR Estimation in Each Sub-band.....	29
2.6.2 Subspace Based SNR Estimator.....	30
2.6.2.1 Estimation of Subspace Based SNR.....	32
2.6.2.2 Subspace based SNR estimator.....	34
2.7 Applications Which May Benefit From Knowledge of the SNR.....	35
2.7.1 Power Control.....	36
2.7.2 Resource Management Algorithms.....	36
2.7.3 Diversity Combining.....	37
2.7.4 Equalization.....	38
2.7.5 Synchronization.....	38
2.7.6 Adaptive Arrays.....	38
2.7.7 Viterbi Equalization and Decoding.....	39
2.8 Summary.....	39

CHAPTER 3: NOVEL FRONT-END SNR ESTIMATION TECHNIQUE FOR OFDM SYSTEMS..... 40

3.1 Introduction.....	40
3.2 Formulation of Proposed Front-End SNR Estimation Technique.....	42
3.2.1 Selection of a Preamble.....	43
3.2.2 Proposed Front-End SNR Estimator.....	46
3.2.2.1 Ist Part: Front End Noise Power and SNR Estimation Technique for AWGN channel and Wireless Multipath Channels.....	46
a. Autocorrelation Based Front-End SNR Estimator.....	49

b. Signal Power and Noise Power Estimation.....	50
c. Signal Power Estimation.....	55
d. Noise Power Estimation.....	57
e. SNR Estimation.....	57
3.3.2.2 2nd Part: Front-End Noise Power and SNR Estimation of Colored Noise Using Wavelet Packet.....	58
a. Signal Power and Noise Power Estimation in Sub-Bands.....	58
b. Signal Power Estimation in each Sub-band.....	60
c. Noise power Estimation in each Sub-band.....	61
d.SNR Estimation in each Sub-band.....	61
3.3 Methodology for Analyzing Various SNR Estimators.....	62
3.3.1 Methodology for Analyzing Reddy’s SNR Estimator.....	63
3.3.2 Methodology for Analyzing Subspace Based SNR Estimator.....	66
3.3.3 Methodology for Analyzing Proposed Front-End SNR Estimator.....	68
3.3.3.1 1st Part: For Multipath Channels With AWGN	68
3.3.3.2 2nd Part: For Multipath Channel with Colored Noise using Wavelet Packet Filter Banks.....	71
3.4 Summary.....	75
CHAPTER 4: RESULTS AND DISCUSSION.....	76
4.1 Introduction.....	76
4.2 Analysis Results of SNR Estimation Technique for Multipath Channels AWGN in OFDM Systems	77
4.2.1 Performance Evaluation.....	77
4.2.1.1 Comparison with Other Techniques.....	81
4.2.1.2 Performance over AWGN, Rayleigh and Rician.....	83
4.2.1.3 Performance over SUI Multipath Channels.....	91
4.2.1.4 Performance over Indoor Channel Model for Wi-Fi.....	98

4.2.2 Computational Complexity.....	100
4.2.3 Sensitivity Analysis.....	103
4.3 Analysis Results of SNR Estimation Technique for Multipath Channel Colored Noise using Wavelet-Packet Transform in OFDM Systems.....	107
4.3.1 Performance Comparisons of colored noise estimator.....	110
4.4 Summary.....	110
CHAPTER 5: CONCLUSION.....	111
5.1 Introduction.....	111
5.2 Conclusion.....	111
5.3 Suggested Future Work.....	113
REFERENCES.....	115
PUBLICATIONS.....	121
APPENDIXES.....	122
Appendix A: About Wavelet Packet Analysis.....	123
A.1 Introduction.....	123
A.2 Matlab® Wavelet Toolbox.....	126
A.3 Wavelet Packet.....	126
A.4 From Wavelets to Wavelet Packets: Decomposing the Details.....	127
Appendix B: Implementation of FFT Using Discrete Wavelet Packet Transform and its Application to SNR Estimation in OFDM Systems.....	131
B.1 Introduction.....	131
B.2 Proposed Wavelet Packet Based FFT (DWPT-FFT).....	133
B.3 SNR Estimation inside FFT Block.....	136

B.3.1 Autocorrelation based SNR Estimator.....	138
B.3.2 Signal Power and Noise Power Estimation.....	140
B.3.2.1 Signal Power Estimation in each Sub-band.....	141
B.3.2.2 Noise Power Estimation in each Sub-band.....	142
B.3.2.3 SNR Estimation in Each Sub-band.....	143
B.4 Results and Discussions.....	143
B.4.1 Performance Comparison.....	144
B.5 Summary.....	146

LIST OF TABLES

Table 3.1	Ideal vs. calculated SNR for first-part of proposed technique.....	57
Table 3.2	Ideal vs. calculated SNR for second-part of proposed technique.....	61
Table 3.3:	Parameters for OFDM Systems Simulation.....	64
Table 3.4:	Parameters of proposed Technique for first part (IEEE802.16, 2004)...	70
Table 3.5:	Parameters of proposed Technique for first part (IEEE802.11a).....	70
Table 3.6:	Parameters for Second-Part of proposed technique.....	73
Table 4.1:	Description of Rayleigh and Rician channel.....	79
Table 4.2:	Terrain types and corresponding SUI channels.....	79
Table 4.3:	Description of SUI channels.....	80
Table 4.4:	Description of Indoor channel models for Wi-Fi.....	80
Table 4.5:	Complexity comparison of SNR estimators.....	102
Table A.1:	Analysis-Decomposition Functions.....	128
Table A.2:	Synthesis-Reconstruction Functions.....	128
Table A.3:	Decomposition Structure Utilities.....	128
Table A.4:	De-Noising and Compression.....	129
Table B.1:	Parameters for the simulation.....	144

LIST OF FIGURES

Figure 2.1:	Multipath propagation.....	10
Figure 2.2:	Intersymbol interference.....	11
Figure 2.3:	Frequency division multiplexing.....	13
Figure 2.4:	Orthogonal Frequency division multiplexing.....	14
Figure 2.5:	Spectrum of a single subchannel.....	14
Figure 2.6:	Spectrum of an OFDM signal.....	15
Figure 2.7:	OFDM modulator.....	17
Figure 2.8:	OFDM demodulator.....	17
Figure 2.9:	No ISI with introduction of guard time.....	18
Figure 2.10:	Effect of ICI with no signal in the guard time.....	19
Figure 2.11:	No ICI with cyclic prefix in the guard time.....	19
Figure 3.1:	Preamble signal loaded on even subcarriers using PN sequence.....	47
Figure 3.2:	Power spectrum of an OFDM signal.....	50
Figure 3.3:	Multiplication of $h(n)$ and $h(n+N/2)$	52
Figure 3.4:	(a) Transmitted Preamble.....	54
Figure 3.4:	(b): Received Preamble after coming through a channel (Plots show two identical halves with no cyclic prefix).....	55
Figure 3.5:	(a): Autocorrelation plot of transmitted signal.....	56
	(b): Autocorrelation plot of received signal.....	56
Figure 3.6:	Autocorrelation of received preamble in time domain.....	59
Figure 3.7:	Wavelet decomposition of transmitted OFDM data Estimation of colored noise using white noise in small segments.....	59
Figure 3.8:	(a): Autocorrelation plot of transmitted signal.....	60
Figure 3.9:	(b): Autocorrelation plot of received signal.....	60
Figure 3.10:	Methodology of Reddy's SNR estimator.....	63
Figure 3.11:	OFDM signal in frequency domain (IEEE802.16d).....	64
Figure 3.12:	Reddy's estimator flow chart.....	65
Figure 3.13:	Methodology of subspace based SNR estimator.....	66
Figure 3.14:	Flow chart of subspace estimator.....	67
Figure 3.15:	Methodology of first part of proposed estimator.....	69
Figure 3.16:	OFDM preamble signal with CP.....	69
Figure 3.17:	Flow chart of proposed SNR estimation technique for white noise.....	71
Figure 3.18:	Methodology of proposed SNR estimation technique for colored noise.....	72
Figure 3.19:	Flow chart of proposed SNR estimation for colored noise.....	74
Figure 4.1:	SNR-NMSE vs. actual SNR comparison of proposed technique	

	with Reddy's and subspace Estimators.....	82
Figure 4.2:	Estimated SNR vs. actual SNR comparison of proposed technique with Reddy's and subspace.....	82
Figure 4.3:	Autocorrelation of AWGN.....	84
Figure 5.4:	SNR-NMSE vs. actual SNR with AWGN channel.....	84
Figure 4.5:	Estimated SNR vs. Actual SNR with AWGN channel.....	85
Figure 4.6:	SNR-NMSE vs. actual SNR with Rayleigh 3-Tap channel.....	85
Figure 4.7:	Estimated SNR vs. Actual SNR with Rayleigh 3-Tap channel.....	86
Figure 4.8:	SNR-NMSE vs, actual SNR with Rayleigh 5-Tap channel.....	86
Figure 4.9:	Estimated SNR vs. Actual SNR with Rayleigh 5-Tap channel.....	87
Figure 4.10:	SNR-NMSE vs. actual SNR with Rayleigh 10-Tap channel.....	87
Figure 4.11:	Estimated SNR vs. Actual SNR with Rayleigh 10-Tap channel.....	88
Figure 4.12:	SNR-NMSE vs. actual SNR with Rician 3-Tap channel.....	88
Figure 4.13:	Estimated SNR vs. Actual SNR with Rician 3-Tap channel.....	89
Figure 4.14:	SNR-NMSE vs. actual SNR with Rician 5-Tap channel.....	89
Figure 4.15:	Estimated SNR vs. Actual SNR with Rician 5-Tap channel.....	90
Figure 4.16:	SNR-NMSE vs. actual SNR with Rician 10-Tap channel.....	90
Figure 4.17:	Estimated SNR vs. Actual SNR with Rician 10-Tap channel.....	91
Figure 4.18:	SNR NMSE vs. actual SNR with SUI-1 Channel.....	92
Figure 4.19:	Estimated SNR vs. Actual SNR with SUI-1 Channel.....	92
Figure 4.20:	SNR NMSE vs. actual SNR with SUI-2 Channel.....	93
Figure 4.21:	Estimated SNR vs. Actual SNR with SUI-2 Channel.....	93
Figure 4.22:	SNR NMSE vs. actual SNR with SUI-3 Channel.....	94
Figure 4.23:	Estimated SNR vs. Actual SNR with SUI-3 Channel.....	94
Figure 4.24:	SNR NMSE vs. actual SNR with SUI-4 Channel.....	95
Figure 4.25:	Estimated SNR vs. Actual SNR with SUI-4 Channel.....	95
Figure 4.26:	SNR NMSE vs. actual SNR with SUI-5 Channel.....	96
Figure 4.27:	Estimated SNR vs. Actual SNR with SUI-5 Channel.....	96
Figure 4.28:	SNR NMSE vs. actual SNR with SUI-6 Channel.....	97
Figure 4.29:	Estimated SNR vs. Actual SNR with SUI-6 Channel.....	97
Figure 4.30:	SNR-NMSE vs. Actual SNR for IEEE802.11a.....	99
Figure 4.31:	Estimated SNR vs. Actual SNR for IEEE802.11a.....	99
Figure 4.32:	Sensitivity of estimated SNR w.r.t. (L-N) peak.....	105
Figure 4.33:	Sensitivity of estimated SNR w.r.t. (L-N/2) peak.....	105
Figure 4.34:	Sensitivity of estimated SNR w.r.t. (L) peak.....	106
Figure 4.35:	Combined results of sensitivity of estimated SNR.....	106
Figure 4.36:	Mean-square-error performance of the proposed technique with colored noise.....	109
Figure 5.37:	Estimated SNR vs. Actual SNR with colored noise.....	109
Figure A.1:	Wavelet packet decomposition.....	125

Figure A.2:	Wavelet Packet Decomposition Tree at Level 3.....	127
Figure B.1:	Block Diagram of DWPT-FFT.....	133
Figure B.2:	Last stage of length 8 DWPT-FFT.....	135
Figure B.3:	Butterfly operation in DWPT-FFT.....	135
Figure B.4:	Two-scale discrete wavelet packet transforms.....	135
Figure B.5:	Preamble signal loaded on even subcarriers using PN sequence.....	136
Figure B.6:	Power spectrum of an OFDM signal.....	140
Figure B.7:	(a): Transmitted Preamble.....	141
	(b): Received Preamble after coming through a channel.....	141
Figure B.8:	a)Autocorrelation plot of Transmitted.....	142
	(b) Received (b) 5 th band signal.....	142
Figure B.9:	FFT result with and without wavelet packet.....	143
FigureB.11:	MSE performance of the proposed technique.....	144
FigureB.10:	Actual SNR vs. Estimated SNR of colored noise.....	145

LIST OF ABBREVIATIONS

AWGN	Additive White Gaussian Noise
BER	Bit Error Rate
BPSK	Binary Phase Shift Keying
BS	Base Station
CCI	Co-Channel Interference
CIR	Channel Impulse Response
CPE	Customer Premises Equipment
CSI	Channel State Information
DA	Data Aided
DFT	Discrete Fourier Transform
DVB	Digital Video Broadcasting
FBWA	Fixed Broadband Wireless Access
FDM	Frequency Division Multiplexing
FFT	Fast Fourier Transform
ICI	Inter-carrier Interference
IDFT	Inverse Discrete Fourier Transform
IFFT	Inverse Fast Fourier Transform
ISI	Intersymbol Interference
LAN	Local Area Network
LOS	Line-Of-Sight
MAN	Metropolitan Area Networks
MDL	Minimum Descriptive Length
MF	Matched Filter
ML	Maximum Likelihood
MLSE	Maximum-Likelihood Sequence Estimation
MRC	Maximum Ratio Combining
MSE	Mean Squared Error
NLOS	Non-Line-Of-Sight

NMSE	Normalized Mean-Squared-Error
OFDM	Orthogonal Frequency Division Multiplexing
PAPR	Peak to Average Power Ratio
Pdf	Power Density Function
PN	Pseudorandom Noise
PSK	Phase Shift Keying
QAM	Quadrature Amplitude Modulation
QPSK	Quadrature Phase Shift Keying
RMS	Root-Mean-Squared
SINR	Signal to Interference + Noise Ratio
SIR	Signal-to-Interference-Ratio
SNR	Signal to Noise Ratio
SS	Subscriber Station
SSME	Split Symbol Moment Estimator
SUI	Stanford University Interim
Wi-Fi	Wireless Fidelity
WiMAX	Worldwide Interoperability for Microwave Access
WP	Wavelet Packet
WSSUS	Wide-Sense Stationary and Uncorrelated Scattering

1.1 Background

Fourth Generation wireless and mobile systems characterized by broadband wireless systems are currently the focus of research and development among the researchers everywhere. The broadband wireless systems favor the use of orthogonal frequency division multiplexing (OFDM) modulation that allows high data-rate communication. A major advantage of OFDM systems is its ability to divide the input high rate data stream into many low-rate streams that are transmitted in parallel. Doing so increases the symbol duration and reduces the intersymbol interference over frequency-selective fading channels [Van Nee, 2000]. This and other features of equivalent importance have motivated the adoption of OFDM as a standard for several applications such as digital video broadcasting (DVB) and broadband indoor wireless local area networks, broadband wireless metropolitan area networks and many others.

In order to exploit all these advantages and maximize the performance of OFDM systems; channel state information (CSI) plays a very important role. Signal-to-noise ratio (SNR) is a quantity that gives a comprehensive measure of CSI for each frame. An on-line SNR estimator thus provides the knowledge to decide whether a transition to higher bit rates would be favorable or not.

Signal-to-noise ratio (SNR) is broadly defined as the ratio of desired signal power to the noise power. Noise variance and hence signal to noise ratio (SNR) estimates of the

received signal are very important for the channel quality control in communication systems. The search for a good SNR estimation technique is also motivated by the fact that various algorithms require knowledge of the SNR for optimal performance. For instance, in OFDM systems, SNR estimation is used for power control, adaptive coding and modulation, turbo decoding, diversity combining, etc.

One of the purposes of acquiring SNR estimates in a wireless communication channel is to use this information to evaluate the link reliability. In worldwide inter operability for microwave access (WiMAX) systems, the knowledge of the SNR is used for throughput optimization by selecting one out of seven burst where the selected profile changes according to the measured SNR. As in adaptive modulation and coding, a higher modulation and coding rate is used in high SNR conditions, while a lower and noise robust modulation formats is used in low SNR conditions. Each burst profile has some threshold values of SNR. These threshold values of SNR are used to adapt different burst profiles on the basis of channel state information.

Several SNR estimation algorithms have been suggested in the past for single carrier systems presuming ISI free reception of the system. SNR estimation for multicarrier systems (OFDM) were presented first in nineties. There is not that much work found for SNR estimation in OFDM systems. SNR estimation algorithm for multicarrier systems suggested in the past by [Shousheng et.al, 1998], [Reddy, S. et al, 2003], [Bournard, S, et al,2003], [Taesang, Y. et al, 2004],[Xiaodong X. et al ,2005], [Yucek et al, 2005], [Doukas et al, 2006] and have been successfully implemented previously in OFDM systems by making use of the pilot symbols that are inserted in the OFDM symbol. Extracting pilots and using them for SNR estimation is computationally complex. The need is of an SNR estimator of low computational complexity so as to keep hardware costs minimum while keeping estimation error minimum. This is the motivating factor for the pursuit of an SNR estimator that does not require the manipulation of pilot symbols. SNR estimator presented in the past performed SNR at the back-end of the receiver. So, there is enough interest in estimating SNR at the front-end of the receiver which has added advantages of fast and efficient inline diversity combining, adaptive

modulation and coding. For systems that use preamble for synchronization and channel estimation, this is feasible and designed in this thesis.

1.2 Types of SNR Estimators

All the estimation algorithms mentioned above can be divided into two classes. One class is data-aided estimator (DA-SNR estimator) for which known (training sequence or pilot) data is transmitted and the SNR estimator at the receiver uses the known data to estimate the SNR. The other class is the non-data-aided estimator. For this class of estimator, no known data is transmitted, and therefore the SNR estimator at the receiver has to blindly estimate the SNR value.

Various specific DA-SNR estimators are discussed in more detail in later sections, but there are two general types classified according to whether the data is used to aid the SNR estimation is known or estimated. An estimator that uses an exact, known copy of the transmitted message sequence will be referred to as a TxDA estimator.

A DA-SNR estimator that uses an estimate of the transmitted message sequence provided by receiver decisions will be referred to as an RxDA estimator. As a further classification, any SNR estimator that can generate SNR estimates from the unknown, information-bearing portion of the received signal is often referred to as an in-service estimator. RxDA-SNR estimators are of the in-service type.

In TxDA-SNR estimation, the fidelity of the message sequence used for SNR estimation is assured by making an exact copy of the transmitted message sequence available to the receiver. As an example, short blocks of known data may be inserted periodically into the information-bearing sequence. DA equalization techniques use so-called training sequences for a similar purpose [J.G.Proakis, 1989].

A throughput penalty is incurred since some channel capacity must be devoted to the transmission of non information- bearing data (training sequences are not considered to

carry information because the data is already known to the receiver). However, in systems which already employ training sequences for equalization or synchronization, there would be no additional throughput penalty since those same known sequences could be used to maximize the performance of a DA-SNR estimator.

Note that since TxDA-SNR estimates can only be generated when known data is available at the receiver, the use of a TxDA-SNR estimator may not be appropriate in some situations where a continuous stream of SNR estimates is required.

Since receiver decisions are subject to error, the performance of RxDA-SNR estimation is inferior to that of TxDA-SNR estimation at low SNR where decision errors are more likely. An advantage of RxDA-SNR estimation is that the SNR information is extracted directly from the information-bearing signal with no loss of throughput due to resource overhead. Since RxDA-SNR estimates may be generated whether the transmitted symbols are known or unknown, RxDA-SNR estimators may be used in applications that require a continuous stream of SNR estimates

1.3 SNR Estimation Problem Statement

In this work, an estimator of type Rx-DA-SNR is proposed. It makes use of the synchronization preamble. Most synchronization schemes of today are based on Schmidl & Cox technique [Schmidl et al, 1997], which uses alternate loading of subcarriers with known PN sequence. Such alternate loading leads to two identical halves property in the preamble. Since the preamble used for the proposed method is the timing synchronization preamble in OFDM system so there is no additional throughput penalty.

According to best knowledge of the author, there is no work done at front-end of the receiver for OFDM systems. Herein, a front-end estimation of noise power and SNR based on one OFDM preamble symbol used for synchronization is proposed.

There are two main tasks that need to be addressed in preamble based SNR estimation. Firstly, selection of training or preamble signal that will sound out the channel effectively

and efficiently. In an OFDM system, this means that the preamble signal should have equal power in all subcarriers and peak to average power ratio (PAPR) of the preamble signal should be as small as possible. Given the same system power, the preamble with a lower PAPR can be power boosted more. This results in a better estimation of signal to noise ratio (SNR).

After selecting an efficient preamble, the other major task is the development of SNR estimation technique that can estimate the SNR at front-end of the receiver with only one OFDM preamble symbol.

1.4 Objectives of the Research

There are three main objectives of the research work. These are outlined as follows:

- A complete end-to-end IEEE802.16d compliant OFDM-FBWA system will be developed in Matlab® for the purpose of evaluating the performance of proposed SNR estimation technique in both frequency non-dispersive and dispersive channels with real additive white Gaussian noise (AWGN) and also colored noise.
- Front-end SNR estimation technique based on one OFDM preamble will be developed that has desirable properties of minimal estimation error in mean squared sense and will provide accurate estimates of SNR in term of only one training symbol. The results will be compared with other works reported in the literature.
- The technique will also be extended to obtaining noise power estimates of colored noise using wavelet-packet based filter bank analysis of the noise.

1.5 Contribution of This Thesis

- A novel SNR estimation technique for OFDM systems is reported. It makes use of timing synchronization preamble used in many OFDM systems. There is no extra

overhead as the preamble used for SNR estimation is already employed in OFDM systems. It estimates the SNR by auto correlating the received preamble. Complexity of proposed estimator to find SNR estimates is much lower than other SNR estimators because it is based on only one OFDM preamble.

- The proposed technique, when employed up-front in the presence of cyclic prefix (CP), gives better estimates of SNR over AWGN channel and multipath channels (Rayleigh & Rician). The technique is also extended to estimates the SNR over colored noise using wavelet packet.
- The proposed technique, when employed after CP removal, can also estimate SNR over colored noise using wavelet packet analysis.
- Wavelet packet based FFT implementation is also reported in this thesis in appendix B where SNR estimation is performed inside FFT for both AWGN and colored noise.

1.6 Organization of Thesis

This thesis is structured as follows. Chapter 2 presents the background of OFDM systems and its advantages when used in wireless channels. It is followed by the literature review of SNR estimation for different systems and later by literature review about SNR estimation for OFDM systems, - the topic of this thesis. Formulation of SNR estimation algorithms used later for comparing them with the proposed technique is also presented. This chapters ends with the applications which may be benefited from the knowledge of SNR.

Chapter 3 presents the formulation of proposed front-end SNR estimation. The proposed technique makes use of one OFDM synchronization preamble - the preamble which has two identical halves property. Benefit of using this preamble is discussed in selection of preamble section. Proposed technique is designed for additive white Gaussian noise (AWGN) channel and multipath channels and also extended to obtain the noise power

estimates of colored noise using wavelet-packet based filter bank analysis of the noise. The proposed technique is deployed at the front-end of the receiver unlike all other SNR estimators for OFDM systems discussed in chapter 2. In the last section methodologies of proposed estimator as well as the estimators used later for comparison are presented. It lists the selected parameters for proposed as well as other SNR estimators that have been used for comparison in our simulations.

In chapter 4, results of proposed work is presented and discussed. The results are compared with previously published SNR estimators for both white noise and colored noise scenario respectively. The results shows that the proposed estimator with one OFDM preamble perform better than other SNR estimators which makes use of many OFDM symbols to obtain the accurate estimates of SNR. The purposed method is also checked with the WiMAX systems (IEEE802.16d) using SUI channels and also with IEEE802.11g systems using indoor channel models.

Chapter 5 presents the conclusions and suggests the future works.

Appendix A discusses Wavelet Packets used in this technique.

Appendix B presents the wavelet packet based FFT and its use in SNR estimation for both AWGN and colored noise.

2.1 Introduction

In Chapter 1, motivations of SNR estimation in OFDM systems and types of SNR estimators were introduced. Multipath is a phenomenon that occurs in wireless channel when multiple reflected versions of the signal arrive at the receiver at slightly different time and with various amplitudes and phases. The two channel impairments caused by multipath are multipath fading and intersymbol interference (ISI).

The key enabling technology to overcome these channel impairments is OFDM, introduced in this chapter. The principles of OFDM technology will be explored. Following this, literature review on SNR estimation and SNR estimation algorithms used later for comparison with the purposed technique will be presented. It will be followed by applications that may benefit from SNR. It is shown that in order to fully harness the power of OFDM technology, accurate SNR estimates must be obtained at the receiver. This establishes the importance of SNR estimation in an OFDM system.

2.2 Wireless Channel

Before introducing both OFDM and SNR estimation, we introduce the wireless channel itself and the 2 main impairments of multipath wireless channel, ISI and multipath fading. We undertake this in order to appreciate how OFDM technology is able to

overcome these impairments. The following literature is borrowed from the Rappaport's book [Rappaport, 2002].

The wireless channel is the single most important factor that limits the performance of wireless communication system. It is extremely hostile to communication. The transmission path from the transmitter to the receiver can vary from a simple LOS to one that is heavily obstructed by buildings, mountains and foliage. The signal from the transmitter is reflected, diffracted and scattered by various objects in the surrounding before reaching the receiver. When the signal impinges on an object that is very large compared to its wavelength, it will be reflected. Examples of reflecting objects are the earth's surface, buildings and walls. Some of the signal's energy will be transmitted through refraction while the rest will be reflected.

On the other hand, diffraction happens when the signal seemingly bends around obstacles that obstruct the path between the transmitter and receiver. Although one would expect the signal strength to be zero behind the obstacle, this is actually not the case. There is signal energy behind and beyond the obstacle. Due to this, although there is no LOS between the transmitter and receiver, the latter can still receive the signal. This phenomenon can be explained using Huygen's principle, which states that all points on a wavefront can be considered as point sources for the production of secondary wavelets and these wavelets combine to produce a new wavefront in the direction of propagation. When the signal impinges on objects that are small compared to its wavelength, scattering occurs. These objects usually have rough surfaces. Foliage, street signs and lamp posts are some objects that produce scattering.

The three signal propagation mechanisms (reflection, diffraction and scattering) affect the received signal strength. Naturally, the signal strength will be lower the farther the receiver is from the transmitter due to the spread of the signal in all direction through free space. But reflection, diffraction and scattering cause the signal strength to decrease faster as the distance increases. There are models that predict the mean received signal strength given the distance of the receiver from the transmitter. Due to the randomness of

the wireless channel, these models are statistically based and they are known as large-scale propagation models.

Making matters worse, a signal from the transmitter can take multiple different paths before reaching the receiver as shown in Fig. 2.1. This can be caused by reflecting or even scattering objects. The multiple reflected versions of the signal will arrive at the receiver at slightly different time and with various amplitudes and phases. This phenomenon is called multipath. The multipath signals add up vectorially. The received signal strength will be amplified if the signals reinforce each other or are in phase with one another. The received signal strength can also drop drastically to a level that impedes any communication if the signals cancel each other or are out of phase. This is also known as multipath fading and is detrimental to wireless communications. Due to multipath, the signal strength at the receiver can change drastically and rapidly in a short period of time and over short distances. This is called small scale fading. Although the transmitters and receivers in a FBWA system are stationary, movement of other objects

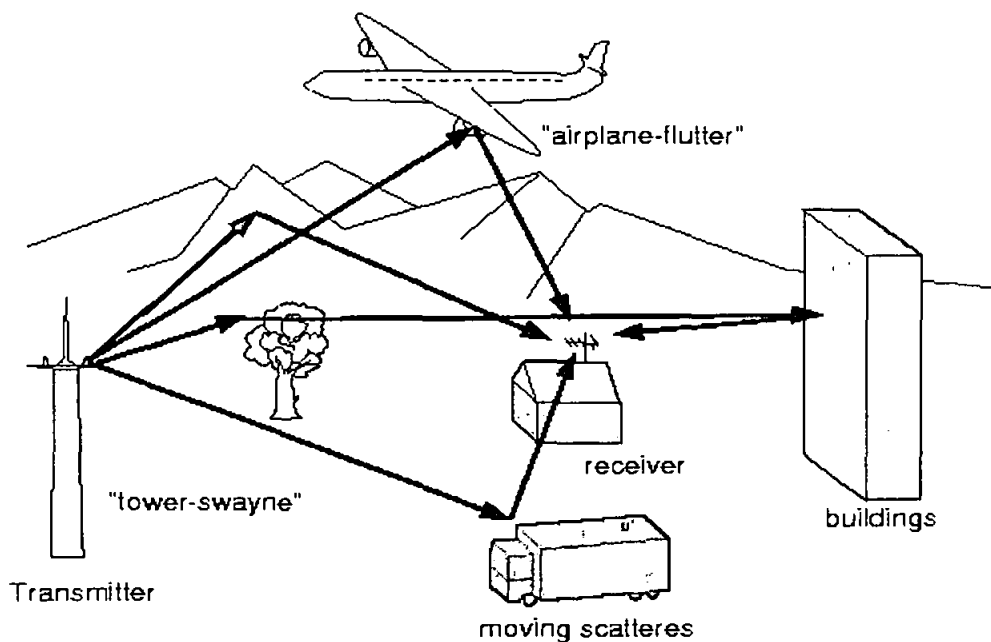


Figure 2.1: Multipath propagation

in the surrounding environment still causes fading to occur. It has been reported in [Sampath, Talwar, Tellado, Erceg & Paulraj, 2002] that FBWA system experiences fades that are as bad as mobile wireless communication systems when the measurements are done over a large timescale of the order of tens of hours.

In order for communication links to work even in deep fades, the transmit power required for a given link reliability should be much higher, depending on the severity of the fades expected. This extra power is known as fade margin. If effective techniques are used to mitigate the fades, the extra power will not be needed, making the BS and CPEs cheaper. On the other hand, the extra power can be used to increase the reliability or extend the range of the system to cover a larger geographical area.

Multipath can also cause signal distortion. When different copies of the transmitted signal arrive at slightly different times, it can overlap across different symbol times. The delayed previous symbol interferes with the current symbol causing what is known as intersymbol interference (ISI) as shown in Fig2.2. When the symbol rate increases, ISI will be worse because the delayed previous symbol can interfere with many symbols after it. This means that ISI becomes a major problem with high data rate wireless communication systems like FBWA. This signal distortion needs to be corrected using various equalization techniques [Sklar, 1997].

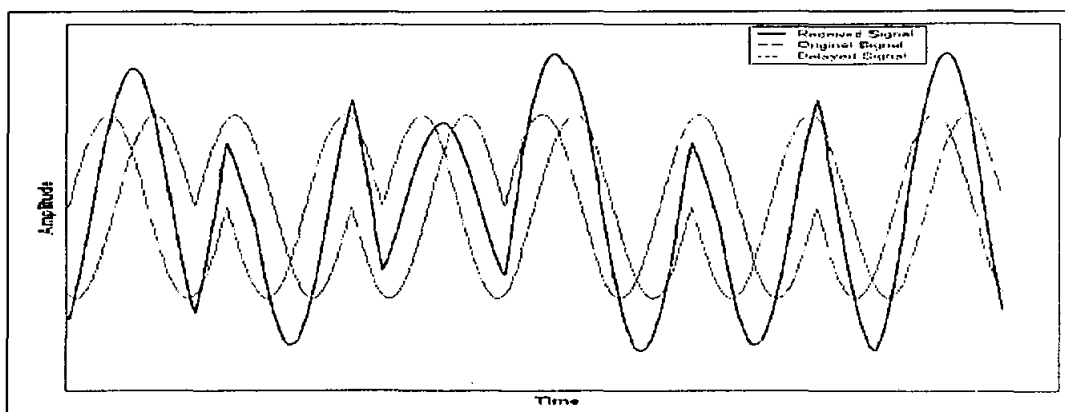


Fig.2.2 Intersymbol interference

In the frequency domain, ISI manifests itself as frequency selective fading where the gain and phase shift are different for different frequencies. Therefore the 2 most important challenges presented by the wireless channel to a FBWA system are multipath fading and ISI.

2.3 Orthogonal Frequency Division Multiplexing (OFDM)

In high rate communication systems, OFDM, as a technique, proves very effective in overcoming ISI in frequency selective fading channels. It is a special form of multicarrier modulation. In OFDM, a single high rate data stream is transmitted over a number of lower rate data streams. For example, in a packet based system, N data bits of a single high rate data stream are mapped to 1 bit on each of the parallel data streams. So, the symbol period of each of the data stream is N times the symbol period of the single data stream. The symbol duration of each of the lower rate data streams are now N times longer. ISI now only causes an overlap into the next symbol by an amount that is reduced by a factor of N . The relative dispersion in time due to ISI is therefore reduced considerably because of this. In fact, ISI is completely eliminated by introducing a guard time in each OFDM symbol. In the guard time, the OFDM symbol is cyclically extended to avoid inter-carrier interference (ICI). This cyclic extension is called cyclic prefix and the reasons for it will be further explained in the Section 2.3.1.

In OFDM, the broad bandwidth of the signal has been divided into N narrower sub-channels. If the OFDM system is designed properly, each of these narrow sub-channels will undergo flat fading as opposed to frequency selective fading when using single carrier systems. Therefore in OFDM, equalization is very much simplified and involves just a complex multiplication for each of the subcarrier.

The concept of using parallel data transmission and frequency division multiplexing (FDM) is not new. In FDM, the total frequency band is divided into N non-overlapping frequency sub-channels in order to avoid inter-channel interference. There would also be

guard bands between the sub-channels so that each subcarrier can be filtered and demodulated. This is shown in Fig.2.3.

However, this leads to inefficient use of the available spectrum. In order to avoid this spectrum wastage, ideas were proposed that made use of overlapping sub-channels instead. This is shown in Fig.2.4. Comparing with Fig.2.3, one can see that there is significant savings in bandwidth in OFDM compared with conventional FDM.

The question remains as to how the subcarriers can be separated and demodulated without suffering interference from other subcarriers. A technique, that allows the sub-channels to overlap and yet not interfere with one another, is to have the subcarriers mathematically orthogonal to each other [Van Nee, 2000]. A set of signals $\phi_j(t)$ is said to be orthogonal over an interval (a,b) if it satisfies the following: [Soliman & Srinath, 1990]

$$\int_a^b \phi_i(t) \phi_k(t) dt = \begin{cases} C & \text{for } i = k \\ 0 & \text{for } i \neq k \end{cases} \quad (2.1)$$

where C is a constant.

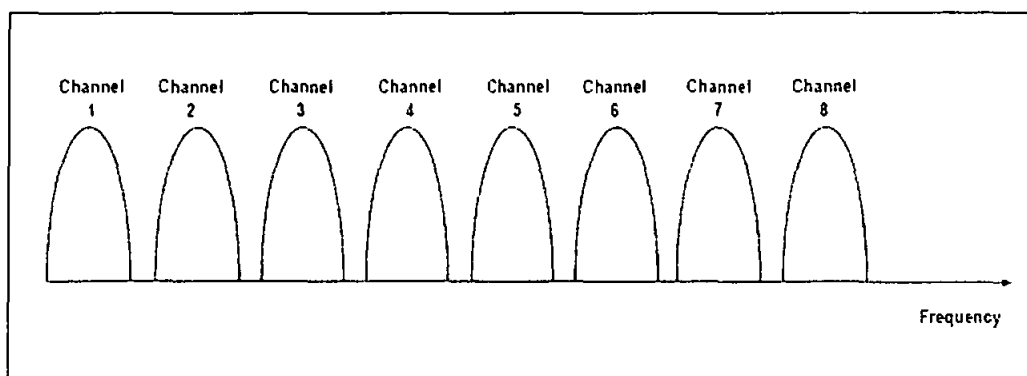


Fig.2.3 Frequency division multiplexing

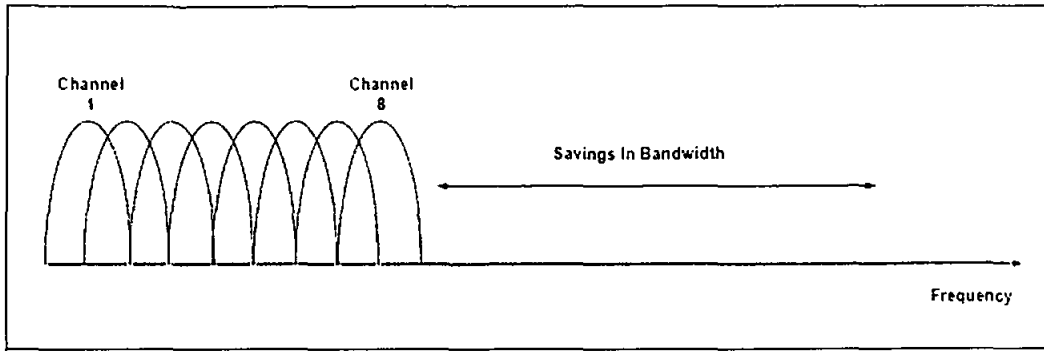


Fig.2.4 Orthogonal Frequency division multiplexing

Fig.2.5 shows the spectrum of a single sub-channel and Fig.2.6 shows the spectrum of an 7 subcarrier OFDM signal. From Fig.2.6, it can be seen that sub-channels overlap but the peak of any sub-channel is at the nulls of other sub-channels. This means that there is no interference and ICI between the sub-channels at the centre frequency of each sub-channel.

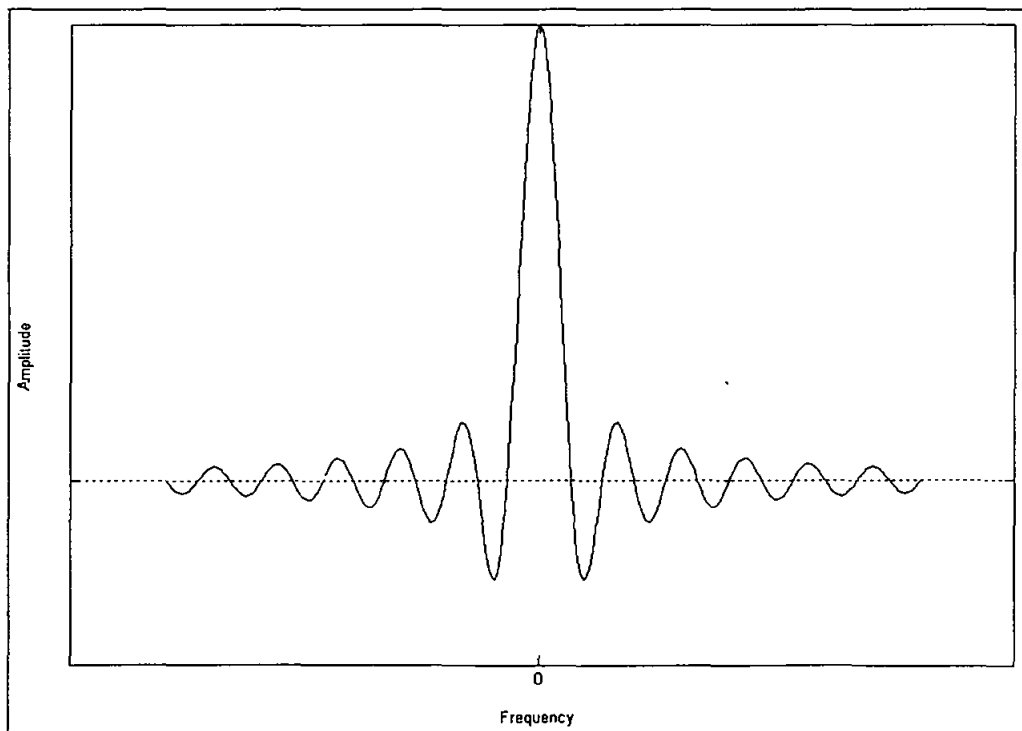


Figure 2.5: Spectrum of a single subchannel

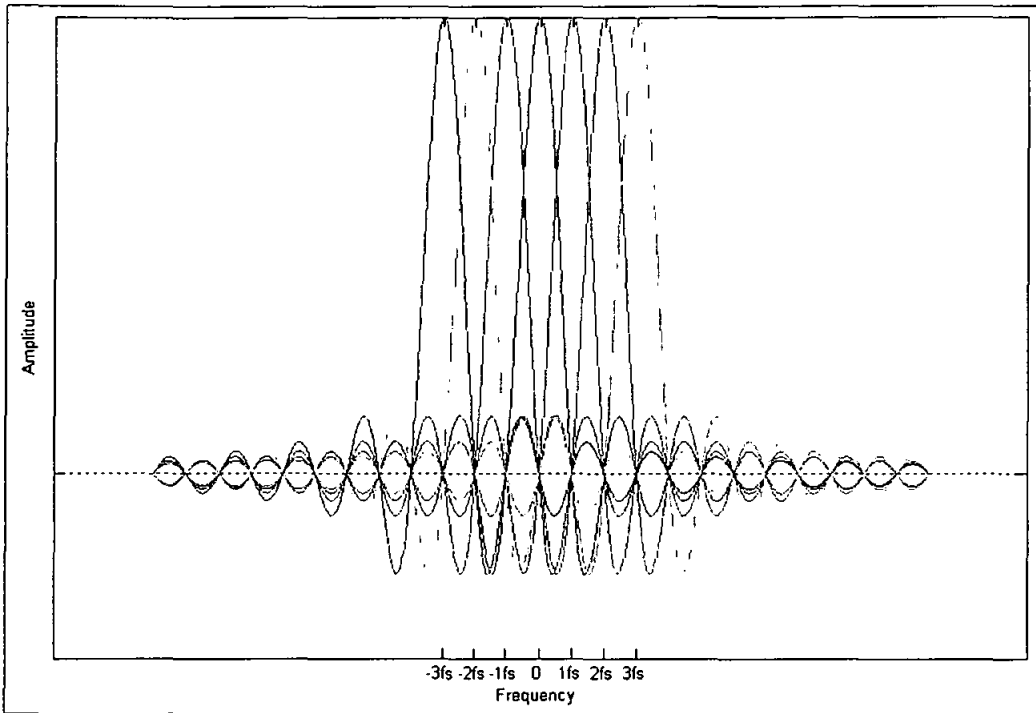


Figure 2.6: Spectrum of an OFDM signal

The next challenge is to have an efficient implementation of the OFDM. Initially, the OFDM was implemented using banks of subcarrier oscillators and coherent demodulators. Today, the use of discrete Fourier transform (DFT) and inverse discrete Fourier transform (IDFT) and their efficient implementation of fast Fourier transform (FFT) and inverse fast Fourier transform (IFFT) makes OFDM a practical and viable technique.

2.3.1 OFDM Principles

An OFDM signal is made up of many subcarriers that are independently modulated using either phase shift keying (PSK) or quadrature amplitude modulation (QAM).

Mathematically, one OFDM symbol $s(t)$ starting at time $t = t_s$ is written as [Van Nee, 2000]

$$s(t) = \text{Re} \left\{ \sum_{i=-\frac{N_s}{2}}^{\frac{N_s}{2}-1} d_{i+\frac{N_s}{2}} \exp(j2\pi(f_c + \frac{i+0.5}{T})(t-t_s)) \right\}, \quad t_s \leq t \leq t_s + T$$

$$s(t) = 0, \quad t < t_s \text{ \& } t > t_s + T \quad (2.2)$$

and its equivalent complex baseband notation

$$\hat{s}(t) = \text{Re} \left\{ \sum_{i=-\frac{N_s}{2}}^{\frac{N_s}{2}-1} d_{i+\frac{N_s}{2}} \exp(j2\pi \frac{i}{T}(t-t_s)) \right\}, \quad t_s \leq t \leq t_s + T$$

$$\hat{s}(t) = 0, \quad t < t_s \text{ \& } t > t_s + T \quad (2.3)$$

In the complex baseband representation, the real and imaginary parts are the in-phase and quadrature phase parts of the OFDM signal. Both parts need to be multiplied by a cosine and sine of the carrier frequency respectively to produce the final OFDM signal.

Fig.2.7 shows the baseband OFDM modulator block diagram and Fig.2.8 shows the baseband OFDM demodulator block diagram.

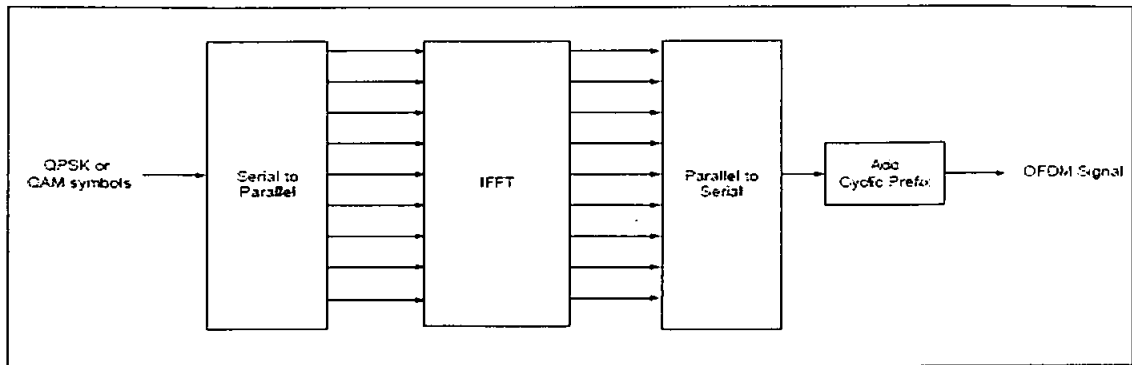


Figure 2.7 OFDM modulator

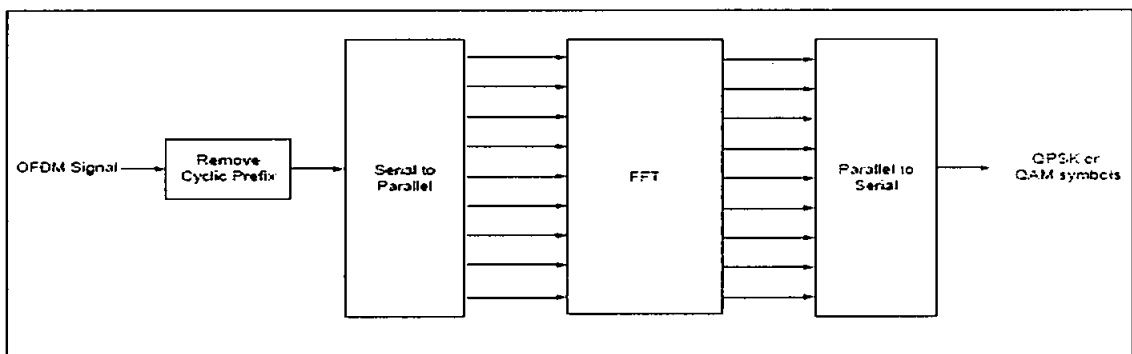


Fig2.8 OFDM demodulator

It is important to note that each of the subcarrier has a frequency that is an integer multiple of $1/T$ where T is the OFDM useful symbol period. This makes the sinc function spectrum of each of the subcarriers to be $1/T$ spaced from each other resulting in the OFDM spectrum as shown in Fig.2.6. This property makes the subcarriers orthogonal to each other because the peak of any subcarrier corresponds to the nulls of all other subcarriers.

In order to completely eliminate ISI in OFDM, a guard time is introduced at the beginning of each OFDM symbol. The guard time is chosen to be larger than the maximum expected delay spread of the channel so that multipath from one symbol will not interfere with the next symbol. Fig.2.9 shows how ISI is eliminated in OFDM by

introducing a guard time. Note in the figure that the delayed symbol 1 does not spill over to symbol 2 due to the guard time. Notice also that if the delay is longer than the guard time, ISI will occur.

This guard time could consist of no signal at all as in the case of Fig.2.9 but this will introduce ICI as shown in Fig.2.10, causing the loss of orthogonality among the subcarriers. Fig.2.10 shows subcarrier i and a delayed subcarrier j . During the demodulation of subcarrier i , there would be some interference from subcarrier j because there is no integer number of cycles of subcarrier j within the FFT integration interval and vice versa.

To eliminate this ICI, the OFDM symbol is cyclically extended in the guard time. This ensures that delayed replicas of the OFDM symbol always have an integer number of cycles within the FFT interval, as long as the delay spread is smaller than the guard time. Fig.2.11 shows that there is no ICI when cyclic prefix is used in the guard time.

In order to exploit the advantages and maximize the performance of OFDM technology; using high data rates, channel state information is necessary. Key role in the channel state information has Signal-to-Noise Ratio (SNR).

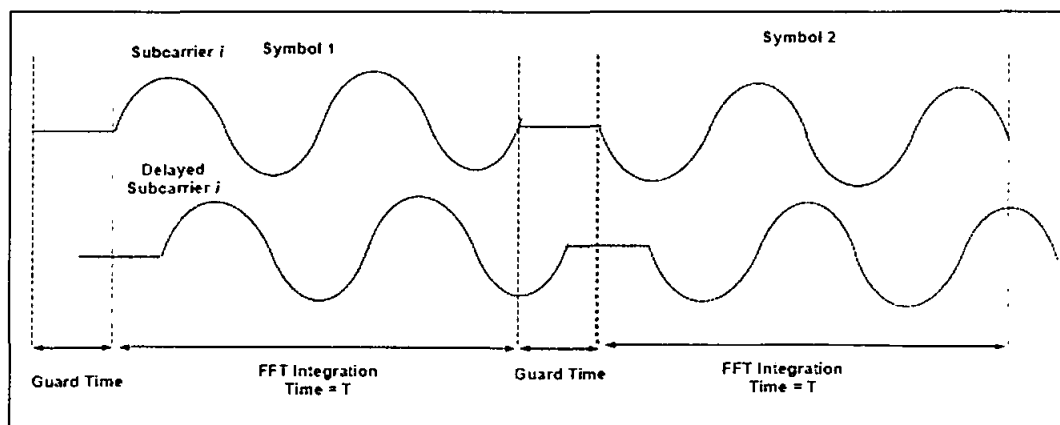


Fig.2.9 No ISI with introduction of guard time

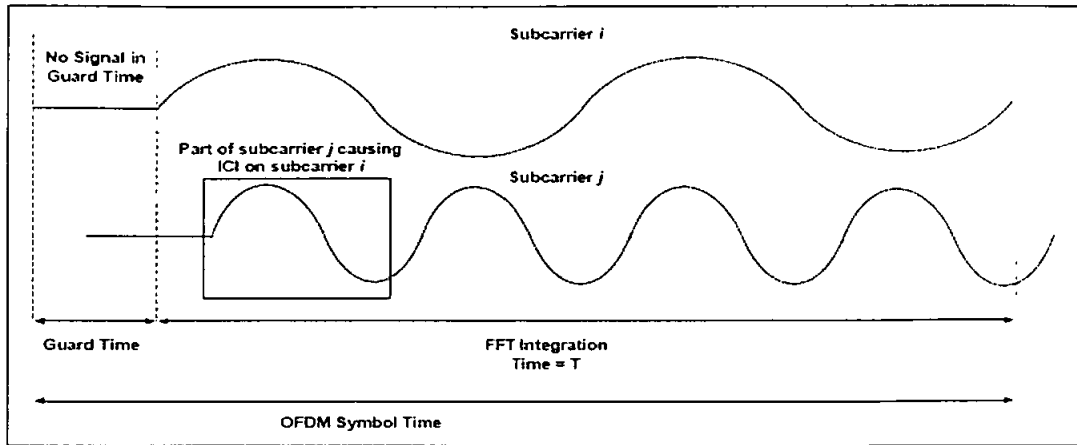


Fig 2.10 Effect of ICI with no signal in the guard time

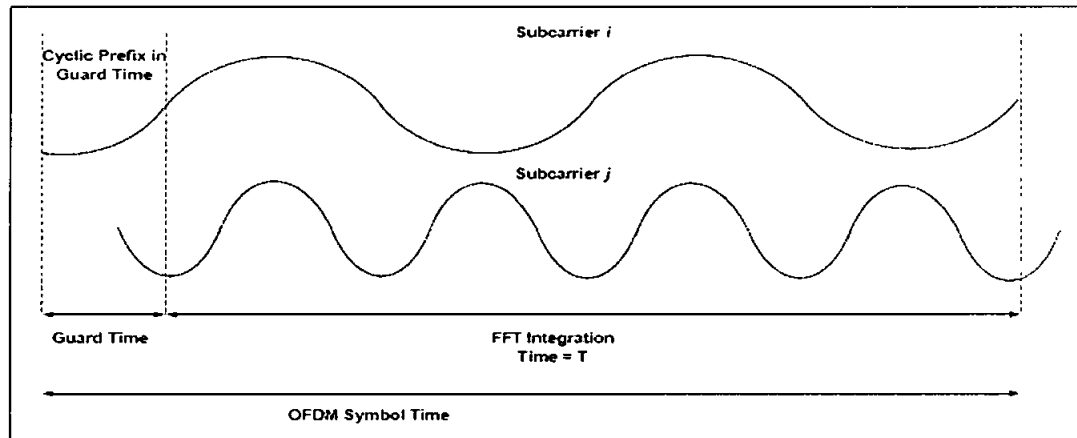


Fig.2.11 No ICI with cyclic prefix in the guard time

2.4 Literature Review

2.4.1 Overview of SNR Estimation

The signal-to-noise ratio (SNR) is broadly defined as the ratio of the desired signal power to the noise power and has been accepted as a standard measure of signal quality for communication system. The SNR estimators reported in the literature fall in two categories called data-aided (DA) and non-data-aided (NDA) estimators.

SNR estimators which extract the SNR from a single channel on which both a desired signal and noise are present using knowledge of the transmitted message sequence are referred to as data-aided (DA) estimators. A DA SNR estimator performs best when the message sequence used by the estimator is identical to the true transmitted message sequence. An example of this type of SNR estimator may be implemented using the correlation between the noisy signal and the known transmitted signal.

Non-data-aided SNR estimators generate estimates of the SNR assuming knowledge only of the statistics of the signal and channel. These estimation techniques are usually moment-based methods. Since no knowledge of the transmitted symbols is required, these techniques can derive SNR estimates from the information-bearing portion of the received signal and so are classified as in-service estimators.

- Interest in techniques to generate estimates of the SNR began in the mid- to late-1960's. The earliest recorded work on SNR estimation that could be found is a university report written by Nahi and Gagliardi [Nahi et al, 1964]. A subset of this work was published by Nahi and Gagliardi [Nahi et al, 1967]. The estimators described by Nahi and Gagliardi form estimates of the SNR by measuring the power of a hard limited, received (noisy) signal at the output of a filter. Both the signal and noise are assumed to be Gaussian stochastic processes with correlation functions of known shape. An expression is given by Nahi and Gagliardi showing the output power as a function of the filter transfer function and the SNR. The expression is not easily inverted so that, if the output power is known (measured), the SNR must be found implicitly using iterative techniques or a lookup table.
- Other early work on SNR estimation includes that of Benedict and Soong [Benedict et al, 1967]. The authors present three different methods to estimate separately the carrier strength and the noise level based on a finite number of samples. A maximum likelihood (ML) estimator, an estimator based on amplitude moments, and an estimator based on square-law moments are presented along with plots of the

bias and root mean square (RMS) error of the simulated signal and noise estimates for the three estimation techniques.

- Benedict and Soong refer to work done by [Middleton 1962] which predates that of Nahi [Nahi et al, 1967]. However, the estimation method developed by Middleton assumes that the noise level is known and so is not applicable to this study. The maximum likelihood (ML) estimator derived by Benedict and Soong is complicated. The ML SNR estimation problem was formulated in a different manner by Kerr [Kerr et al, 1966], [Gagliardi et al, 1968], [Thomas et al, 1967] and [Gilchriest et al, 1966] to yield much simpler expressions.
- Kerr proposes two different variations of a maximum likelihood SNR estimator where antipodal signaling in AWGN is assumed [Kerr et al, 1966]. The estimators derived by Kerr can be manipulated into the form of the SNR estimator derived by Gagliardi and Thomas. The probability density function (pdf) of the ML SNR estimator and analytical expressions for the bias and variance are offered by Gagliardi [Gagliardi et al, 1968].
- In the Jet Propulsion Laboratory report by Gilchriest [Gilchriest et al, 1966], a simple, intuitive SNR estimator is proposed based on the absolute mean and variance of an antipodal (BPSK) signal corrupted by AWGN. An analysis of the pdf of this estimator is presented along with confidence intervals. This work was extended by Layland to study the performance of this SNR estimator at low levels of SNR [Layland et al, 1967]. It is indicated in this work that this intuitive SNR estimator is a type of ML estimator. An analog method for determining the SNR of BPSK signals in additive white Gaussian noise (AWGN) was published by Edbauer [Edbauer et al, 1977]. The method is based on the processing of the in-phase and quadrature branches of a Costas demodulator.
- Simon and Mileant introduced an SNR estimator called the split symbol moments estimator (SSME) which is designed for BPSK signals in wideband AWGN

channels [Simon et al, 1986]. Shah and Hinedi study the SSME in narrowband channels and provide plots of the means and inverse normalized variances of theoretical and simulated SSME estimates [Shah et al, 1990]. In a Jet Propulsion Laboratory memo, Shah and Holmes discuss a modification of the SSME designed to improve performance in narrowband channels. The channel models of this work assume that all of the filtering occurs after noise is added.

- Matzner presented an SNR estimator whose structure was first introduced by Benedict and Soong in 1967 as the "square-law method of carrier strength and noise level estimation [Matzner et al, 1993]. Matzner evaluates the performance of the SNR estimator as opposed to the performances of the separate estimators of carrier strength and noise level as treated by Benedict and Soong. Matzner also provides more derivation details. The derivation assumes complex baseband signals in complex AWGN, but the estimator structures developed are also applicable, with relatively minor modifications, to real baseband signals in real AWGN. The mean square error (MSE) of the logarithm (dB) of simulated SNR estimates is plotted by Matzner as a function of the block length and as a function of the true SNR.
- A hardware implementation is described by Matzner, Engleberger, and Sietvert [Matzner et al, 1997]. The complex form of this SNR estimator may be modified to be used as a more general signal-to-interference ratio (SIR) estimator in fading channels with co-channel interference (CCI) and AWGN. The "signal-to-variation ratio (SVR) estimator proposed by Brand is an SIR estimator used to measure the quality of signals in channels corrupted by multipath, CCI, and AWGN [Brand et al, 1996]. This estimator may be modified to be used as an SNR estimator for complex signals in complex AWGN, or for real signals in real AWGN. The SVR estimator is identified as being of the "in-service type which is a term sometimes used to refer to an estimator that forms estimates from the information-bearing received signal, thus avoiding the need to perform SNR measurements off-line.

- Plots provided by Brand showing the theoretical and simulated SVR estimates as a function of signal power for three different fading channels [Brand et al, 1994]. [Yoshida et al, 1991] and [Yoshida et al, 1992] describe an in-service estimator that, like the SVR estimator, also reflects the multipath spread and level of CCI in a wireless channel.
- Pauluzzi et al in 2000 compares different SNR estimation techniques for AWGN channel [Pauluzzi et al, 2000]. Ramesh proposed SNR estimation in generalized fading channels [Ramesh et al, 2001]. Wiesel proposed non data aided (NDA) SNR estimation for PSK signals in AWGN [Wiesel et al, 2002]. Xu extend the work done by Wiesel and proposed NDA-SNR estimation for QAM signals [Xu et al, 2004]. NDA-SNR estimation is derived based on a statistical ratio of observables over a block of data. This estimator performs well with only large block of data.
- The entire estimator presented above derived the SNR estimates solely from the received signal at the output of the matched filter (MF). The perfect carrier and intersymbol interference (ISI) is assumed. Nidal proposed an SNR estimation technique for AWGN channel [Nidal et al, 2007], which can operate on data collected at the front-end of the receiver without any restriction on ISI.

2.5 SNR Estimation in OFDM Systems

All the estimators presented in the literature so far handle the issue considering single carrier transmission and presume ISI free reception of the signal. There is not that much work found for the SNR estimation in OFDM systems. OFDM is a multicarrier transmission scheme as described before in section 2.3 and one can received ISI free signal at the receiver using cyclic prefix (CP) of proper guard band length.

- Shousheng proposed SNR estimator for OFDM systems but the wireless channel used is flat fading [Shousheng et al, 1998]. Additionally no quantitative results are

given to connect the estimated and actual SNR values but only constellation diagram demonstrating the received vector scatter in the complex plain.

- Arslan & Reddy presented a method to estimate the noise power and SNR for OFDM systems [Arslan et al, 2003]. In this work noise power estimation, which takes into account the color and variation of noise statistics over OFDM sub-carriers, is considered. Instead of averaging the instantaneous noise samples estimates over all of the OFDM sub-carriers, dividing the total number of sub-carriers into several sub-groups and averaging the sub-carriers separately within each sub-group is proposed. It is observed that this estimator gives better results when the number of OFDM symbols is large. Due to averaging each sub-carrier separately complexity is increased.
- Xiaodong reported a subspace based noise variance and SNR estimation technique for OFDM systems which is based on eigenvector decomposition of the estimated channel correlation matrix [Xiaodong et al, 2005]. Subspace based estimator gives accurate measurements of the noise variance and SNR after an observation interval of about 20 OFDM symbols for various fading channels. Due to large number of OFDM symbols complexity of the system is high.
- Yucek and Arslan proposed MMSE noise power and SNR estimation for OFDM systems in which noise variance, and hence SNR, is calculated by using two cascaded filter in time and frequency directions whose coefficients are calculated using the statistics of noise/interference variance [Yucek et al, 2005]. Averaging is used over 20 OFDM symbols and considers estimation over subcarriers only.
- Doukas reported SNR estimation for low bit rate OFDM systems in AWGN channel [Doukas et al, 2006]. Doukas introduced two new methods to estimate SNR, SNV-SNR estimator and MMSE-SNR estimator in AWGN. Satisfactory SNR estimation can be achieved using these estimators with 1000 OFDM samples. Due

to large number of samples used to find the SNR estimate, complexity of the system increased.

- According to the best knowledge of author, all the SNR estimators for OFDM systems discussed above gives SNR estimate at the back-end of the receiver. Unlike all the SNR estimators for OFDM systems which perform SNR estimation at the back-end of the receiver, the SNR estimator proposed in this thesis gives SNR estimates at the front-end of the receiver. The proposed method based on one OFDM preamble used for timing synchronization.
- In contrast to other SNR estimators, the proposed technique operates on data collected at the front-end of the receiver, imposing no restriction on ISI. This will improve the SNR estimates in severe ISI channels and also help extending the implementation of SNR estimators towards systems that require SNR estimates at the input of the receiver. One such application is antenna diversity combining, where at least two antenna signal paths are communicably connected to a receiver. The combiner can use the SNR estimates obtained for each antenna signal to respectively weight each signal and thereby generate a combined output signal.

Reddy's SNR estimator and subspace based SNR estimator are selected to comparing them with our purposed SNR estimation technique and discussed in the next section.

2.6 Previous SNR Estimation Algorithms for OFDM Systems

The two back-end SNR estimators, the Reddy's estimator [Reddy et al, 2003], and subspace based estimator [Xiaodong et al, 2005], used later for comparison are discussed below.

2.6.1 Reddy's SNR Estimation

An OFDM based system model is used. Time domain samples of an OFDM symbol can be obtained from frequency domain symbols as

$$\begin{aligned}
x_m(n) &= IDFT \{X_m(k)\} \\
&= \sum_{k=0}^{N-1} X_m(k) e^{j2\pi nk/N} \quad 0 \leq n \leq N-1
\end{aligned} \tag{2.4}$$

where $X_m(k)$ is the symbol that is transmitted on k -th subcarrier of the m -th OFDM symbol, and N is the number of sub-carriers. After the addition of cyclic prefix and D/A conversion, the signal is passed through the mobile radio channel. Assuming a wide-sense stationary and uncorrelated scattering (WSSUS) channel, the channel $H(f, t)$ can be characterized for all time and all frequencies by the two-dimensional spaced-frequency, spaced-time correlation function

$$\phi(\Delta f, \Delta t) = E \{H^*(f, t) H(f + \Delta f, t + \Delta t)\} \tag{2.5}$$

In this technique, it is assumed that the channel remains constant over an OFDM symbol, but time-varying across OFDM symbols, which is a reasonable assumption for low and medium mobility.

At the receiver, the signal is received together with the noise. The noise power is assumed to be varying across OFDM sub-carriers as well as in time. After down converting, synchronization and removing the cyclic prefix, the simplified received baseband model of the samples can be formulated as

$$Y_m(n) = \sum_{l=0}^{L-1} x_m(n-l) h_m(l) + n_m(n) \tag{2.6}$$

where L is the number of channel taps, $n_m(n)$ is the noise sample which is combination of white Gaussian noise and colored interference source. The channel is assumed quasi static, therefore the time domain channel impulse response (CIR), $h_m(l)$, over an OFDM

symbol is given as time-invariant linear filter. After taking DFT of the OFDM symbols, the received samples in frequency domain can be shown as

$$\begin{aligned} Y_m(k) &= DFT \{y_m(n)\} = \sum_n y_m(n) e^{-j2\pi nk/N} \\ &= S_m(k) H_m(k) + N_m(k) \end{aligned} \quad (2.7)$$

where $H_m(k)$ and $N_m(k)$ are DFT of $h_m(l)$ and $n_m(l)$, respectively.

Note that, in this technique, the noise is not assumed to be white. In practical wireless communication systems, often the received signal is impaired by dominant interference sources. For example, in cellular systems, the dominant interference source can be a co-channel or an adjacent channel interferer.

2.6.1.1 Estimation of Noise Power and Signal Power

The noise power estimation is performed in frequency domain. The instantaneous noise estimate for each OFDM carrier is calculated by finding difference between noisy received sample and the best hypothesis of the noiseless received signal. The variance of the noise estimator is thus given by

$$\sigma_{N(m)}^2(k) = |Y_m(k) - \hat{X}_m(k) \cdot \hat{H}_m(k)|^2 \quad (2.8)$$

where $\hat{X}_m(k)$ is the best hypothesis of the received symbol and $\hat{H}_m(k)$ is the channel estimate for the k -th carrier of the m -th OFDM symbol. For noiseless channel estimates and for correctly detected symbols, the above equation will provide the absolute square of the exact instantaneous noise samples. However, the channel estimation error and incorrect decisions will bias the noise estimates. The problem with incorrect symbol estimates can be resolved by estimating noise samples using only known data (training symbols), or by finding the error after decoding and re-encoding the detected symbols.

Using the decoded information improves performance as the decoder corrects the incorrect decisions.

2.6.1.2 Signal Power Estimation

Signal power can be estimated from the knowledge of channel estimates. The channel estimates in frequency domain can be obtained using OFDM training symbols, or by transmitting regularly spaced pilot symbols in between the data symbols and by employing frequency domain interpolation. In this technique, transmission of training OFDM pilots is assumed. Using the knowledge of the training pilots, channel frequency response can be estimated as

$$\begin{aligned}\hat{H}_m(k) &= \frac{Y_m(k)}{S_m(k)} \\ \hat{H}_m(k) &= H_m(k) + w_m(k)\end{aligned}\tag{2.9}$$

where $Y_m(k)$ is the received pilot value and $w_m(k)$ is the channel estimation error. It is to be noted that interpolation is critical for the pilot based estimation because pilots are inserted at fixed places in an OFDM symbols. For example in IEEE 802.16d std. (WiMAX) eight pilots are used in 256 bit longer frame. Pilots are used in each frame unlike preamble which is used at the front of OFDM data symbols only once.

2.6.1.3 Noise Power Estimation in Sub-bands

In conventional noise power estimation algorithms, the absolute square of the instantaneous noise samples are averaged over all OFDM sub-carriers, providing an averaged noise power estimate. The conventional approaches assume the noise to be white and of Gaussian distribution and estimate a single noise variance (power) for all the OFDM sub-carriers. Therefore, these approaches do not provide any information about the variation of noise within the transmission bandwidth.

In this technique, noise power estimates for overall OFDM subcarriers as well as noise power estimates for noise varying within the transmission bandwidth (colored noise) are derived. For the noise power estimation of colored noise, the whole OFDM data is divided (i.e. the total number of sub-carriers) into sub-bands (i.e. to a set of subcarriers). If the number of sub-carriers in each sub-band is k , then the number of sub-bands will be N/k . Then, the absolute square of the instantaneous noise estimates in each sub-band are averaged,

$$\hat{\sigma}_{N_m}^2(j) = \frac{1}{k} \sum_{l=1}^k \hat{\sigma}_{N_m}^2(l) \quad 1 \leq j \leq N/k \quad (2.10)$$

where $\hat{\sigma}_{N_m}^2(j)$ is the estimated noise power in the j -th sub-band.

2.6.1.4 Signal Power Estimation in Each Sub-band

Using the knowledge of channel estimates, signal power over each sub-band is estimated as

$$\hat{P}_s(j) = \frac{1}{k} \sum_{l=1}^k |Y_m(l)|^2 \quad (2.11)$$

where $\hat{P}_s(j)$ is the estimated signal power in the j -th sub-band.

2.6.1.5 SNR Estimation in Each Sub-band

Having knowledge of noise power estimates and signal power estimates in each sub-band, the SNR is computed as

$$S\hat{N}R(j) = \frac{\hat{P}_s(j)}{\hat{\sigma}_{N_m}^2(j)} \quad (2.12)$$

where $S\hat{N}R(j)$ is the estimated value of actual SNR in the j -th sub-band.

The size of k depends on the color of the noise. If the noise is completely white, then it is desired that averaging be done across all the available OFDM sub-carriers, i.e. to have k equal to N . Therefore, increasing the number of samples over which averaging is done yields a lower mean-squared-error in the case of white noise, but the same does not apply for colored noise. The averaged noise estimates over each sub-band are further averaged across several OFDM symbols to get global SNR estimates (Over-all SNR values).

The methodology and parameters to perform simulation for this technique is discussed in the chapter 3 and results of this method are used for comparison with the proposed front-end SNR estimator are shown in chapter 4.

2.6.2 Subspace Based SNR Estimation

In this technique, an OFDM system that consists of N subcarriers among which N_t subcarriers at the central spectrum are used for transmission and the other subcarriers at both edges form the guard bands. A cyclic prefix is also added as guard interval for every OFDM symbol to avoid intersymbol interference caused by multipath fading channels. Each transmission subcarrier is modulated by a data symbol $X_{i,n}$, where i represent the OFDM symbol number and n represents the subcarrier number. It is assumed that the signal is transmitted over a multipath Rayleigh fading channel characterized by

$$h(t, \tau) = \sum_{l=1}^L h_l(t) \delta(t - \tau_l) \quad (2.13)$$

where $h_l(t)$ are the different path complex gains, τ_l are different path time delays, and L is the number of paths. $h_l(t)$ are wide-sense stationary (WSS) narrow-band complex Gaussian processes and the different path gains are uncorrelated with respect to each other where total channel energy is normalized to one. At the receiver side, with the assumption that the channel is quasi-stationary (in other words, the guard interval duration is longer than the channel maximum excess delay and the channel does not

change within one OFDM symbol duration), then the n^{th} subcarrier output during the i^{th} OFDM symbol can be represented by

$$Y_{i,n} = X_{i,n} \cdot H_{i,n} + N_{i,n} \quad (2.14)$$

where $N_{i,n}$ is a white Gaussian noise with variance, $H_{i,n}$ is the channel frequency response given by

$$H_{i,n} = \sum_{l=1}^L h_l(i, T_s) \cdot e^{-j2\pi \frac{n\tau_l}{NT}} \quad (2.15)$$

where $h_l(i, T_s)$ denotes the channel l -th path gain during the i -th OFDM symbol and T is the sampling time interval of the OFDM signal. In this technique the SNR during the i -th OFDM symbol is defined as the ratio of the channel power to noise power and may be written as

$$\hat{SNR} = \frac{\sum_{i=1}^N |h_l(iT_s)|^2}{\sigma_N^2} \quad (2.16)$$

2.6.2.1 Estimation of Subspace Based SNR

Consider an OFDM system that uses M pilot subcarriers to estimate channel. It is assumed that M ($M > L$) pilots are evenly inserted in OFDM symbols. Let P denote the set that contains the position indexes of M pilots sub-carriers. At the pilot position we have

$$X_{i,p(m)} = \gamma_m \quad m = 0, 1, \dots, M-1 \quad (2.17)$$

where $\{\gamma_m\}$ are the pilot subcarrier symbols with unit amplitude. Then the channel frequency response at the pilot subcarriers during the i -th OFDM symbol can be expressed as

$$\begin{aligned} \hat{H}_{i,p(m)} &= \frac{Y_{i,p(m)}}{\gamma_m} \\ &= \sum_{l=1}^L h_l(i.T_s).e^{-j2\pi \frac{p(m)\tau_l}{NT}} + \frac{N_{i,p(m)}}{\gamma_m} \end{aligned} \quad (2.18)$$

Eq.2.18 can also be written in matrix as

$$\hat{H}_{i,p} = W_p h_i + N_p \quad (2.19)$$

where $\hat{H}_{i,p}$ is $M \times 1$ column vector and N_p is $M \times 1$ noise column vector, W_p is the $M \times L$ matrix with m -th Row given by

$$\left[e^{-j2\pi \frac{p(m)\tau_1}{NT}} \dots \dots \dots e^{-j2\pi \frac{p(m)\tau_L}{NT}} \right] \quad (2.20)$$

here h_i is $L \times 1$ column vector representing the path complex gains. It should be noted that in mobile communications the multipath time delays are slowly varying in time. In contrast, the amplitude and relative phase of each path are relatively fast varying [Yang et al, 2001]. So we can regard W_p is unchanged during the K continuous OFDM symbols and h_i varies from symbol to symbol.

Because the noise vector N_p is zero mean and independent of the h_i , it follows that the correlation matrix of $\hat{H}_{i,p}$, is given by

$$R = \Psi + \sigma_N^2 \cdot I \quad (2.21)$$

Where I is the identity matrix and

$$\Psi = W_p E(h_l \cdot h_l^H) W_p^H \quad (2.22)$$

where

W_p = FFT matrix of pilot symbols

h_l = channel impulse response for l -th multipath

$(\cdot)^H$ = Hermitian conjugate matrix transpose

P = pilot symbol index $p \in \{1, 2, \dots, M\}$

M = number of pilot symbols

E = expectation operator

Because the matrix W_p is of full column rank and the correlation matrix of h_l is nonsingular, it follows that the rank of Ψ is L , or equivalently, the $M - L$ smallest eigenvalues of Ψ are equal to zero. Denoting the eigenvalues of R by $\lambda_1 \geq \lambda_2 \dots \geq \lambda_m$ it follows, therefore, that the smallest $M - L$ eigenvalues of R are all equal to σ_N^2 , i.e.,

$$\lambda_{L+1} = \lambda_{L+2} \dots \lambda_m = \sigma_N^2 \quad (2.23)$$

And we also have

$$\text{Trace}(R) = M(\sigma_S^2 + \sigma_N^2) = \sum_{i=1}^M \lambda_i \quad (2.24)$$

Where $\sigma_S^2 = E(h_l \cdot h_l^H)$ denotes the channel power. This implies that the observation space can be partitioned into a signal subspace spanned by the columns of W_p and a noise subspace. Now if we get the estimate of the channel correlation matrix R and the

multipath number L (also is the dimension of the signal subspace), the noise variance and then the SNR can be derived.

Since we want to track time variations of the SNR, we form a moving average of the correlation matrix from the K most recent observation vectors. Let m denote the m^{th} OFDM symbol, then we have

$$\hat{R}(m) = \frac{1}{K} \sum_{i=m-K+1}^m H_{i,p} \cdot H_{i,p}^H \quad (2.25)$$

The estimate of L can be decided by the well-known Minimum Descriptive Length (MDL) criterion presented by [Wax et al, 1985] as,

$$MDL(k) = -K(M-k) \log \left(\frac{\prod_{i=k+1}^M \hat{\lambda}_i^{1/(M-K)}}{\frac{1}{M-K} \sum_{i=k+1}^M \hat{\lambda}_i} \right) + \frac{1}{2} k(2M-k) \log(K) \quad (2.26)$$

The number of multipath is estimated as

$$\hat{L} = \arg \min_k MDL(k) \quad k \in \{0, 1, 2, \dots, M-1\} \quad (2.27)$$

From equations (2.23, 2.24, 2.26, 2.27), we can obtain subspace based SNR estimator.

2.6.2.2 Subspace based SNR estimator

1. Make an Eigen vector decomposition of the correlation matrix \hat{R} .

2. Estimate the current dimensions of the signal subspace \hat{L} using equations (3.26 & 3.27).
3. According to eq.3.23 and eq.3.24 , estimate the noise power as

$$\hat{\sigma}_N^2 = \frac{1}{M - \hat{L}} \sum_{i=\hat{L}+1}^M \hat{\lambda}_i \quad (2.28)$$

And channel power as

$$\hat{\sigma}_s^2 = \frac{1}{M} \left(\sum_{i=1}^{\hat{L}} \hat{\lambda}_i - \hat{L} \cdot \hat{\sigma}_N^2 \right) \quad (2.29)$$

4. The estimate of the SNR is then obtained as

$$S\hat{N}R = \frac{\hat{\sigma}_s^2}{\hat{\sigma}_N^2} \quad (2.30)$$

where $S\hat{N}R$ is the estimated value of actual SNR.

The methodology and parameters to perform simulation for this technique is discussed in the chapter 4 and results of this method are used for comparison with the proposed front-end SNR estimator are shown in chapter 5.

2.7 Applications Which May Benefit From Knowledge of the SNR

In many applications, the total received power is estimated for simplicity rather than the SNR. Goldsmith [Goldsmith et al, 1994] discusses power measurement for time-varying cellular channels, and point out that real-time measurement of the received power is required for operations such as power control, handoff, and dynamic channel allocation. Examples of applications that use total power or received signal strength estimates are

described by Holtzman [J. M. Holtzman1992], Vijayan [R. Vijayan et al,1992], Whitehead [J. F. Whitehead et al,1993], Zhang [N. Zhang et al,1994]. In fact, the use of SNR estimates can improve the performances of the signal-strength-based algorithms used in these applications. Some references are listed below which describe applications that ideally require knowledge of the SNR.

2.7.1 Resource Management Algorithms

Measurement of the SNR is of great interest today as wireless service providers are finding that co-channel interference (CCI) is the greatest factor limiting the extent to which cell sizes can be reduced in an effort to increase frequency reuse and system capacity. For this reason, methods to measure the SNR (where the impairment, in this case, is mainly CCI are attracting much attention for use in resource management algorithms such as those used for handoff, dynamic channel allocation, and power control.

2.7.2 Power Control

Zander [J. Zander,1992] indicates that power control is important "to adjust the power of each transmitter for a given channel allocation such that the interference levels at the receiver locations are minimized". He points out that, in practice, power control algorithms typically keep the total received power at a constant level; however, he adds that keeping the signal-to-interference power ratio constant instead could improve system capacity. This view is supported by Jalali [Jalali et al, 1994]. Zander admits that a practical implementation of the power control algorithm would be difficult since the path gains of the desired signal and interferers are, in general, unknown. A means to estimate the SNR would facilitate the practical implementation of this power control algorithm.

2.7.3 Diversity Combining

The classic pre-detection maximal-ratio combiner is described by Brennan [D.G.Brennan,1959], Lee [W.C.Lee, 1982] and Jakes [W.C.Jakes,1974]. These combiners form the weighted sum of two or more diversity branches where the weights are proportional to the amplitude of the signal, and inversely proportional to the noise variance. The weights for this diversity scheme are often implemented using the signal-plus-noise envelope as opposed to the signal amplitude to-noise variance ratio described by Adachi [F.Adachi et al.,1967]. If an algorithm were available to estimate the signal and noise powers separately, the desired weightings for each of the branches of the maximal-ratio combiner could be formed trivially as the ratio of the square root of the signal power to the noise power. If the SNR is determined as an inseparable parameter, $\rho = S/N$, then the signal power and noise power could be computed by also estimating the total received power, $P = S + N$, so that simultaneous equations for ' ρ ' and P may be solved for S and N to yield $N = P / (1 + \rho)$ and $S = P - N$. The branch weights are then formed trivially as $\sqrt{S/N}$.

Adachi [F.Adachi, 1993] presents an optimal post detection diversity combiner that weights the differentially-detected symbols of each of the branches based on a formula which depends explicitly on both the SNR and the signal-to-interference ratio. The implementation of this formula actually requires two separate estimators-one to measure the SNR, the other to measure the signal-to-interference ratio.

A postdetection selection diversity combiner is described by Hladik [Hladik et al, 1992] where the SNR of each diversity branch is measured on a symbol-by- symbol basis. Each symbol interval, the differentially-detected symbol corresponding to the branch with the largest instantaneous SNR is the one that is presented to the decision device. The specific SNR estimator is not given there but is simply described as an approximation to the maximum-likelihood (ML) estimate of the SNR.

2.7.4 Equalization

Balaban [Balaban et al, 1991] describe an equalizer for frequency-selective fading channels. The tap update algorithm of the equalizer requires both an estimate of the channel impulse response and an estimate of the SNR, thus illustrating another application requiring some means to estimate the SNR.

2.7.5 Synchronization

A maximum likelihood estimator of the bit timing is presented by Wintz [Wintz et al, 1992] which is a function of the noise variance. For additive white Gaussian noise (AWGN), the noise variance drops from the estimator expression as shown by equation (11) of Wintz work. However, in time-varying channels, the noise variance cannot be assumed to be constant so it, or the SNR, must be estimated for optimal performance. Though a noise power estimator is required here, an SNR estimator could be used together with a total received power estimator to derive the noise power, as described in Section 2.5.3. Chennakeshu [Chennakeshu et al, 1993] present a method to achieve timing and frequency synchronization by maximizing the SIR with respect to the timing and frequency offset.

2.7.6 Adaptive Arrays

Adaptive arrays are used in wireless communications systems to cancel interference and mitigate fading effects by appropriately weighting and combining the output of two or more antennas. The optimal weight equation is given by Winters [Winters et al, 1993] or, equivalently, by Winters [Winters et al, 1984], and is found to be a function of the noise variance. Again, using a technique such as that described in Section 2.5.3 an estimate of the noise power may be found from estimates of the SNR and the total received signal power.

2.7.7 Viterbi Equalization and Decoding

The path metric used in Viterbi equalization and decoding is shown by Hagenauer [Hagenauer et al, 1989] to depend on what the authors call the 'instantaneous SNR, $E_s(k)/N_o$, where E_s is the energy per symbol, N_o is the noise power spectral density, and k is the time index. The time dependence arises as a result of the time-varying nature of the multipath channel assumed in this equalization and decoding.

2.8 Summary

In this chapter, background of the for FBWA-OFDM systems is discussed. There are two main impairments in wireless channels that are ISI and multipath fading. OFDM is highly effective in mitigating these channel impairments. The principles of OFDM technology are discussed and it is shown that how guard interval makes the OFDM system ISI free. Following this, literature review of SNR estimation and formulation of SNR estimation algorithms used later for comparing them with proposed methods are discussed and applications which may be benefited from SNR are discussed. It is shown that in order to fully harness the power of OFDM technology, accurate SNR estimates must be obtained at the receiver. This establishes the importance of SNR estimation in an FBWA-OFDM system.

3.1 Introduction

In the last chapter we discussed the background of OFDM systems and SNR estimation. The completion of the background study now sets the stage for the development of an improved SNR estimation technique. Formulation of proposed SNR estimation technique will be discussed in this chapter. In order to validate the proposed technique, schemes of Reddy [Reddy, S et al, 2003] and subspace [Xiaodong et al, 2005] are used. The formulation of these techniques is also described before the formulation of our technique. Methodologies of these estimation techniques will be discussed in the next chapter.

SNR estimation indicates the reliability of the link between the transmitter and receiver. In adaptive system, SNR estimation is commonly used for measuring the quality of the channel and accordingly changing the system parameters. For example, if the measured channel quality is low, the transmitter may add some redundancy or complexity to the information bits (more powerful coding), or reduce the modulation level (better Euclidean distance), or increase the spreading rate (longer spreading code) for lower data rate transmission. Therefore, instead of implementing fixed information rate for all levels of channel quality, variable rates of information transfer can be used to maximize system resource utilization with high quality of user experience.

Many SNR estimation algorithms have been suggested and implemented in the last ten years in OFDM systems at the back-end of receiver using the system pilot symbols. The

essential requirement for an SNR estimator in OFDM system is of low computational load. This is in order to minimize hardware complexity as well as the computational time. Most of these techniques derive the symbol SNR estimates solely from the received signal at the output of the matched filter (MF). The estimators assume perfect carrier and symbol synchronization while at the same time implicitly assuming intersymbol interference (ISI)-free output of the MF (the decision variable). However, in practice, multipath wireless communication gives rise to much intersymbol interference, especially in indoor and urban areas. In these ISI dominated scenarios, SNR estimators that do not presume ISI-free reception are highly desirable.

In contrast to other SNR estimators, the proposed technique operates on data collected at the front-end of the receiver, imposing no restriction on ISI. This will improve the SNR estimates in severe ISI channels and also help extending the implementation of SNR estimators towards systems that require SNR estimates at the input of the receiver. One such application is antenna diversity combining, where at least two antenna signal paths are communicably connected to a receiver. The combiner can use the SNR estimates obtained for each antenna signal to respectively weight each signal and thereby generate a combined output signal.

In many SNR estimation techniques, noise is assumed to be uncorrelated or white. But, in wireless communication systems, where noise is mainly caused by a strong interferer, noise is colored in nature.

In this chapter, formulation and methodology of Proposed SNR estimation technique are presented. A front-end noise power and SNR estimator for the white noise as well as for colored noise in OFDM system is proposed. The algorithm is based on the two identical halves property of time synchronization preamble used in some OFDM systems. The proposed technique is divided in to two parts. In the first part, SNR estimation technique for AWGN channel and multipath channels is considered. In the second part, the proposed estimator is taking into consideration the different noise power levels over the OFDM sub-carriers. The OFDM band is divided into several sub-bands using wavelet

packet and noise in each sub-band is considered white. The second-order statistics of the transmitted OFDM preamble are calculated in each sub-band and the power noise is estimated. Therefore, the proposed approach estimates both local (within smaller sets of subcarriers) and global (over all sub-carriers) SNR values. The short term local estimates calculate the noise power variation across OFDM sub-carriers. When the noise is white, the proposed algorithm works as well as the conventional noise power estimation schemes, showing the generality of the proposed method.

The remainder of the chapter is organized as follows. Section 3.2 describes the Formulation of our proposed SNR estimation technique. In Section 3.3 we discuss the formulation of our proposed technique.

3.2 Formulation of Proposed Front-End SNR estimation Technique

In this section, we presented our proposed front-end SNR estimation technique. This is a data-aided technique based on the preamble appended to data frames. According to the best knowledge of the author, there is no estimation technique that estimates SNR at front-end of the receiver for OFDM systems. The motivation in using a preamble for SNR estimation is that a preamble is always present in most OFDM systems, and, therefore, using it will not cause any additional burden. Preamble is used both for channel estimation and timing and frequency synchronization. A good preamble must sound the channel very efficiently. It will also have low peak-to-average power ratio (PAPR). Also it will have features that are best utilized for synchronization. For example popular Schmidl & Cox [Schmidl et al, 1997] technique for synchronization loads a PN-sequence on alternate subcarriers. This generates a preamble that has two identical halves, whose correlation gives an identification of the start of the frame. This also implies that channel will have to be interpolated at subcarriers where PN-sequence was not loaded.

Next subsection discusses the work that has been done in the literature on arriving at a suitable preamble.

3.2.1 Selection of a Preamble

For the proposed technique we aim to select a preamble which is already employed in OFDM systems for timing & frequency synchronization and channel estimation. Given below is a brief historical development of the work done in developing synchronization schemes and a suitable preamble for it.

There have been several papers on the subject of synchronization for OFDM in recent years. Moose gives the maximum likelihood estimator for the carrier frequency offset which is calculated in the frequency domain after taking the FFT [Moose et al, 1994]. He assumes that the symbol timing is known, so he just has to find the carrier frequency offset. The limit of the acquisition range for the carrier frequency offset is the subcarrier spacing. He also describes how to increase this range by using shorter training symbols to find the carrier frequency offset. For example shortening the training symbols by a factor of two would double the range of carrier frequency acquisition. This approach will work to a point, but the estimates get worse as the symbols get shorter because there are fewer samples over which to average, and the training symbols need to be kept longer than the guard interval so that the channel impulse response does not cause distortion when estimating the frequency offset.

Nogami present algorithms to find the carrier frequency offset and sampling rate offset [Nogami et al, 1995]. They use a null symbol where nothing is transmitted for one symbol period so that the drop in received power can be detected to find the beginning of the frame. The carrier frequency offset is found in the frequency domain after applying a Hanning window and taking the FFT. The null symbol is also used by Bot [Bot et al,1994]. This extra overhead of using a null symbol is avoided by using the technique described in this work. If instead of a continuous transmission mode, a burst mode is

used, it would be difficult to use a null symbol since there would be no difference between the null symbol and the idle period between bursts.

Beek describes a method of using a correlation with the cyclic prefix to find the symbol timing [Beek et al, 1995]. If this method were used to find the symbol timing, while using one of the previous methods to find the carrier frequency offset, there would still be a problem of finding the start of the frame to know where the training symbols are located.

Classen introduces a method which jointly finds both the symbol timing and carrier frequency offset [Classen et al, 1995]. However, it is very computationally complex because it uses a trial and error method where the carrier frequency is incremented in small steps over the entire acquisition range until the correct carrier frequency is found. It is impractical to do the exhaustive search and go through a large amount of computation at each possible carrier frequency offset.

Schmidl introduces some modifications of Classen's method which both greatly simplify the computation necessary for synchronization and extend the range for the acquisition of carrier frequency offset [Schmidl et al, 1997]. The method in this paper avoids the extra overhead of using a null symbol, while allowing a large acquisition range for the carrier frequency offset. By using one unique symbol which has a repetition within half a symbol period, this method can be used for bursts of data to find whether a burst is present and to find the start of the burst. Acquisition is achieved in two separate steps through the use of a two-symbol training sequence, which will usually be placed at the start of the frame. First the symbol/frame timing is found by searching for a symbol in which the first half is identical to the second half in the time domain. Then the carrier frequency offset is partially corrected, and a correlation with a second symbol is performed to find the carrier frequency offset.

After studying we select an OFDM synchronization preamble proposed by Schmidl [Schmidl et al, 1997]. As will be shown later, the preamble has two identical halves property. In this preamble, the two halves of the training symbol in time obtained by transmitting a pseudonoise (PN) sequence on the even frequencies, while zeros are used on the odd frequencies. This means that at each even frequency one of the points of a QPSK constellation is transmitted. In order to maintain approximately constant signal energy for each symbol the frequency components of this training symbol are multiplied by $\sqrt{2}$ at the transmitter. Transmitted data will not be mistaken as the start of the frame since any actual data must contain odd frequencies. Note that an equivalent method of generating this training symbol is to use an IFFT of half the normal size to generate the time domain samples. The repetition is not generated using the IFFT, so instead of just using the even frequencies, a PN sequence would be transmitted on all of the subcarriers to generate the time domain samples which are half a symbol in duration. These time-domain samples are repeated (and properly scaled) to form the first training symbol. The second training symbol contains a PN sequence on the odd frequencies to measure these sub-channels, and another PN sequence on the even frequencies to help determine frequency offset.

The selection of a particular PN sequence should not have much effect on the performance of the synchronization algorithms. Instead the PN sequence can be chosen on the basis of being easy to implement or having a low peak-to-average power ratio so that there is little distortion in the transmitter amplifier.

3.2.2 Proposed Front-End SNR Estimator

The second stage after selecting synchronization preamble - the preamble which has two identical halves property, is to develop a preamble based front-end SNR estimation technique. The selected preamble has low PAPR and can sound the channels well and can be power boosted more with the same system power requirements. This translates into higher signal to noise ratio (SNR). The proposed technique is divided in to two parts. The first part is the front-end SNR estimation technique for AWGN channel and multipath channels (Rayleigh, Rician, SUI channels and indoor channel models) using white noise scenario. The second part is the extension of first part to noise power estimation of colored noise using wavelet-packet based analysis of the noise.

3.2.2.1 First Part: Front-End Noise Power and SNR Estimation Technique for AWGN Channel and Wireless Multipath Channels

As discussed earlier, the preamble used for timing synchronization is derived from alternate loading of subcarriers with PN-sequence modulated constellation as follows:

$$P_{even}(k) = \begin{cases} \sqrt{2} \cdot P(m) & k=2m \quad m=1,2,3,\dots,N/2 \\ 0 & otherwise \end{cases} \quad (3.1)$$

Here, $P(m)$ is the PN sequence loaded onto even subcarriers taken from IEEE802.16d. The factor $\sqrt{2}$ is related to the 3 dB boost and k shows the sub-carriers index.

In actual practice, an OFDM signal is provided with a guard band on either side of its spectrum. Accordingly the data are not loaded on the sides. For example, for a typical IEEE802.16d signal of length 256 subcarriers wide, 28 carriers on either side are null carriers as shown in Fig.3.1.

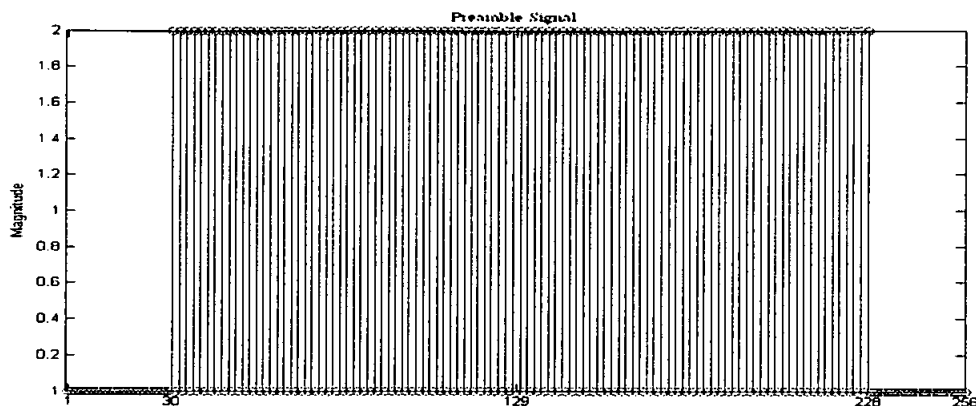


Fig.3.1 Preamble signal loaded on even subcarriers using PN sequence

Therefore for our purposes, eq.3.1 is rewritten as

$$P_{\text{even}}(k) = \begin{cases} \sqrt{2} \cdot P(m) & k=2m & m=15,16,17,\dots,(N/2-14) \\ 0 & & m=1,2,3,\dots,14 \\ 0 & & m=N/2-13, N/2-12, \dots, N/2 \end{cases} \quad (3.2)$$

The corresponding time-domain preamble $P(n)$, is obtained by Inverse discrete Fourier transform (IDFT) of $P_{\text{even}}(k)$ as follows.

$$\begin{aligned} p(n) &= \text{IDFT} \{P_{\text{even}}(k)\} \\ &= \sum_{k=0}^{N-1} P_{\text{even}}(k) \cdot e^{j2\pi nk/N} \quad 0 \leq n \leq N-1 \end{aligned} \quad (3.3)$$

Since $P_{\text{even}}(k)$ has values only at even subcarriers, this can be seen from the properties of

$e^{j2\pi nm/N/2}$ (also written as $W_{N/2}^{-nm}$, where W_N is the N -th root of unity).

For $k = 2m$,

$$e^{j2\pi n2m/N} = e^{j2\pi nm/N/2} \quad (3.4)$$

So, for $n = n + N/2$,

$$\begin{aligned} e^{j2\pi(n+N/2)m/N} &= e^{j2\pi nm/N} \cdot e^{j2\pi m \cdot N/2/N} \\ &= e^{j2\pi nm/N} \end{aligned} \quad (3.5)$$

In other words

$$p(n) = p(n + N/2) \quad (3.6)$$

To avoid intersymbol interference (ISI) caused by multipath fading channels, cyclic prefix (CP) of length l_{CP} is added so that the total length of OFDM data becomes $N_{total} = N + l_{CP}$. It is assumed that the signal is transmitted over Rayleigh multipath fading channel characterized by

$$h(t, \tau) = \sum_{l=1}^L h_l(t) \delta(t - \tau_l) \quad (3.7)$$

where $h_l(t)$ are the different path complex gains, τ_l are different path time delays, and L is the number of paths. $h_l(t)$ are wide-sense stationary (WSS) narrow-band complex Gaussian processes. At the receiver side, with the assumption that the guard interval duration is longer than the channel maximum excess delay, the received OFDM data can be represented by

$$y(n) = x(n) + n(n) \quad (3.8)$$

where

$$x(n) = s(n) * h(n)$$

* = Linear convolution

$s(n) = IDFT \{S(K)\}$, $S(K)$ are the constellation symbols, and $S(n)$ is the transmitted signal in time-domain.

$n(n)$ = white Gaussian noise with variance σ^2 .

$h(n)$ = discretized version of impulse response of the system.

a. Autocorrelation based Front-End SNR Estimator

The proposed estimator is deployed right at the front-end of the receiver. It makes use of two identical halves property of time synchronization preamble padded with cyclic prefix and relies on the autocorrelation of the same. From eq.3.9, it can be shown that the autocorrelation function of the received signal, $R_{yy}(m)$, has the following relationship to the autocorrelation of the data signal, $R_{xx}(m)$ and the noise, $R_{nn}(m)$:

$$R_{yy}(m) = R_{xx}(m) + R_{nn}(m) \quad (3.9)$$

where

$$R_{yy}(m) = \sum_n y(n) y^*(n+m)$$

$$R_{xx}(m) = \sum_n x(n) x^*(n+m)$$

$$R_{nn}(m) = \sum_n n(n) n^*(n+m)$$

The noise in the channel is modeled as additive white Gaussian noise and its autocorrelation function only has a value at a delay of $m = 0$, with magnitude given by the noise variance (σ^2), expressed as

$$R_{nn}(m) = \sigma^2 \delta(m) \quad (3.10)$$

where $\delta(m)$ is the discrete delta sequence.

b. Signal Power and Noise Power Estimation

We undertake the study of OFDM signal statistics, and observe, as shown in Fig.3.2, that its power spectrum is nearly white. Hence its autocorrelation is generally given by:

$$R_{SS}(m) = P_o \delta(m) \quad (3.11)$$

where P_o is signal power.

However, two identical halves of the preamble OFDM symbol correlate separately and also together at $-N/2$ lag, 0 lag and at $N/2$ lag, giving rise to $R_{SS}(m)$ as:

$$R_{SS}(m) = P_o \left\{ \frac{1}{2} \delta\left(m - \frac{N}{2}\right) + \delta(m) + \frac{1}{2} \delta\left(m + \frac{N}{2}\right) \right\} \quad (3.12)$$

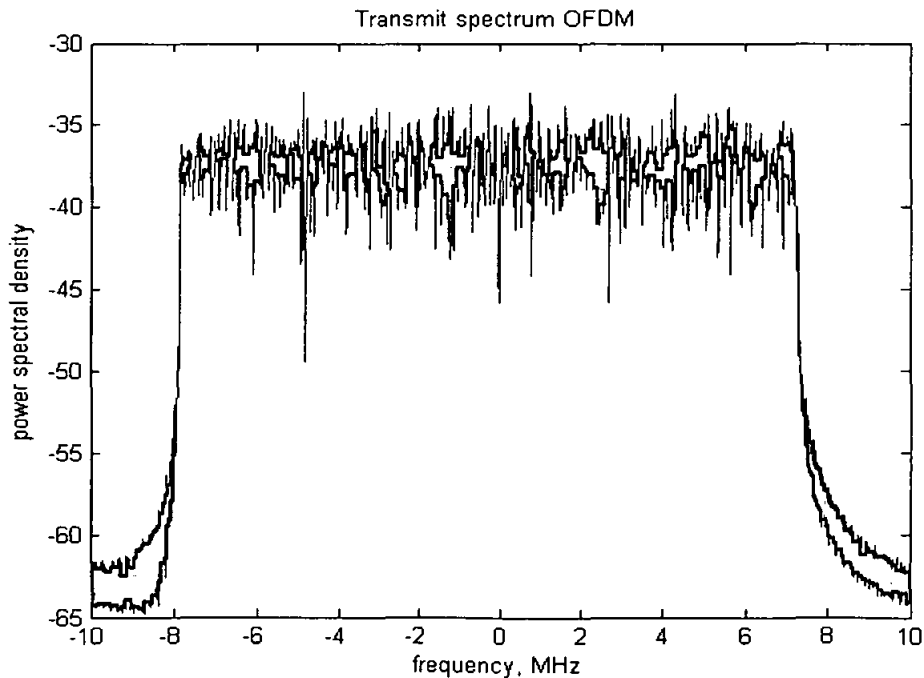


Fig.3.2 Power spectrum of an OFDM signal

As the transmitted signal passes through a channel, $h(n)$ the autocorrelation $R_{xx}(n)$ can be derived as follows:

$$\begin{aligned}
 R_{xx}(m) &= \sum_n s(n) s^*(n+m) \\
 &= \sum_n \left[\sum_i h(i) p(n-i) \right] \left[\sum_j h^*(j) p^*(n+m-j) \right] \\
 &= \sum_i \sum_j h(i) h^*(j) \left[\sum_n p(n-i) p^*(n+m-j) \right] \\
 &= \sum_i \sum_j h(i) h^*(j) \left[\sum_n p(n-i) p^*(n-i+m-j+i) \right] \\
 &= \sum_i \sum_j h(i) h^*(j) \cdot P_o \delta(m-j+i) + \sum_i \sum_j h(i) h^*(j) \cdot \frac{P_o}{2} \delta(m-j+i-N/2) \\
 &\quad + \sum_i \sum_j h(i) h^*(j) \cdot \frac{P_o}{2} \delta(m-j+i+N/2) \\
 &= P_o \sum_i h(i) \left[\sum_j h^*(j) \delta(m-j+i) \right] + \frac{P_o}{2} \sum_i h(i) \left[\sum_j h^*(j) \delta(m-j+i-N/2) \right] \\
 &\quad + \frac{P_o}{2} \sum_i h(i) \left[\sum_j h^*(j) \delta(m-j+i+N/2) \right] \\
 &= P_o \sum_i h(i) h^*(m+i) + \frac{P_o}{2} \sum_i h(i) h^*(m+i-N/2) + \frac{P_o}{2} \sum_i h(i) h^*(m+i+N/2) \tag{3.13}
 \end{aligned}$$

When $m = 0$,

$$R_{xx}(0) = P_o \sum_i |h(i)|^2 + \frac{P_o}{2} \sum_i |h(i)h(i-N/2)| + \frac{P_o}{2} \sum_i |h(i)h(i+N/2)| \tag{3.14}$$

However

$$\sum_i |h(i)h(i - N/2)| = 0$$

$$\sum_i |h(i)h(i + N/2)| = 0$$

As described in Fig.3.3.

So,

$$R_{xx}(0) = P_o \sum_i |h(i)|^2 \tag{3.15}$$

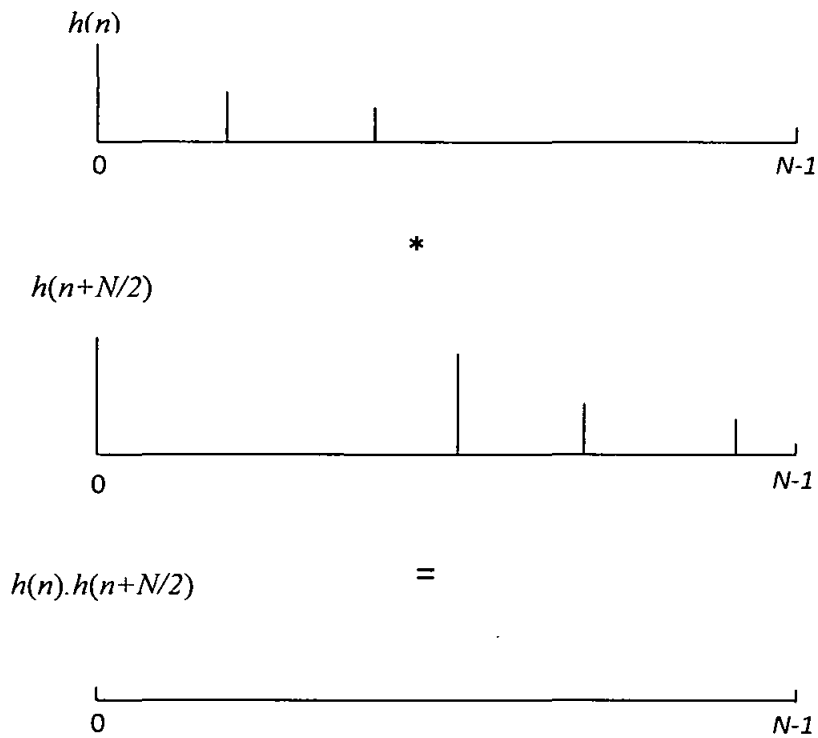


Fig.3.3. multiplication of $h(n)$ and $h(n+N/2)$

Here $P_o \sum_i |h(i)|^2$ is the received power attenuated by $\sum_i |h(i)|^2$ factor.

When $m = N / 2$,

$$R_{xx}\left(\frac{N}{2}\right) = P_o \sum_i |h(i)h(i + N/2)| + \frac{P_o}{2} \sum_i |h(i)|^2 + \frac{P_o}{2} \sum_i |h(i)h(i + N)| \quad (3.16)$$

However, similarly from Fig.3.3.

$$\sum_i |h(i)h(i + N/2)| = 0$$

$$\sum_i |h(i)h(i + N)| = 0$$

So

$$R_{xx}\left(\frac{N}{2}\right) = \frac{P_o}{2} \sum_i |h(i)|^2 \quad (3.17)$$

When $m = -N / 2$,

$$R_{xx}\left(\frac{-N}{2}\right) = P_o \sum_i \left| \sum_i |h(i)h(i - N/2)| \right| + \frac{P_o}{2} \sum_i |h(i)h(i - N)| + \frac{P_o}{2} \sum_i |h(i)|^2 \quad (3.18)$$

However, similarly from Fig.3.3.

$$\sum_i |h(i)h(i - N/2)| = 0$$

$$\sum_i |h(i)h(i - N)| = 0$$

So,

$$R_{xx}\left(\frac{-N}{2}\right) = \frac{P_o}{2} \sum_i |h(i)|^2 \quad (3.19)$$

From the above equations, it is clear that the received signal power ($\frac{P_o}{2} \sum_i |h(i)|^2$) can be estimated from $R_{xx}(\frac{N}{2})$ and $R_{xx}(-\frac{N}{2})$ peak.

Hence, at zero lag (shown at 'L' in Fig.3.4) the autocorrelation $R_{xx}(0)$, contains both the signal power estimate and noise power estimate indistinguishable from each other as shown in eq.3.9 and eq.3.10 before. However, because of the identical halves nature of the preamble, the received signal power can be estimated from auto correlation peak at $N/2$ or at $-N/2$ as shown in Fig.3.3a. In Fig.3.3, $R_{xx}(m)$ has been sketched for $N=256$.

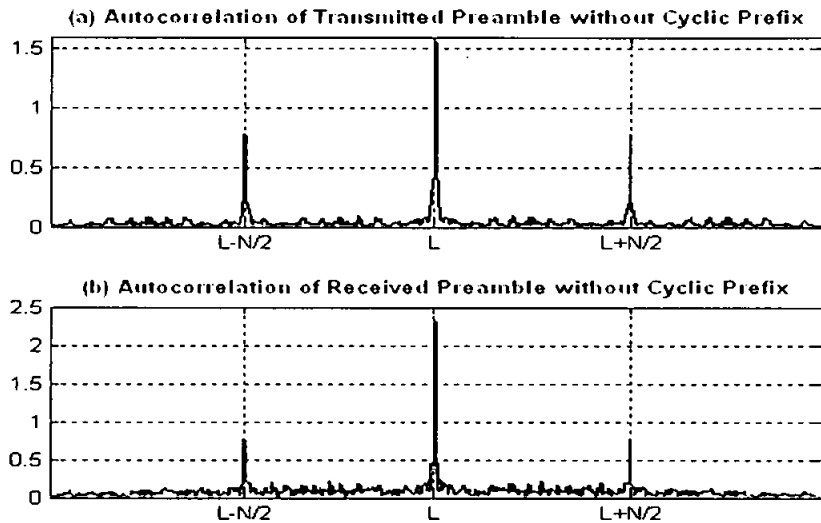


Fig.3.4 (a): Transmitted Preamble (b): Received Preamble after coming through a channel
(Plots show two identical halves with no cyclic prefix).

It is clear that the autocorrelation values apart from the zero-offset are unaffected by the channel effects, so one can find the signal power from the $N/2$ or $-N/2$ lag autocorrelation value.

c. Signal Power Estimation

In Fig.3.4, the auto correlation for preamble has been shown without cyclic prefix. However, all OFDM symbols, including preamble, have cyclic prefix. For example, in WiMAX systems, a cyclic prefix 64 sample long is introduced where the data is 256 points long. In such cases, the autocorrelation also has peaks where cyclic prefix matches with sections. This is shown in Fig.3.5 where the autocorrelation of the clean OFDM signal is shown in Fig.3.5 (a) and that of the received signal with noise at SNR=7dB in Fig.3.5 (b).

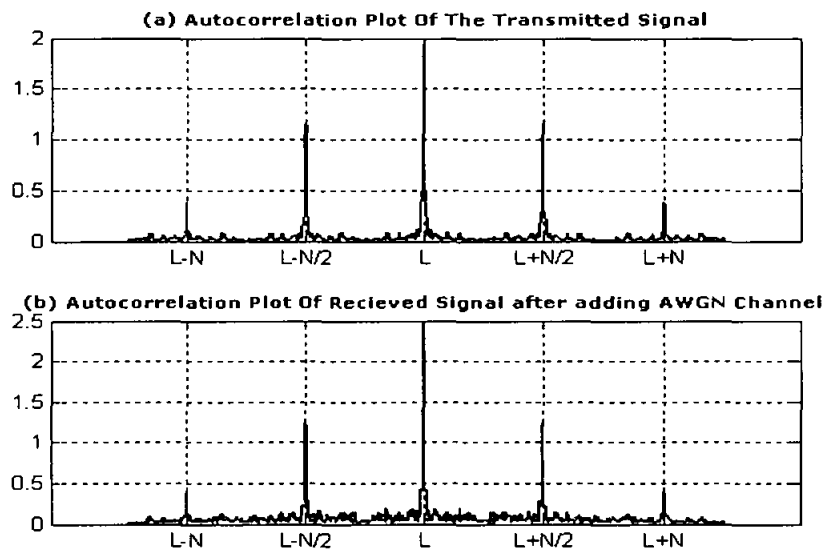


Fig 3.5 (a): Autocorrelation plot of transmitted signal (b): Autocorrelation plot of received signal.

The explanation for the correlation peaks of Fig.3.5 is pictorially given in Fig.3.6.

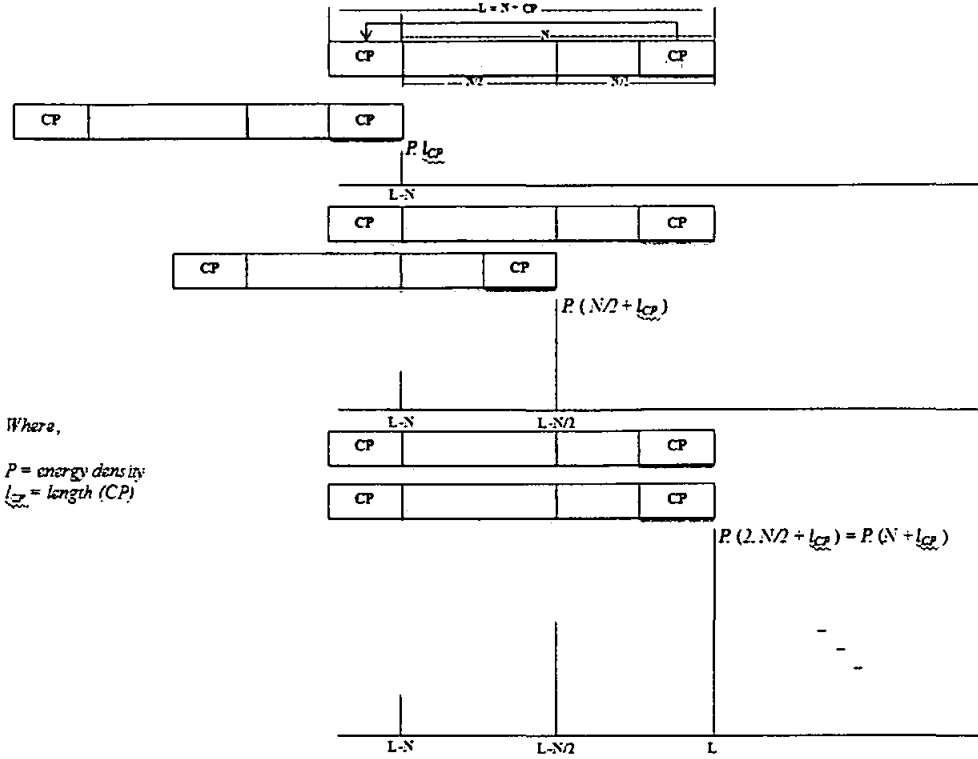


Fig.3.6: Autocorrelation of received preamble signal in time domain

If the energy density of the preamble is ‘ ρ ’ per unit length, the peak heights are equal to the energy of the matched portion of the signal. As it can be seen from the correlation shown in Fig.3.6 that, the first peak rises at $L-N$ when CP matches with itself with energy of $\rho \cdot l_{CP}$. The second peak rises at $L-N/2$ when one half of preamble plus CP matches with itself with energy of $\rho \cdot (N/2+l_{CP})$ and main peak at zero-lag (shown at ‘ L ’ in Fig.3.6) rises when full preamble matcheing with itself with energy of $\rho \cdot (N+l_{CP})$. Taking into consideration the autocorrelation values for ‘ $L-N/2$ ’, ‘ $L-N$ ’, ‘ $L+N/2$ ’, ‘ $L+N$ ’, signal power is given as:

$$\hat{P}_o = 2R_{yy}(L - N / 2) - R_{yy}(L - N) \tag{3.20}$$

Or

$$\hat{P}_o = 2R_{yy}(L + N / 2) - R_{yy}(L + N) \tag{3.21}$$

where \hat{P}_o estimated signal power.

d. Noise Power Estimation

Having obtained the power of signal, noise power, P_N given by noise variance $\hat{\sigma}_N^2$, can be calculated as

$$\text{Noise Power} = \hat{\sigma}_N^2 = R_{yy}(L) - \hat{P}_o \tag{3.22}$$

where $R_{yy}(L)$ is value at zero-lag.

e. SNR Estimation

Finally we can find the SNR estimates using eq.3.20 or eq.3.21 and eq.3.22.

$$S\hat{N}R = \frac{\hat{P}_o}{\hat{\sigma}_N^2} \tag{3.23}$$

where $S\hat{N}R$ is the estimated value for SNR.

Ideally, signal power and noise power are calculated without CP for the original data of length N . For example in WiMAX systems the data length is $N=256$ and after adding cyclic prefix of $\frac{1}{4}N$ it becomes 320. Table 3.1 shows that signal power and noise power calculated for the proposed method is same as ideal case because the energy contained in CP is subtracted from the energy contained by total signal which is data plus CP.

Table 3.1: Ideal vs. calculated SNR for first-part of proposed technique

	(Ideal)	(Calculated)
Signal power= P_{ss}	$\rho \cdot N$	$P_{ss} = \rho\{2(N + l_{CP})\} - \rho \cdot l_{CP} = \rho \cdot N$
Noise Power= P_{NN}	$\hat{\sigma}_N^2 \cdot N$	$P_{NN} = \hat{\sigma}_N^2 (N + l_{CP}) - \hat{\sigma}_N^2 \cdot l_{CP} = \hat{\sigma}_N^2 \cdot N$
SNR	P_{ss} / P_{NN}	P_{ss} / P_{NN}

3.2.2.2 Second Part: Front-End Noise Power and SNR Estimation of Colored Noise Using Wavelet-Packet

For the second part of our proposed technique; we develop a technique that takes into account the color and variation of noise statistics over OFDM sub-carriers. Unlike first part, the OFDM band is divided into several sub-bands using wavelet packet as shown in Fig.3.7 and appendix A shows the details of Wavelet Packet decomposition. The colored noise in each sub-band is considered white as shown in Fig.3.8. The proposed solution provides many local estimates, allowing tracking of the variation of the noise statistics across OFDM sub-carriers, which are particularly of use in sub-band adaptive modulation OFDM systems. The proposed technique estimates both local (within smaller sets of subcarriers) and global (over all sub-carriers) SNR values using noise power estimates knowledge.

After adding cyclic prefix as described in first part, OFDM data is divided into 2^n sub-bands using wavelet packets where 'n' shows the number of levels. The length of each sub-band is $L_{sub} = N_{sub} + l_{CPsub}$, where $N_{sub} = N/2^n$ and $l_{CPsub} = l_{CP}/2^n$.

a. Signal Power and Noise Power Estimation in Sub-Bands

Sub-bands inherit the two identical halves property of synchronization preamble as discussed in first part of proposed technique. So, one can find the signal power and noise power in each sub-band using the same procedure as described in first part of proposed work. Due to wavelet packet decomposition, length of data is changed but location of zero lag and side peaks are unchanged. The autocorrelation of the transmitted and received 5th sub-band signal at SNR = 7 dB are shown in Fig. 3.9 (a) and Fig. 3.9(b), respectively. It is clear that the autocorrelation values apart from the zero-offset are unaffected by the AWGN, so one can find the signal and noise powers from the zero-lag autocorrelation value.

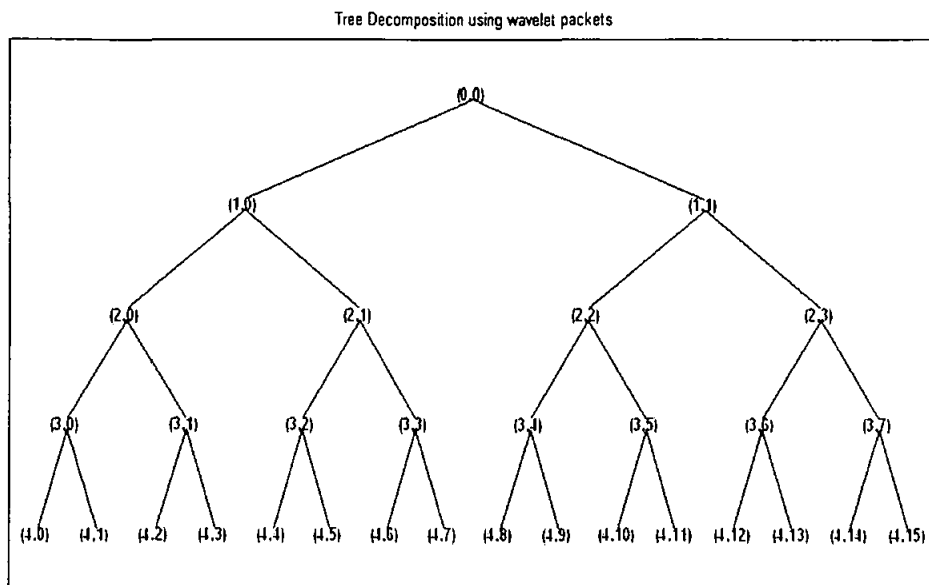


Fig. 3.7: Wavelet decomposition of transmitted OFDM data

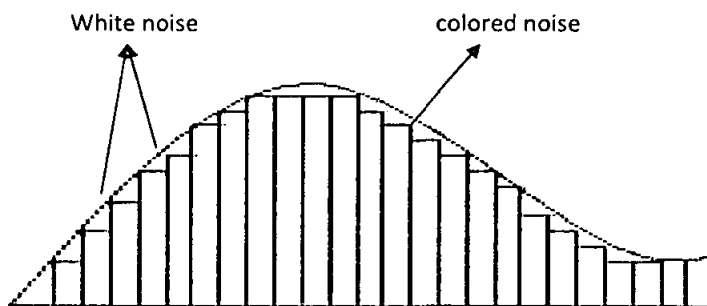


Fig. 3.8: Estimation of colored noise using white noise in small segments

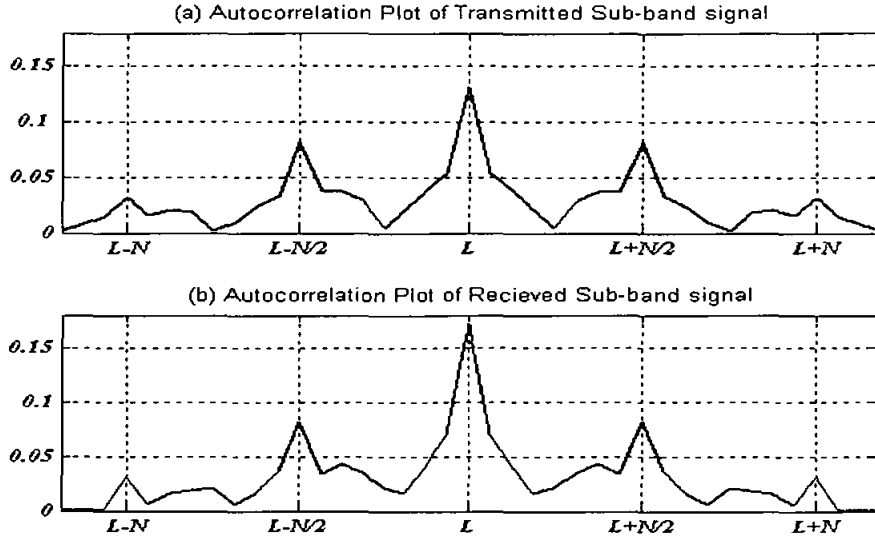


Fig.3.9 (a): Autocorrelation of transmitted signal. (b): Autocorrelation of received signal

b. Signal Power Estimation in each Sub-band

The Explanation for the correlation peaks of Fig.3.9 is same as shown in Fig.3.6 because sub-bands inherit the two identical halves property of synchronization preamble. After wavelet packet decomposition, the length of data and the length of CP are changed. So after correlation of each sub-band, first peak rises at $L_{sub}-N_{sub}$ when CP matches with itself with energy of $\rho \cdot l_{CPsub}$. The second peak rises at $L_{sub}-N_{sub}/2$ when one half of sub-band plus CP_{sub} matches with itself with energy of $\rho \cdot (N_{sub}/2 + l_{CPsub})$ and main peak at zero-lag (L_{sub}) rises when full sub-band matches with itself with energy of $\rho \cdot (N_{sub} + l_{CPsub})$.

Taking into consideration the autocorrelation values for $L_{sub}-N_{sub}/2$ and $L_{sub}-N_{sub}$ lags or $L_{sub}+N_{sub}/2$ and $L_{sub}+N_{sub}$, signal power is given as

$$\hat{P}_{sub} = 2R_{yy}(L_{sub} - N_{sub}/2) - R_{yy}(L_{sub} - N_{sub}) \quad (3.24)$$

Or

$$\hat{P}_{sub} = 2R_{yy}(L_{sub} + N_{sub}/2) - R_{yy}(L_{sub} + N_{sub}) \quad (3.25)$$

where \hat{P}_{sub} is the estimated signal power of each sub-band.

c. Noise power Estimation in each Sub-band

Having obtained the power of signal in certain sub-band, noise power can be calculated as

$$\text{Noise Power} = \hat{\sigma}_N^2 = R_{yy}(L_{sub}) - \hat{P}_{sub} \quad (3.26)$$

where $R_{yy}(L_{sub})$ is value at zero-lag.

d. SNR Estimation in each Sub-band

Finally we can find the SNR estimates in the sub-band by using equation (3.24 or 3.25) and equation (3.26).

$$\hat{SNR} = \frac{\hat{P}_{sub}}{\hat{\sigma}_N^2} \quad (3.27)$$

where \hat{SNR} is the estimated value for SNR.

Ideally, signal power and noise power are calculated without CP for the original data of length N . Table 3.2 shows that signal power and noise power calculated for the proposed method is same as ideal case because the energy contained in CP is subtracted from the energy contained by total signal which is data plus CP.

Table 3.2: Ideal vs. calculated SNR for second-part of proposed technique

	(Ideal)	(Calculated)
Signal power= P_{ss}	$\rho \cdot N_{sub}$	$P_{ss} = \rho\{2(N_{sub} + l_{subCP})\} - \rho \cdot l_{subCP} = \rho \cdot N_{sub}$
Noise Power= P_{NN}	$\hat{\sigma}_N^2 \cdot N_{sub}$	$P_{NN} = \hat{\sigma}_N^2 (N_{sub} + l_{subCP}) - \hat{\sigma}_N^2 \cdot l_{subCP} = \hat{\sigma}_N^2 \cdot N_{sub}$
SNR_{sub}	P_{ss} / P_{NN}	P_{ss} / P_{NN}

The methodology and parameters to perform simulation of proposed front-end based SNR estimation technique is discussed in the chapter 4. The proposed SNR estimation technique is of In-service type SNR estimator. There is no throughput penalty as the proposed technique makes use of synchronization preamble which is already employed in OFDM systems and another advantage of the proposed technique is that it generally works with both white noise as well as colored noise scenario.

According to the best knowledge of author this is the first SNR estimation technique for multicarrier systems like OFDM systems which performs SNR estimation at the front-end of the receiver. Previously, there is only one SNR estimation technique which performs SNR estimation at the front-end of the receiver proposed by Nidal [Nidal, 2007] for single carriers systems using AWGN channel.

3.3 Methodology for Analyzing Various SNR Estimators

In the last section we discussed the formulation of proposed SNR estimation in OFDM systems. The proposed SNR estimator performed SNR estimation at the front-end of the receiver unlike Reddy SNR estimator and subspace SNR estimator discusses in chapter 2 and used later for comparison. The completion of estimator's formulation now set the stage to define the methodology and parameters of developed SNR estimators to perform the simulations. The performance results when using the proposed SNR estimation technique will be obtained and discussed in the next chapter.

The methodology and the parameters needed for the simulations of the SNR estimators (Reddy estimator, Subspace estimator & Proposed front-end estimator) used in this thesis will be discussed in the next section.

3.3.1 Methodology for Analyzing Reddy's SNR Estimator

The methodology of the Reddy's estimator developed in Matlab® is depicted in Fig.3.10. An OFDM system with 256 sub-carriers is considered as shown in Fig.3.11. After the

addition the cyclic prefix of length 64, IFFT is performed and the signal is then passed through the channel. At the receiver side cyclic prefix is removed and FFT is performed to convert the signal back into its original transform. SNR estimation is performed after the FFT process. Other parameters for this technique are shown in Table 3.3. The flow chart in Fig.3.12 shows how this technique works to get the SNR estimates. 8 Pilot (x-pilot) symbols are inserted in each OFDM block transmission. Channel frequency response (H_s) is computed from the pilot symbols for the transmitted signal (x-pilot) and the received signal (y-pilot) as discussed in the last chapter. Each of these pilot symbols are vectors of size 8×1 , which is the number of pilots inserted in the OFDM symbol.

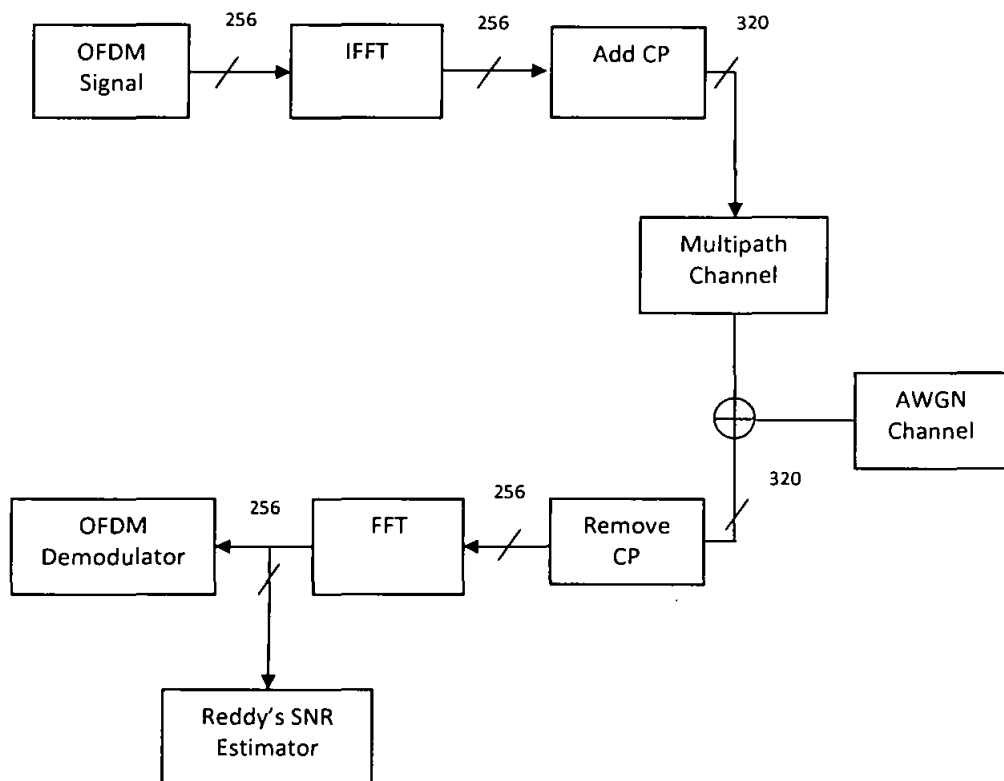


Fig. 3.10 Methodology of Reddy's SNR Estimator

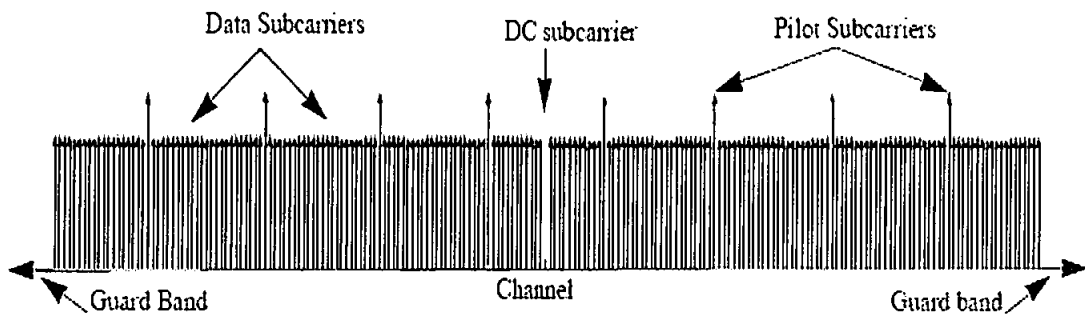


Fig. 3.11 OFDM Signal in frequency domain (IEEE802.16d standard)

Table3.3. Parameters for OFDM Systems Simulation

N_{fft} size (N)	256
N_{used} (data carrier = 192 & Pilot Carrier = 8)	200
Sampling Frequency (F_s)	20MHz.
Number of Lower frequency guard subcarriers	28
Number of Higher frequency guard subcarriers	27
Subcarrier Spacing ($\Delta f = F_s/N_{fft}$)	1×10^5
Useful Symbol Time ($T_b = 1/\Delta f$)	1×10^{-5}
Guard Interval (G)	$\frac{1}{4} (N)$
CP Time ($T_g = G \cdot T_b$)	2.5×10^{-6}
OFDM Symbol Time ($T_s = T_b + T_g$)	1.25×10^{-5}

3.3.2 Methodology for Analyzing Subspace Based SNR Estimator

The methodology of the subspace based estimator developed in Matlab® is depicted in Fig.3.13. An OFDM system with the same parameters as discussed in Reddy’s estimator is considered. Subspace based estimator also performs the SNR estimation at the back end of the receiver. The flow chart in Fig.3.14 shows how this technique works to get the SNR estimates. 8 Pilot (x-pilot) symbols are inserted in each OFDM block transmission. Subspace based estimator accepts the same two inputs (x-pilot & y-pilot) as the Reddy’s estimator, which is used to compute the moving average correlation matrix estimate. The window size of the moving average, which is specified by K in eq.2.26 for minimum descriptive length (MDL) criteria is set to be equal to 10 in the results obtained as this is the suggested size by [Xiaodong et al, 2005]. The subspace estimator then continues to

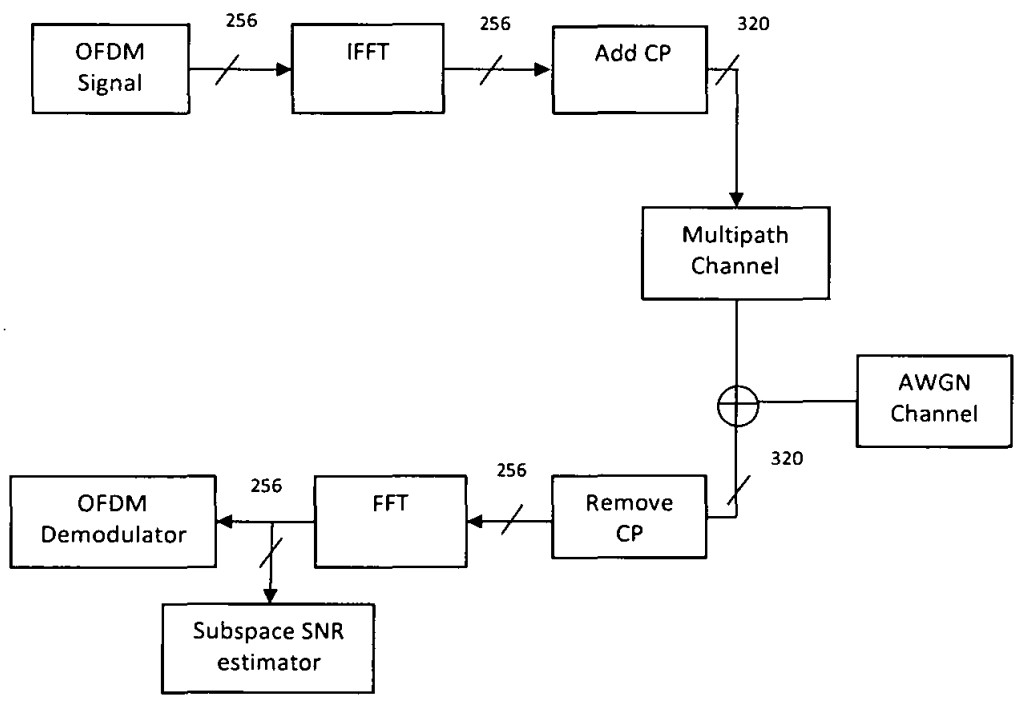


Fig.3.13 Methodology of subspace based SNR estimator

compute the eigenvalues which are used to compute total estimated number of multipath (L). This value of signal path which is calculated to be one for AWGN channel is used to compute the channel power using the eigenvalues. The remaining $M-L$ eigenvalues are used to compute the noise power.

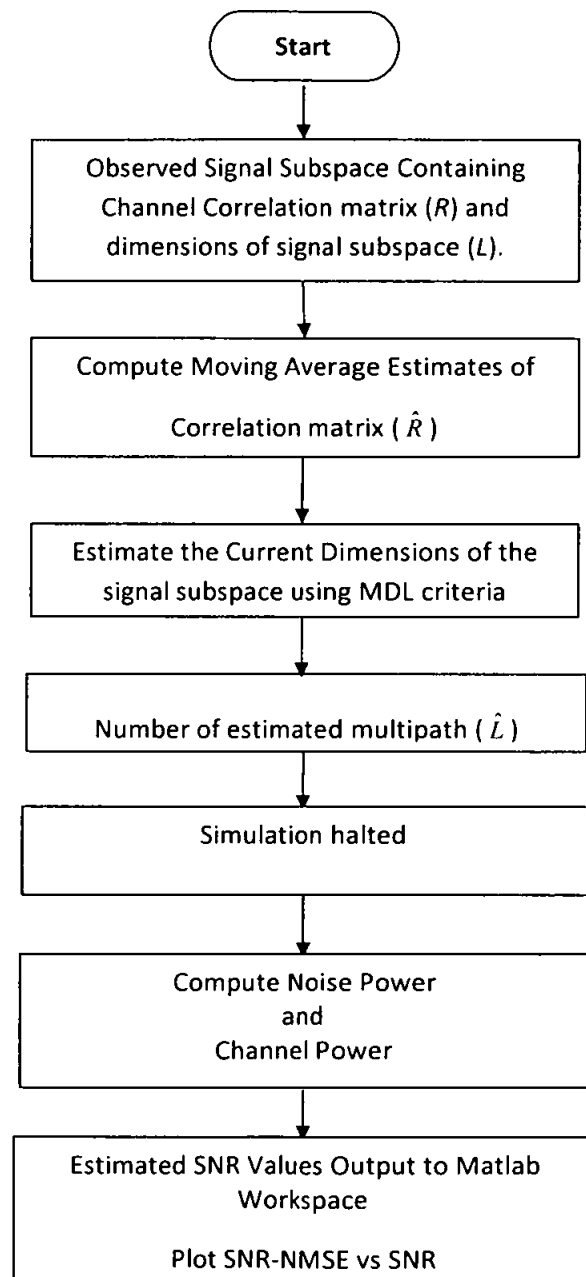


Fig. 3.14 Flow chart of subspace estimator

Simulation results of subspace based SNR estimator for (30 OFDM symbols) are used for comparison with proposed SNR estimator and will be shown in the next results & discussion chapter. The comparison is performed in terms of normalized mean squared error (NMSE) and estimated SNR.

3.3.3 Methodology for Analyzing Proposed Front-End SNR Estimator

The methodology of proposed front-end SNR estimator is divided in to two parts. In the first part methodology of proposed SNR estimation technique for white noise is discussed. The proposed technique is extended for SNR estimation of colored noise using wavelet packet and methodology of SNR estimator for colored noise is discussed in second part.

3.3.3.1: First Part: For Multipath Channels With AWGN

The methodology of proposed SNR estimator is shown in Fig.3.15. An OFDM based system is considered with parameters as shown in Table 3.4 and Table 3.5. The proposed estimator is based on one OFDM preamble signal and performed SNR estimation at the front-end of the receiver unlike Reddy estimator and subspace estimator. The synchronization OFDM preamble-the preamble which has two identical halves property as shown in Fig.3.16, is obtained by loading constellation (QPSK) points with a PN sequence (P_{seq}) at even sub-carriers. For simulations, the parameters are calculated using WiMAX standard (IEEE802.16, 2004) for 256 bit long data and Wi-Fi (IEEE802.11a) for 64 bit long data. Cyclic prefix is chosen $\frac{1}{4}$ of the original data. OFDM training data sent from the transmitter. After the addition the cyclic prefix, IFFT is performed and the signal is then passed through the channel. Autocorrelation is performed on the received signal at the front-end of the receiver. Estimates of the signal power and the noise power are estimated from the autocorrelation results. The flow chart in Fig.3.17 shows how this technique works to get the SNR estimates.

Simulation results of proposed front-end SNR estimator for AWGN and multipath channels (Rayleigh, Rician, SUI channel and indoor channel models), using only one OFDM preamble, are used for comparison with Reddy's estimator and subspace based SNR estimator and will be shown in the next results & discussion chapter. The comparison is performed in terms of normalized mean squared error (NMSE) and estimated SNR.

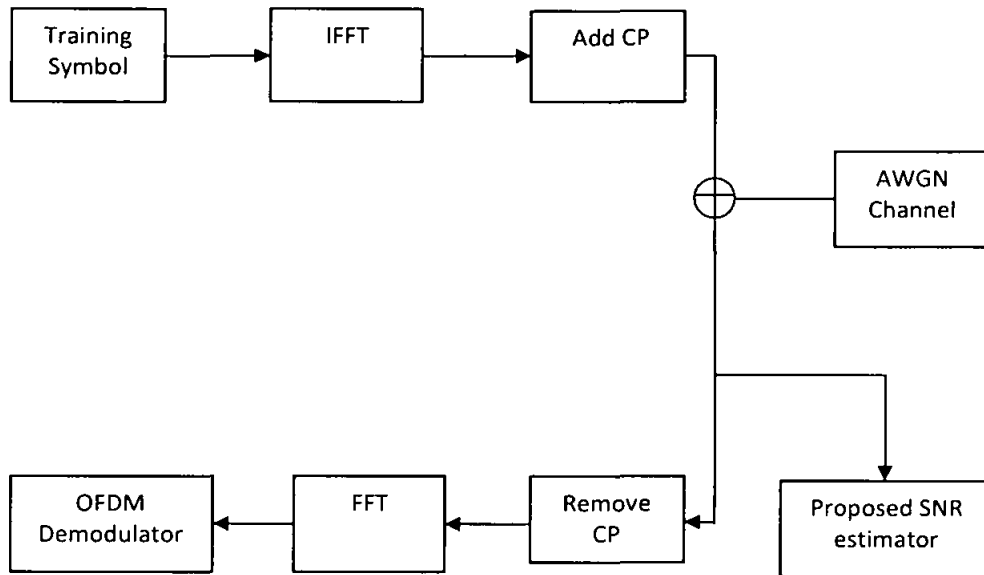


Fig 3.15: Methodology of first part of proposed technique.

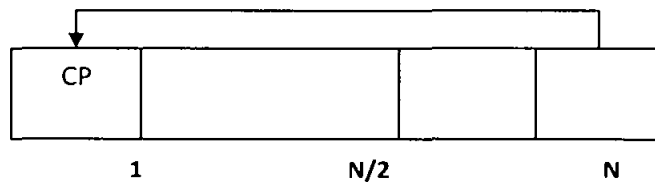


Fig. 3.16: OFDM Preamble symbol with cyclic prefix.

Table 3.4. Parameters of proposed Technique for first part (IEEE802.16, 2004)

N_{fft} size (N)	256
N_{used}	200
Sampling Frequency (F_s)	20MHz.
Number of Lower frequency guard subcarriers	28
Number of Higher frequency guard subcarriers	27
Subcarrier Spacing ($\Delta f = F_s/N_{fft}$)	1×10^5
Useful Symbol Time ($T_b = 1/\Delta f$)	1×10^{-5}
Guard Interval (G)	$\frac{1}{4}(N)$
CP Time ($T_g = G * T_b$)	2.5×10^{-6}
OFDM Symbol Time ($T_s = T_b + T_g$)	1.25×10^{-5}

Table 3.5. Parameters of proposed Technique for first part (IEEE802.11a)

N_{fft} size (N)	64
N_{used}	52
Sampling Frequency (F_s)	20MHz.
Subcarrier Spacing ($\Delta f = F_s/N_{fft}$)	0.3125×10^6
IFFT period ($T_b = 1/\Delta f$)	3.2×10^{-6}
Guard Interval (G)	$\frac{1}{4}(N)$
CP Time ($T_g = G * T_b$)	0.8×10^{-6}
OFDM Symbol Time ($T_s = T_b + T_g$)	4×10^{-6}

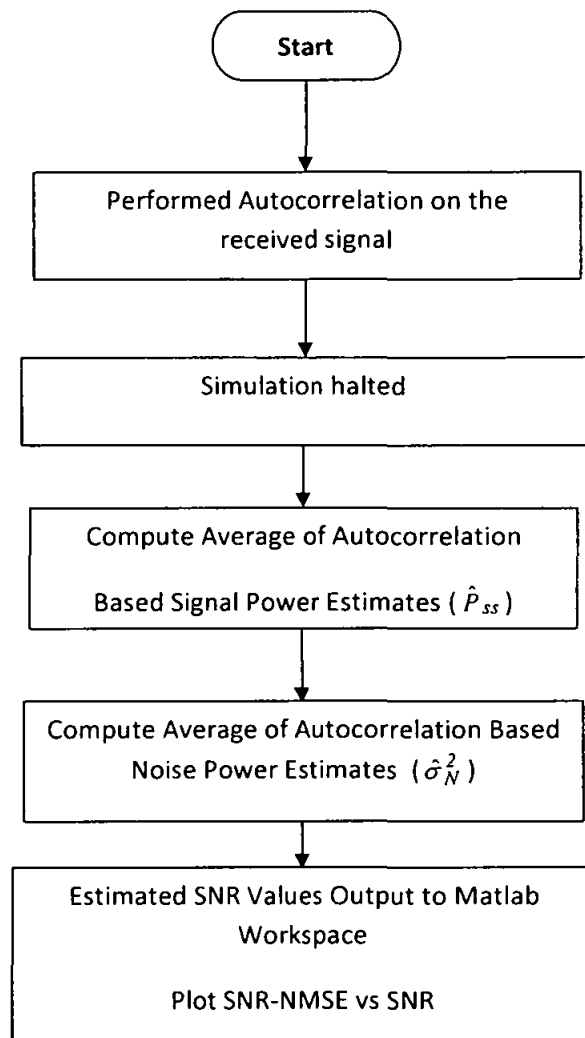


Fig.3.17 Flow chart of Proposed SNR estimation technique for white noise

3.3.3.2: Second part: For Multipath Channel With Colored Noise using Wavelet Packet Filter Banks.

The methodology of proposed SNR estimator is shown in Fig.3.18. For the second part of our proposed technique; An OFDM system, which takes into account the color and

variation of noise statistics over OFDM sub-carriers, is considered. Unlike first part, the received signal at front end of the receiver, is divided into several sub-bands using wavelet packet and noise in each sub-band is considered white. Other parameters used are shown in Table 3.6. The Proposed estimator provides many local estimates, allowing tracking of the variation of the noise statistics across OFDM sub-carriers, which are particularly of use in sub-band adaptive modulation OFDM systems. Autocorrelation is performed on each received sub-band signal at the front-end of the receiver. Estimates of the signal power and the noise power in each sub-band are estimated from the autocorrelation results of each sub-band. Then SNR is estimated within each of the sub-band (local estimates of SNR values) and these local SNR values are averaged over all OFDM data to get global estimates of the SNR. The flow chart in Fig.3.19 shows how this technique works to get the SNR estimates.

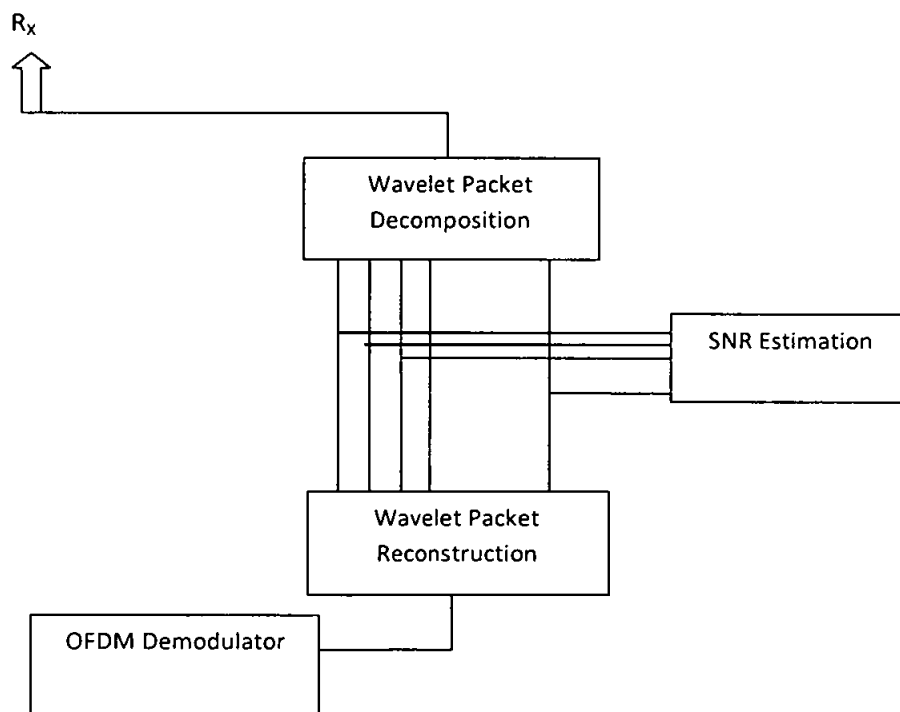


Fig.4.18. Methodology of Proposed SNR estimation technique for colored noise

Table 3.6: Parameters for Second-Part of proposed technique

I_{fft} size	256
N_{used} (preamble on even sub-carriers)	200
Sampling Frequency (F_s)	20MHz.
Number of Lower frequency guard subcarriers	28
Number of Higher frequency guard subcarriers	27
CP Time = $T_g = G * T_b$ where $G = 1/4$	2.5×10^{-6}
OFDM Symbol Time = $T_s = T_b + T_g$	1.25×10^{-5}
$T_s = \frac{5}{4} * T_s$ (Because $\frac{1}{4}$ CP makes the sampling faster by $\frac{5}{4}$ times)	1.5625×10^{-5}
$T_{sub} = \frac{T_s}{16}$	9.7656×10^{-7}
Wavelet Packet Object Structure	
<p>Wavelet Decomposition Command : <code>wpt = wpdec(data,4,'db3')</code> , Size of initial data : [1 320] Order : 2 Depth : 4 Terminal nodes : [15 16 17 18 19 20 21 22 23 24 25 26 27 28 29 30]</p> <p>-----</p> <p>Wavelet Name : db3 Entropy Name : Shannon</p>	

Simulation results of proposed front-end SNR estimator for colored noise (using only one OFDM preamble) is used for comparison with Reddy’s estimator and will be shown in the next results & discussion chapter. The comparison is performed in terms of normalized mean squared error (NMSE) and estimated SNR.

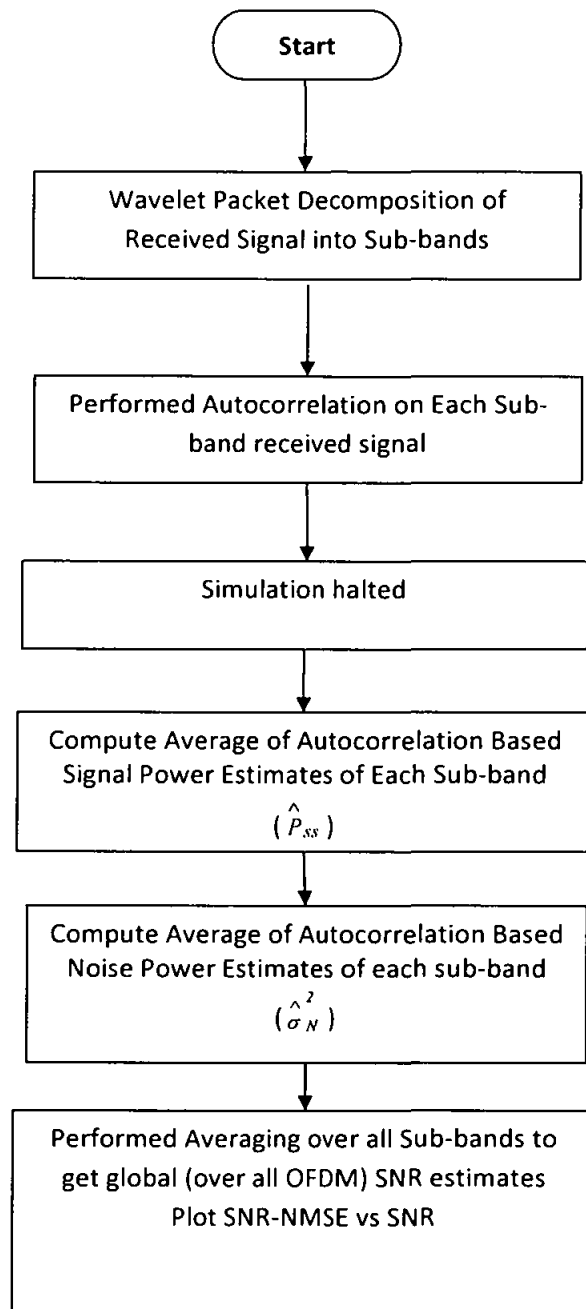


Fig.3.19 Flow chart of Proposed Front-End SNR estimator for Colored noise

3.4 Summary

In this chapter, formulation of Reddy estimator, sub-space estimator and our proposed front-end noise power and SNR estimator technique for OFDM wireless systems is presented. Reddy SNR estimator and subspace based SNR estimator are back end estimators unlike proposed SNR estimator in which SNR estimation is performed at front-end of the receiver. In the first part of proposed technique noise is assumed to be white and SNR estimation is done over all OFDM symbol. In the second part the assumption of the noise to be white is removed. Also, variation of the noise power across OFDM sub-carriers is allowed. Therefore, the proposed approach estimates both local (within smaller sets of subcarriers) and global (over all sub- carriers) SNR values. The short term local estimates calculate the noise power variation across OFDM sub-carriers. These estimates are specifically very useful for adaptive modulation, and optimal soft value calculation for improving channel decoder performance. Methodology and the parameters of Reddy estimator, Sub-space estimator and proposed front-end SNR estimator technique for OFDM wireless systems are presented. Reddy SNR estimator and subspace based SNR estimator are back end estimators unlike proposed SNR estimator in which SNR estimation is performed at front-end of the receiver. Reddy and subspace makes use of pilot symbol for their SNR estimation technique unlike proposed SNR estimator. All estimators discussed in this chapter are using the same parameters to provide a fair comparison of proposed SNR technique. To show the generality of proposed technique, designed methodology is also checked with parameters of Wi-Fi (IEEE802.11a) and WiMAX (IEEE802.16, 2004).

In Appendix B (FFT based on Wavelet Packet and its application to SNR estimation), it can be shown that, if FFT is built using Wavelet Packet algorithm, then for no extra cost, SNR estimates can be obtained inside FFT block after CP has been removed.

4.1 Introduction

The development and methodology of a novel front-end noise power and SNR estimation technique for AWGN channel in OFDM systems has been described in the last chapter. The technique is also extended to obtaining noise power estimates of colored noise using wavelet-packet based filter bank analysis of the noise. This technique is very useful in obtaining the best SNR estimates that are made use of in optimal deployment of OFDM. OFDM technology requires knowledge of the SNR for optimal performance. For instance, in OFDM systems, SNR estimation is used for power control, adaptive coding and modulation, turbo decoding etc.

In this chapter, we present results of the proposed front-end noise power and SNR estimation technique for white noise and for colored noise. In order to benchmark the proposed noise power and SNR estimation technique, a complete end-to-end fixed-broadband-wireless-access-system based on IEEE802.16d simulation has been developed in chapter 3. The simulations are conducted in both frequency non-dispersive and dispersive channels with real additive white Gaussian noise (AWGN) and also colored noise.

The results of SNR estimation technique for AWGN in OFDM systems are shown in section 4.2 and compared with other techniques in terms of normalized mean squared

error (NMSE) and estimated SNR. In section 4.3, the results of SNR estimation technique for colored noise using wavelet-packet in OFDM systems are shown and compared with previous techniques in terms of mean squared error (MSE) and estimated SNR.

4.2 Analysis Results of SNR Estimation Technique for Multipath Channels With AWGN in OFDM Systems

As depicted in chapter 3 on methodology, the proposed SNR estimation technique is hereby evaluated in terms of following criteria.

1. **Performance Evaluation:** This criterion is to establish how good an estimate the technique can provide. Towards this end, we provide comparison of estimated SNR with actual SNR and we also provide normalized mean squared error (NMSE) between actual SNR and estimated SNR at various SNR levels for our technique as well as other techniques. We extend this to predict the performance under various channel conditions. Furthermore, we extend the technique to perform even in colored noise, and evaluate its performance.
2. **Computational Complexity:** Towards this end, we compute the number of multiplications needed to get the SNR estimate and compare that with other techniques.
3. **Sensitivity Analysis:** Towards this end, we analyze which parameter our technique is more sensitive to.

4.2.1 Performance Evaluation

For fixed broadband wireless access systems characterized by IEEE802.16d, OFDM training / synchronization data of length $N=256$ is sent from the transmitter (T_x) where The cyclic prefix length is chosen as $l_{CP}=64$, so that $N_{total}=320$. The other parameters for the simulations are given in Table 3.3 of chapter 3. The proposed SNR estimator is

compared with two existing SNR estimators, the Reddy estimator [Reddy et al, 2003] and Subspace based estimator [Xiaodong et al, 2005] in terms of normalized mean squared error (NMSE) and estimated SNR. SNR is varied from 1 dB to 16 dB and the normalized mean-squared error (NMSE) is derived for the estimated SNR. In order to statistically accurate, mean is obtained over 2000 samples according to the following formula

$$NMSE = \frac{1}{2000} \sum_{m=1}^{2000} \left(\frac{\hat{SNR} - SNR}{SNR} \right)^2 \quad (4.1)$$

The NMSE results shows that proposed estimator with one OFDM symbol performs better than both Reddy's and subspace estimator which gives accurate SNR estimates after an observation interval of 20 OFDM symbols. The performance of proposed estimator (using one OFDM symbol) is compared with Reddy estimator (using 30 OFDM symbols) and subspace estimator (using 30 OFDM symbols). The performance is evaluated via computer simulations using AWGN channel. The results are shown in the Fig 4.1 and Fig 4.2 for SNR-NMSE vs. SNRdB and estimated SNR vs. actual SNRdB. Results shows that the proposed estimator provides enhanced performance in SNR estimation as compared to Reddy and subspace estimators.

The proposed estimator also performs well with other multipath channels (Rayleigh, rician, SUI channels, indoor channel models). The simulations are performed using this multipath channel with different number of taps and results are shown in Figs.4.3 to 4.30. Description of multipath taps used by our technique are given in Table 4.1. It is observed that the performance of proposed estimator is good in terms of NMSE and estimated values of SNR. The results of SUI channels and indoor channel models shows that the proposed technique also performs better estimation of SNR for Wi-Fi (IEEE802.11a) and WiMAX (IEEE802.16, 2004) systems.

In WiMAX (IEEE802.16, 2004) systems, the channel is modeled by the 6 SUI multipath channels with additive white Gaussian noise (AWGN) added to the time samples [Erceg

et al, 2003]. The 6 channels model the typical channels for 3 types of terrains. Terrain type A is hilly terrain with moderate-to-heavy tree densities while type C is flat terrain with light tree densities. Terrain type B is intermediate between type A and terrain type C. Table 4.2 shows the terrain type and corresponding SUI channels that represent them. Table 4.3 shows the description of SUI channels used in our simulations.

It is also seen that the performance of proposed estimator is good with Wi-Fi systems (IEEE802.11a) with indoor channel models of 10 taps. Values of taps are taken from the indoor channel models developed by Zhao [Zhao, 2004]. Description of these channel models are given in Table 4.4.

Table 4.1: Description of Rayleigh and Rician channel

		Taps for Rayleigh Channel & Rician Channel										Unit
3-Taps	Delay	0		1.5			3.2					μ sec
	Power	0		-15			-30					dB
	K-Factor	10 (K=0 for Raleigh channel)										
5-Taps	Delay	0	1.5	3.2	4.5	6					μ sec	
	Power	0	-15	-25	-35	-45					dB	
	K-Factor	10 (K=0 for Raleigh channel)										
10-Taps	Delay	0	1.5	3.2	4.5	6	7.5	10	13	16	19	μ sec
	Power	0	-5	-10	-15	-20	-30	-45	-60	-70	-80	dB
	K-Factor	5 (K=0 for Raleigh channel)										

Table 4.2: Terrain types and corresponding SUI channels

Terrain Type	SUI-Channels
<i>C</i>	<i>SUI-1, SUI-2</i>
<i>B</i>	<i>SUI-3, SUI-4</i>
<i>A</i>	<i>SUI-5, SUI-6</i>

Table 4.3: Description of SUI channels

		Tap1	Tap2	Tap3	Unit
SUI-1	Delay	0	0.4	0.9	μ sec
	Power	0	-21	-32	dB
	K-Factor	16			
SUI-2	Delay	0	0.4	1.1	μ sec
	Power	0	-18	-27	dB
	K-Factor	8			
SUI-3	Delay	0	0.4	0.9	μ sec
	Power	0	-11	-22	dB
	K-Factor	3			
SUI-4	Delay	0	1.5	4	μ sec
	Power	0	-10	-20	dB
	K-Factor	1			
SUI-5	Delay	0	4	10	μ sec
	Power	0	-11	-22	dB
	K-Factor	2			
SUI-6	Delay	0	14	20	μ sec
	Power	0	-16	26	dB
	K-Factor	2			

Table 4.4: Description of Indoor channel models for Wi-Fi

10 Taps for Indoor Channel Models											Unit
Delay	0	10	20	30	40	50	70	90	110	130	n-sec
power	0	-1.8	-3.8	-4.4	-5	-6	-10	-11.8	-13	-15	dB
K-Factor	10										

4.2.1.1 Comparison with Other Techniques

In Fig. 4.1 is shown the normalized mean squared error between estimated SNR and actual SNR (SNR-NMSE) plotted against actual SNR. These results are compared with those of Reddy and subspace.

It can be seen from the Fig.4.1, that the proposed technique has very small NMSE error as compared to Reddy and Subspace. The proposed estimator makes use of only one OFDM symbol unlike Reddy and subspace method which are using 30 OFDM symbols. It is observed that the rise in NMSE at small SNR is due to window effect of the system.

In Fig 4.2 estimated SNR is plotted against actual SNR and compared with Reddy's and subspace techniques.

It is clear from the plot that the proposed estimator gives SNR estimates that have very small bias and are very close to actual SNR value. It is observed that Reddy's technique and subspace technique have more bias in their estimates as compared to our proposed technique.

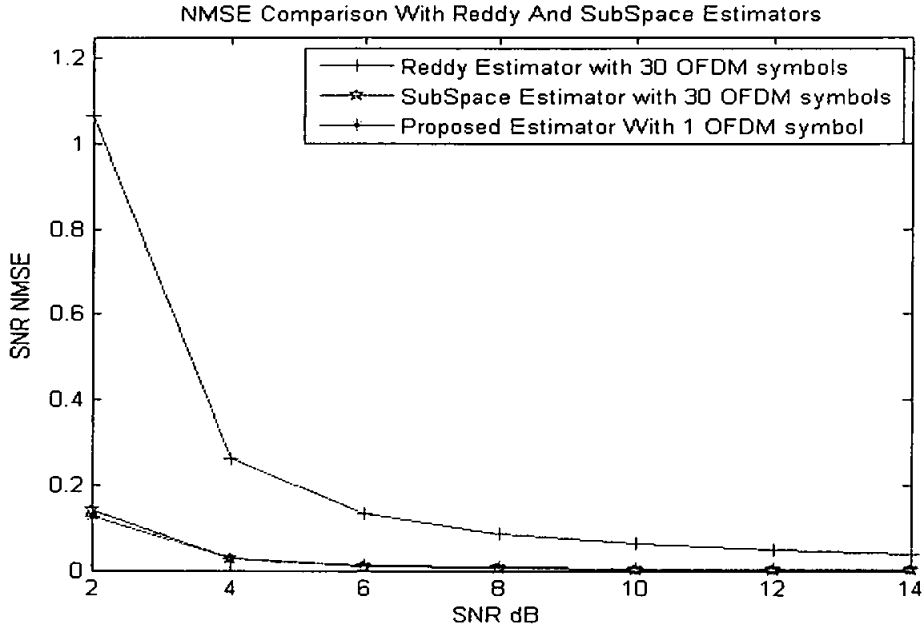


Fig.4.1 SNR-NMSE vs. actual SNR comparison of proposed technique with Reddy’s and subspace Estimators

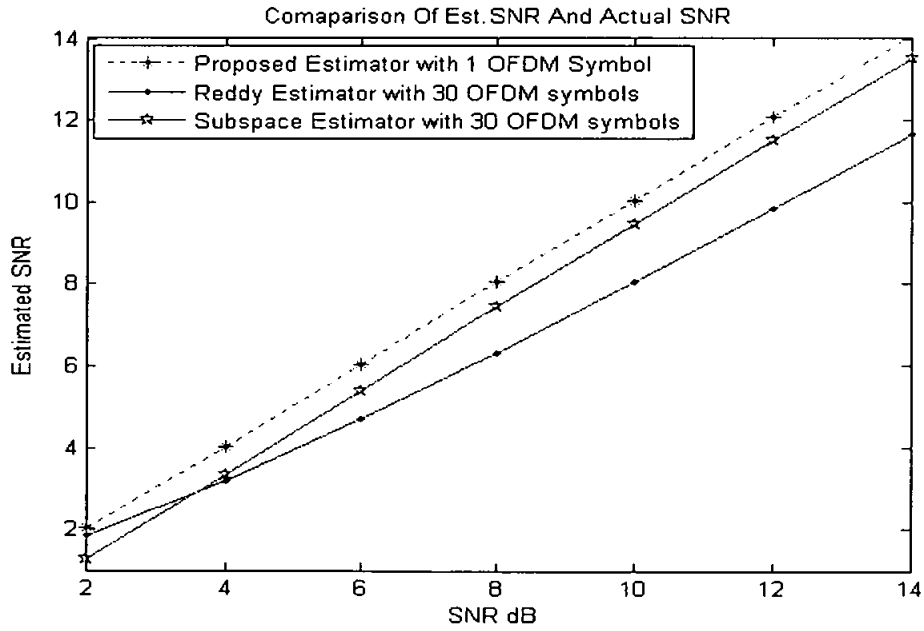


Fig.4.2 Estimated SNR vs. actual SNR comparison of proposed technique with Reddy’s and subspace

4.2.1.2 Performance over AWGN, Rayleigh and Rician

In Fig. 4.4 is shown the SNR-NMSE is plotted against actual SNR using AWGN channel.

It can be seen from the Fig.4.4, that the proposed technique has very small NMSE error. It is observed that the rise in NMSE at small SNR is due to window effect of the system.

In Fig. 4.5 estimated SNR is plotted against actual SNR for AWGN channel. It can be seen that the SNR estimates are very less bias and are very close to the actual SNR.

Fig. 4.6 to Fig. 4.17 performance over Rayleigh and Rician channel for 3 taps, 5 taps and 10 taps, is shown in terms of SNR-NMSE and estimated SNR. The description of Rayleigh and Rician channels is shown in Table 4.1.

It can be seen from the figures, that the proposed technique perform well with Rayleigh and Rician multipath channels and has very small NMSE error. The NMSE is consistently seen to be more for low SNRs. The error could be due to the finite size of the data-window or equivalently, bandwidth window. The effect of finite width window is seen in Fig. 4.3 where autocorrelation of AWGN over the same bandwidth is plotted. As can be seen from figure, the autocorrelation is not zero at delays $\tau \neq 0$. These non zeros values can corrupt the measurement of peaks and cause error.

It also can be seen from these figures that the SNR estimates have very small bias and are very close to the actual SNR.

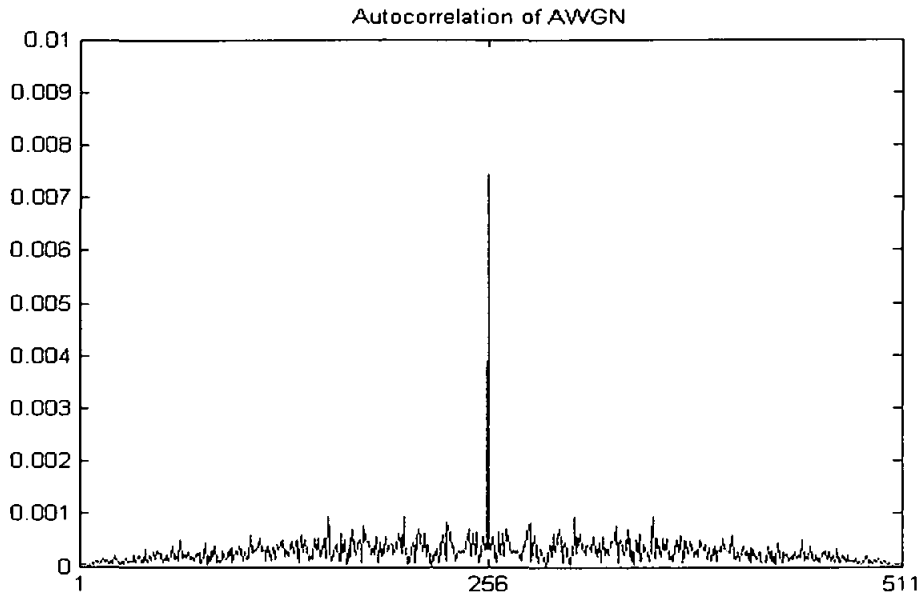


Fig. 4.3 Autocorrelation of AWGN

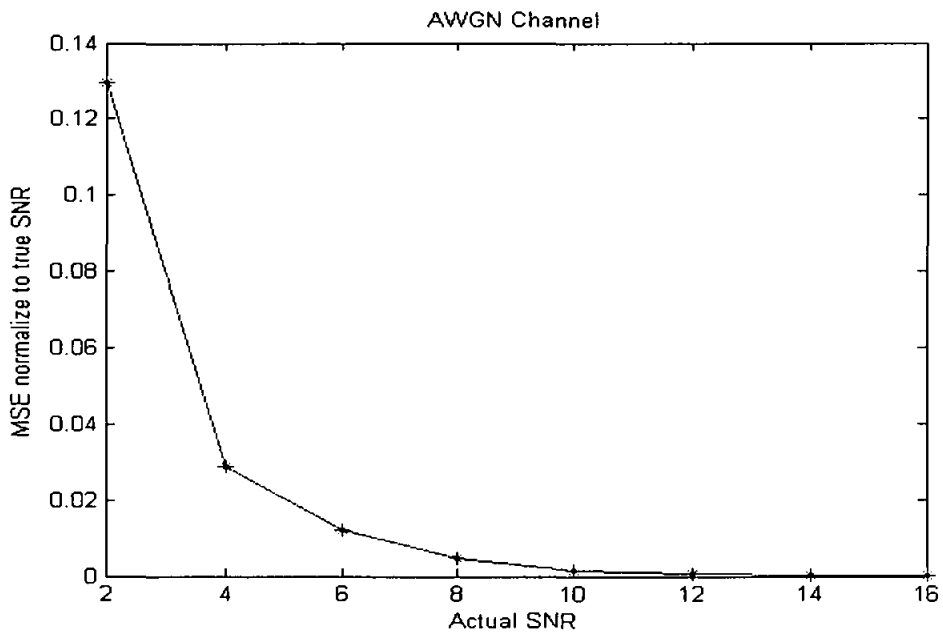


Fig.4.4 SNR-NMSE vs. actual SNR with AWGN channel

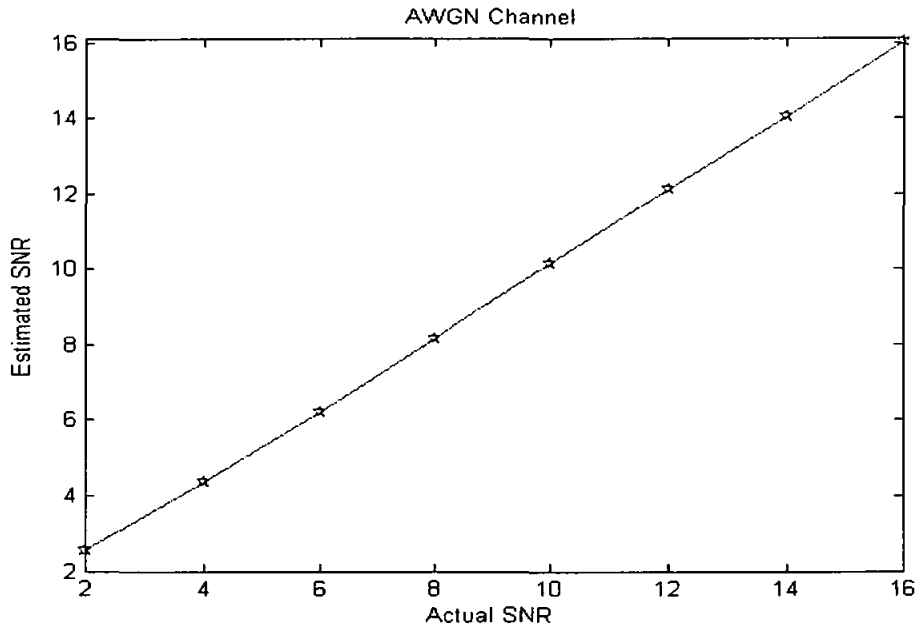


Fig.4.5 Estimated SNR vs. Actual SNR with AWGN channel

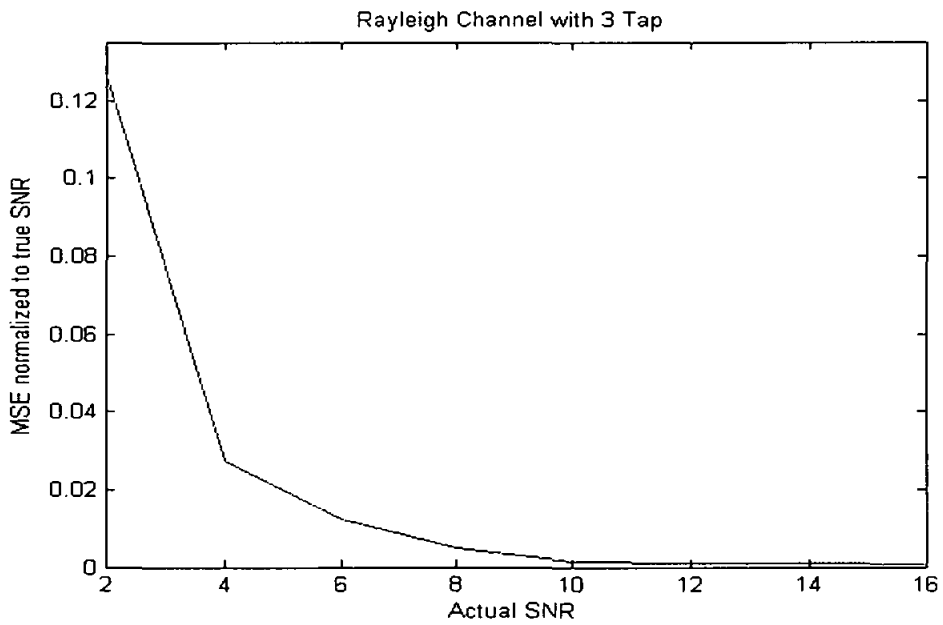


Fig.4.6 SNR-NMSE vs. actual SNR with Rayleigh 3-Tap channel

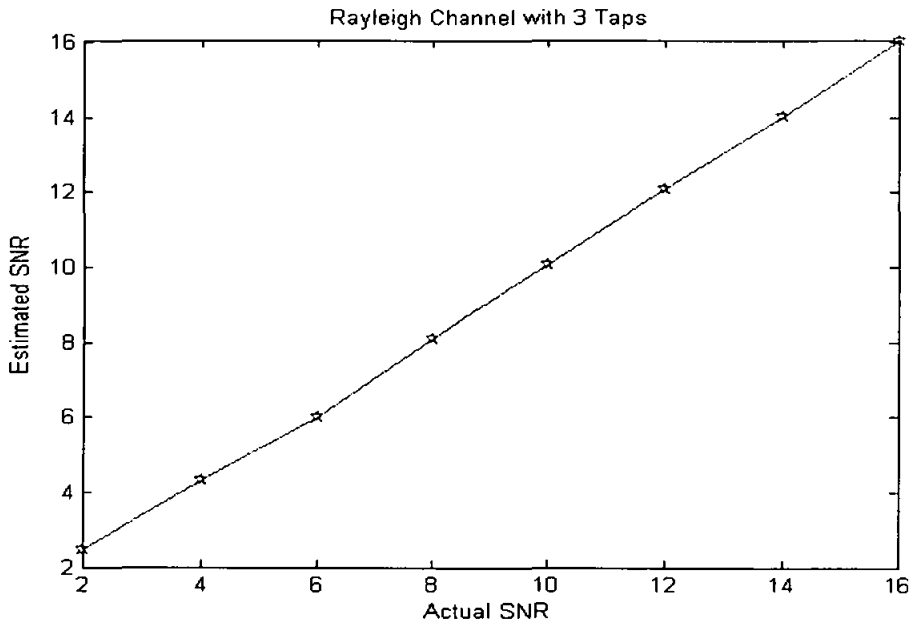


Fig.4.7 Estimated SNR vs. Actual SNR with Rayleigh 3-Tap channel

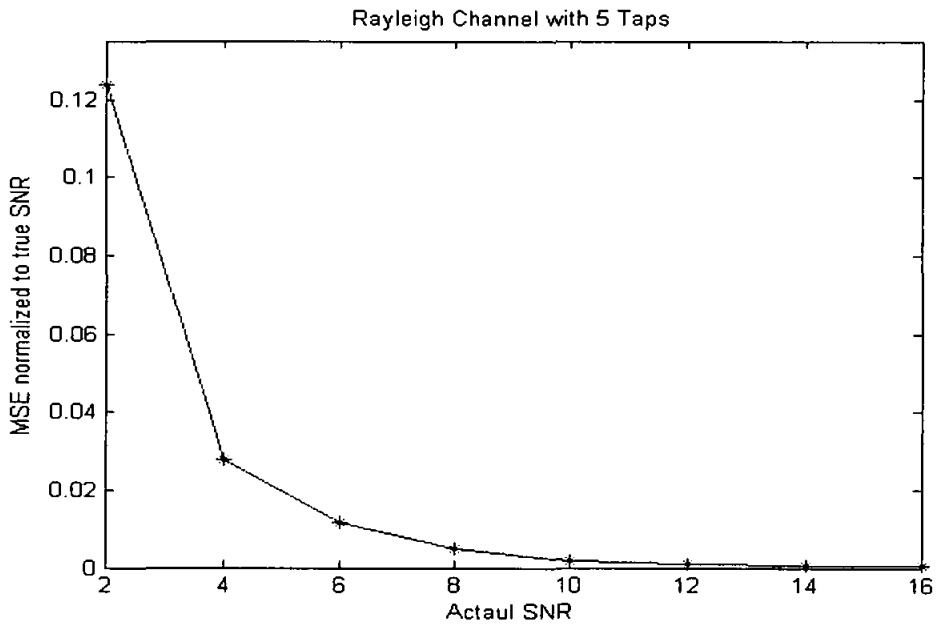


Fig.4.8 SNR-NMSE vs, actual SNR with Rayleigh 5-Tap channel

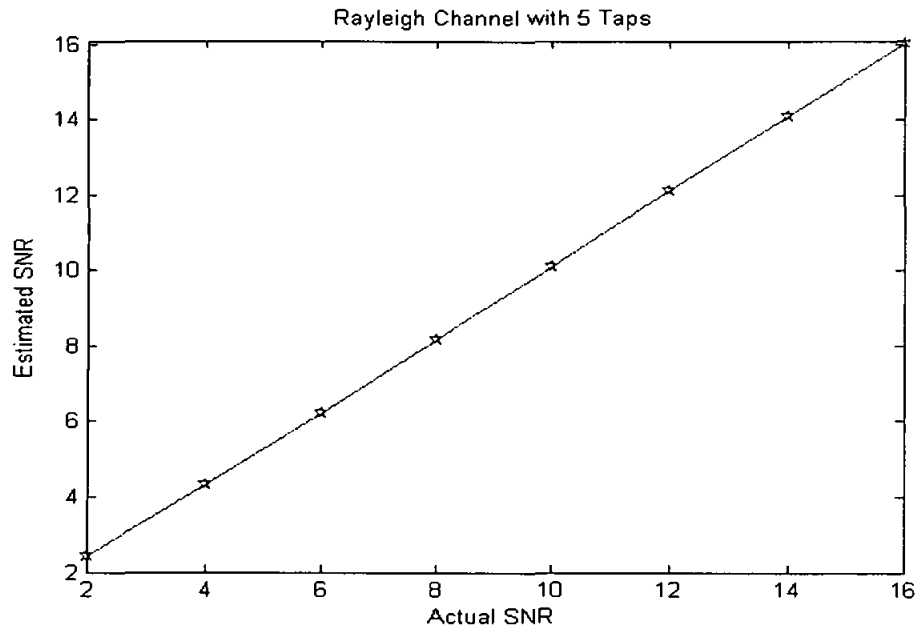


Fig.4.9 Estimated SNR vs. Actual SNR with Rayleigh 5-Tap channel

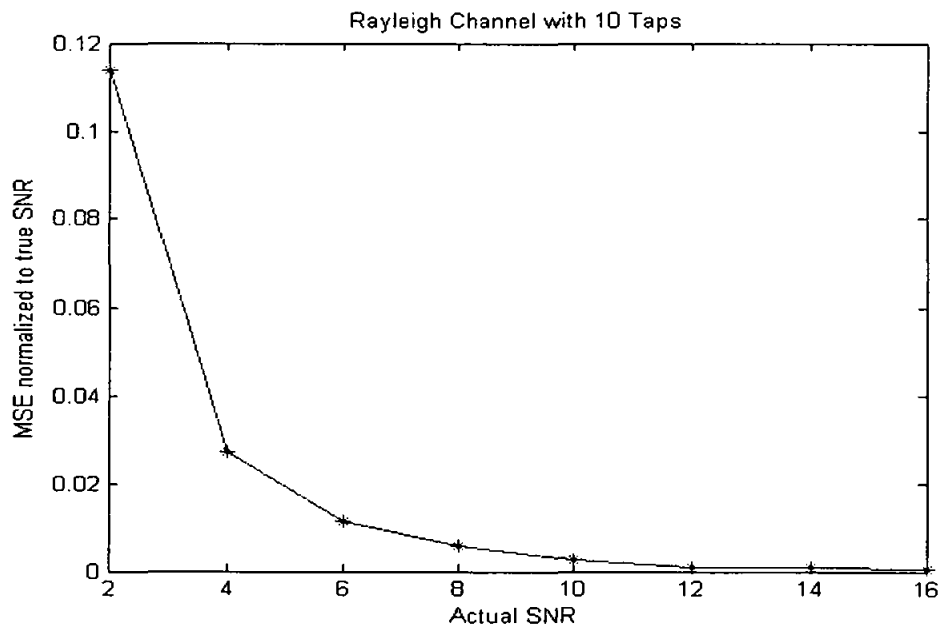


Fig.4.10 SNR-NMSE vs. actual SNR with Rayleigh 10-Tap channel

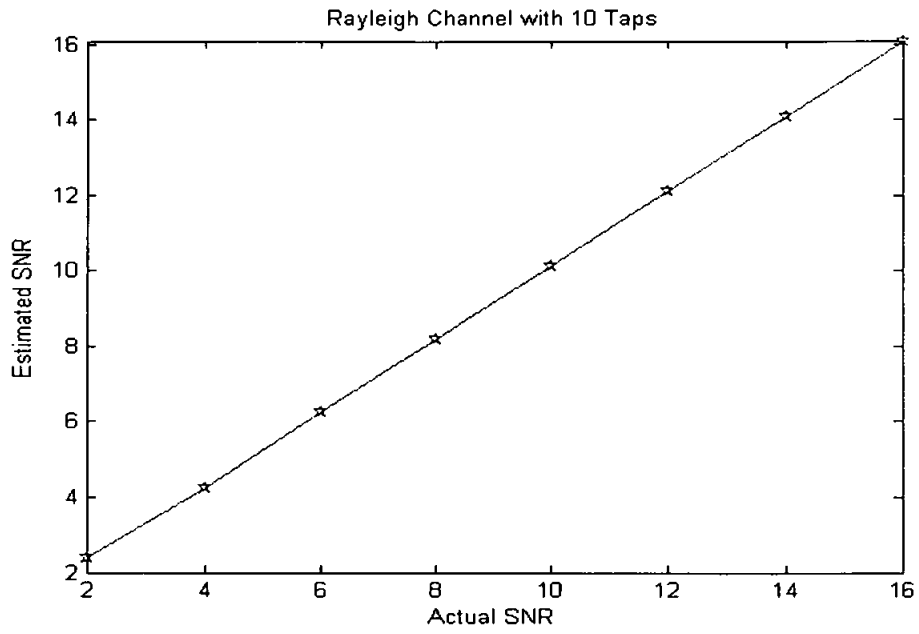


Fig.4.11 Estimated SNR vs. Actual SNR with Rayleigh 10-Tap channel

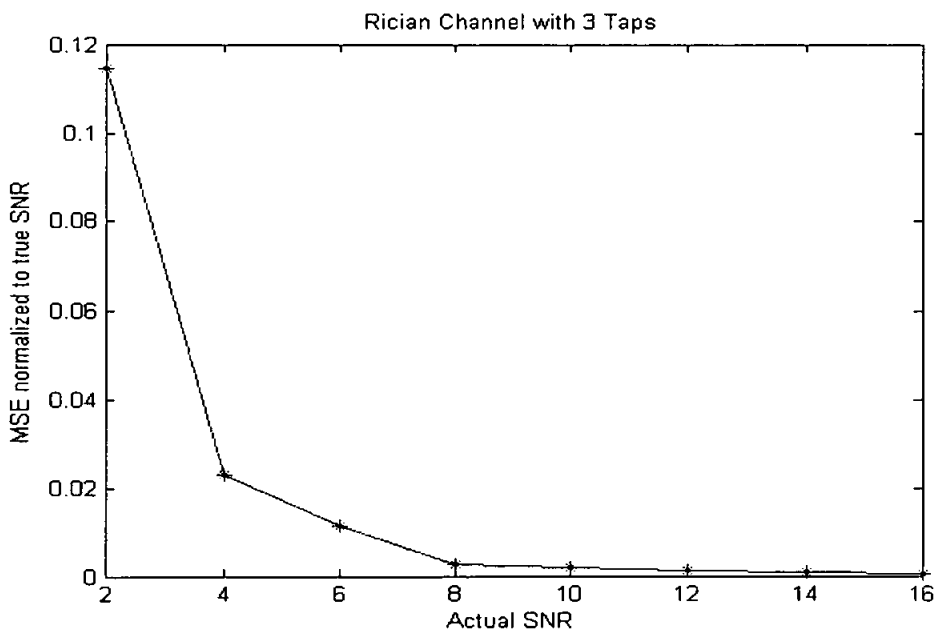


Fig.4.12 SNR-NMSE vs. actual SNR with Rician 3-Tap channel

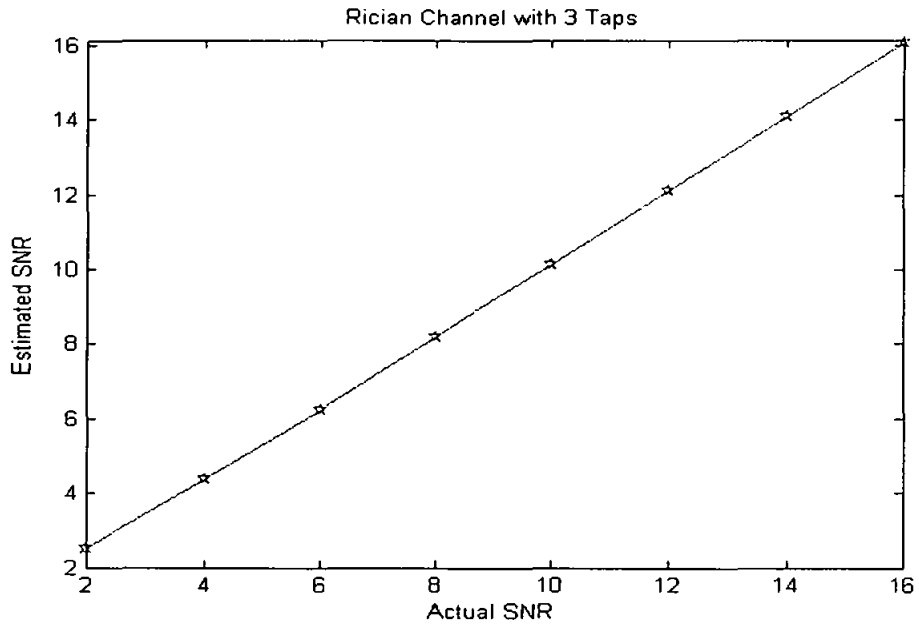


Fig.4.13 Estimated SNR vs. Actual SNR with Rician 3-Tap channel

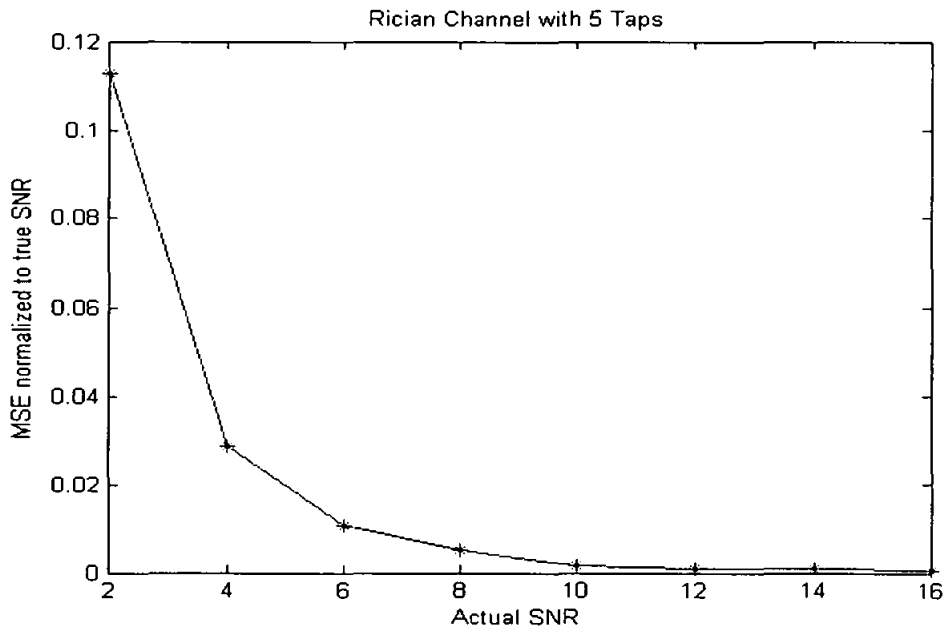


Fig.4.14 SNR-NMSE vs. actual SNR with Rician 5-Tap channel

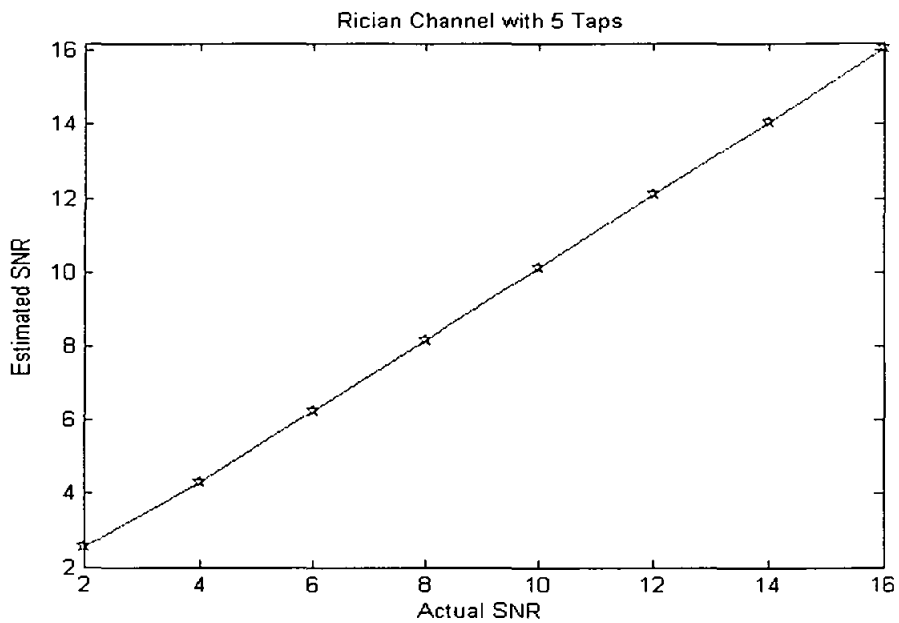


Fig.4.15 Estimated SNR vs. Actual SNR with Rician 5-Tap channel

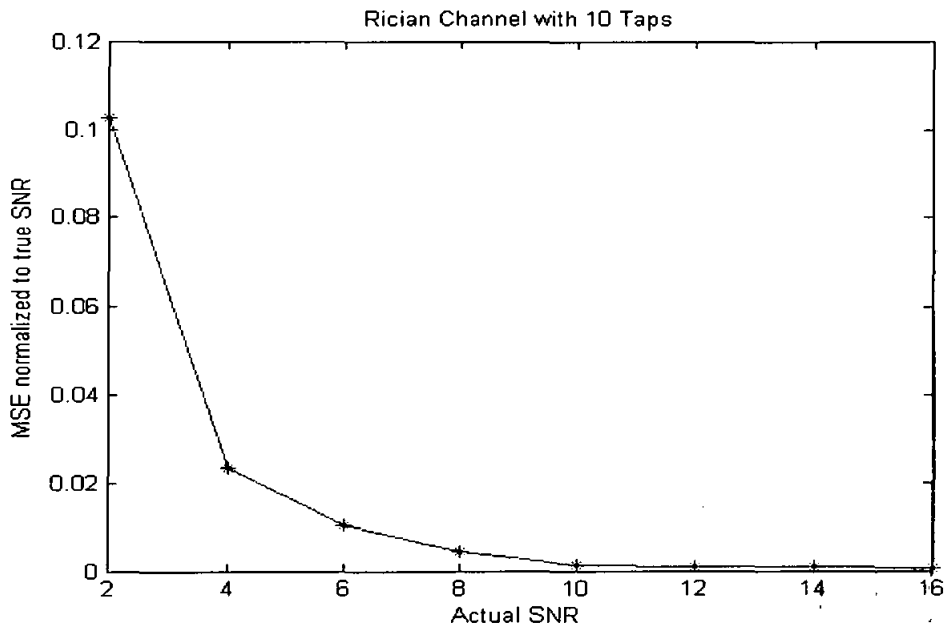


Fig.4.16 SNR-NMSE vs. actual SNR with Rician 10-Tap channel

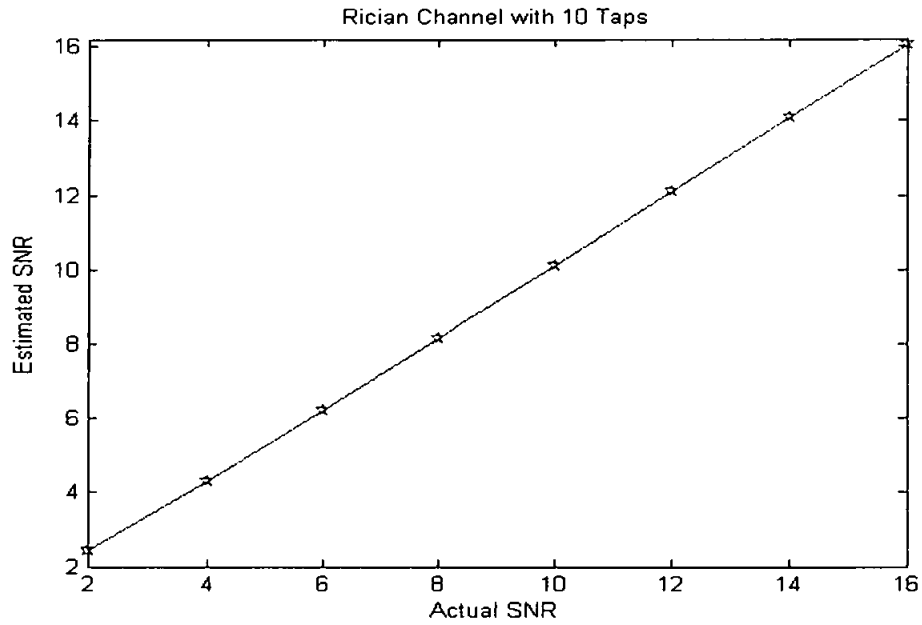


Fig.4.17 Estimated SNR vs. Actual SNR with Rician 10-Tap channel

4.2.1.3 Performance over SUI Multipath Channels

Fig 4.18 to Fig 4.29 performance over SUI multipath channel for 3 taps is shown in terms of SNR-NMSE and estimated SNR. The description of SUI multipath channels is shown in Table 4.3.

It can be seen from the Fig 4.18 to Fig 4.29, that the proposed technique perform well with SUI multipath channels and have very small NMSE error. It is observed that the rise in NMSE at small SNR is due to window effect of the system.

It also can be seen from these figures that the SNR estimates have very small bias and have very close to the actual SNR.

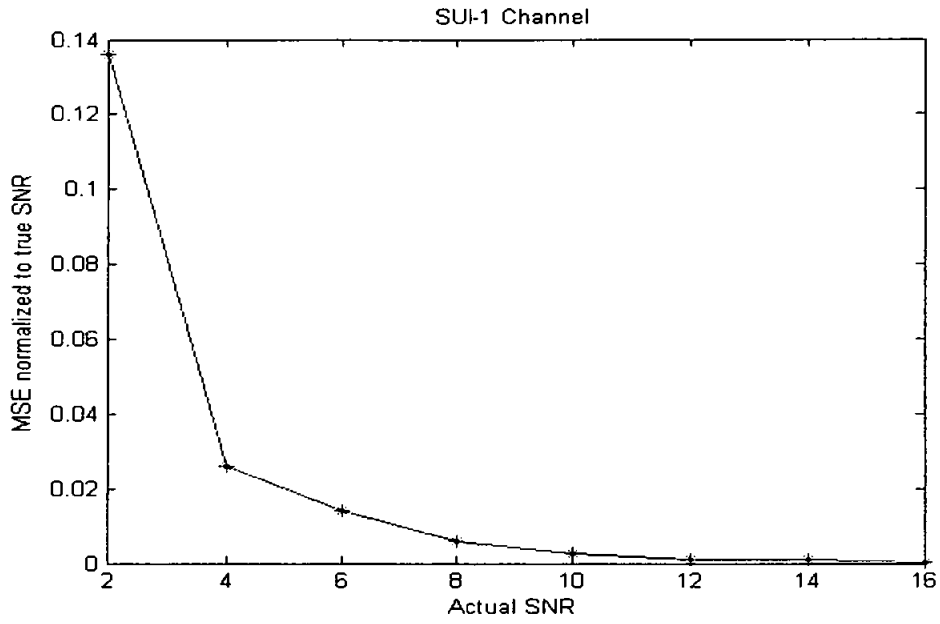


Fig.4.18 SNR NMSE vs. actual SNR with SUI-1 Channel

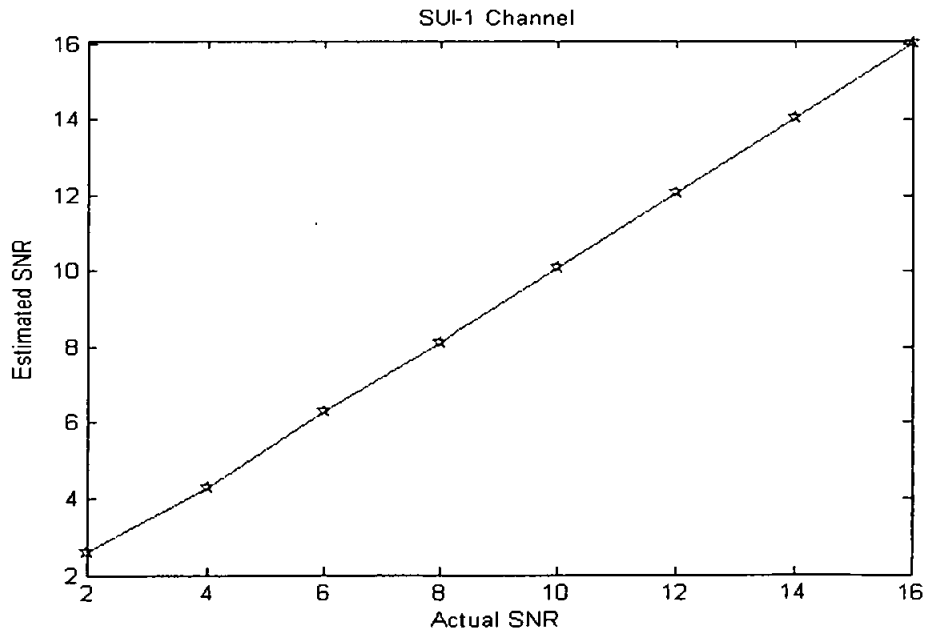


Fig.4.19 Estimated SNR vs. Actual SNR with SUI-1 Channel

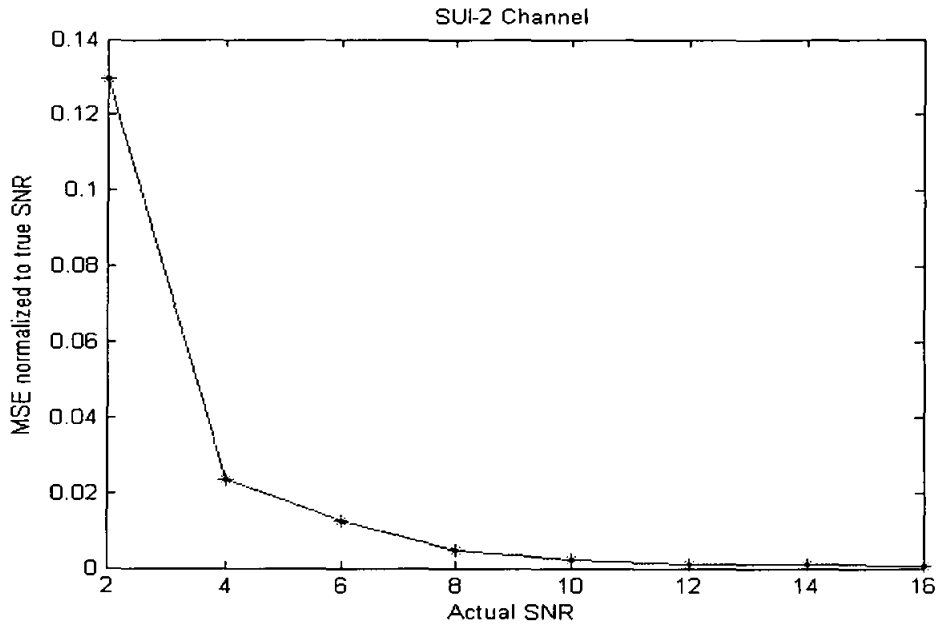


Fig.4.20 SNR NMSE vs. actual SNR with SUI-2 Channel

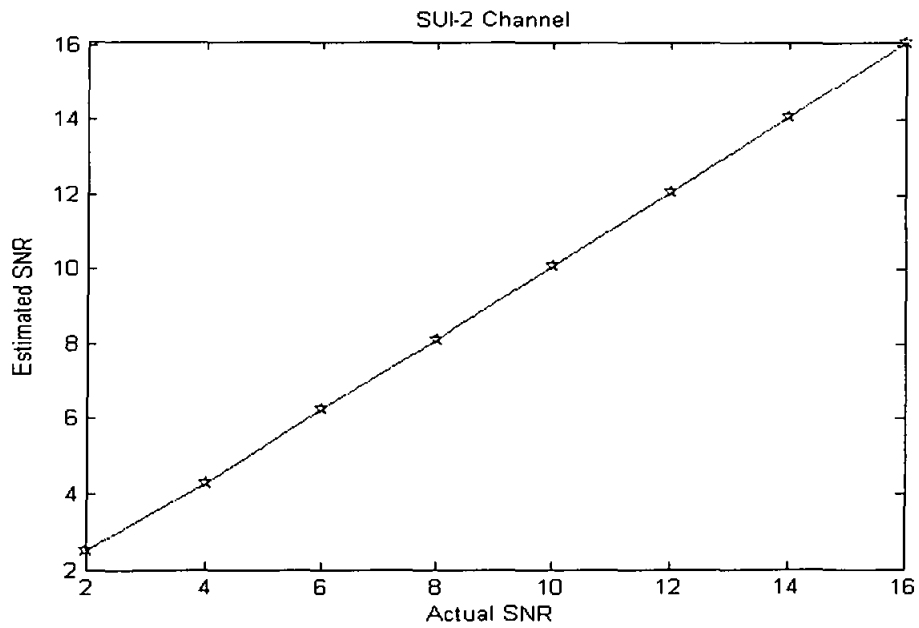


Fig.4.21 Estimated SNR vs. Actual SNR with SUI-2 Channel

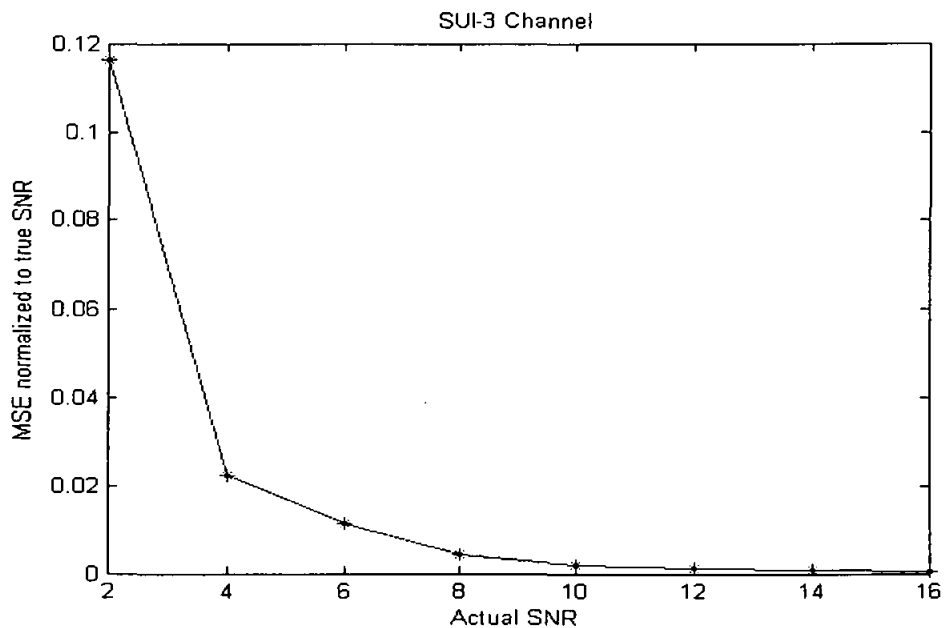


Fig.4.22 SNR NMSE vs. actual SNR with SUI-3 Channel

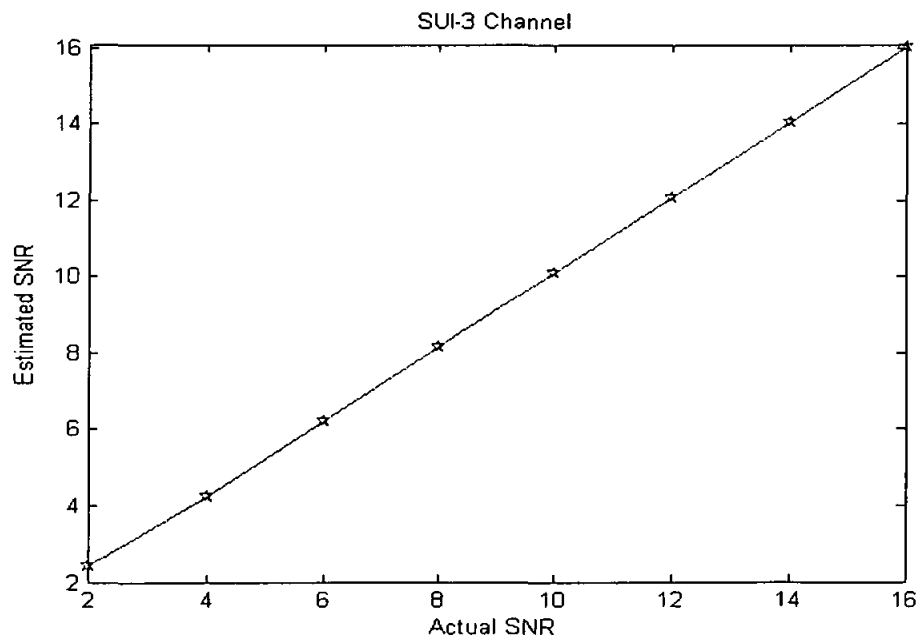


Fig.4.23 Estimated SNR vs. Actual SNR with SUI-3 Channel

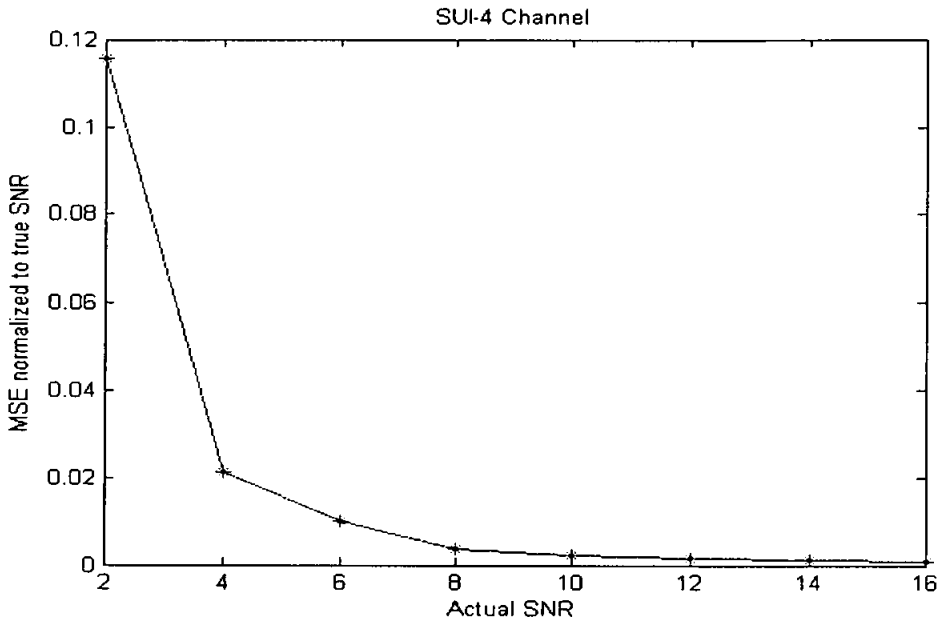


Fig.4.24 SNR NMSE vs. actual SNR with SUI-4 Channel

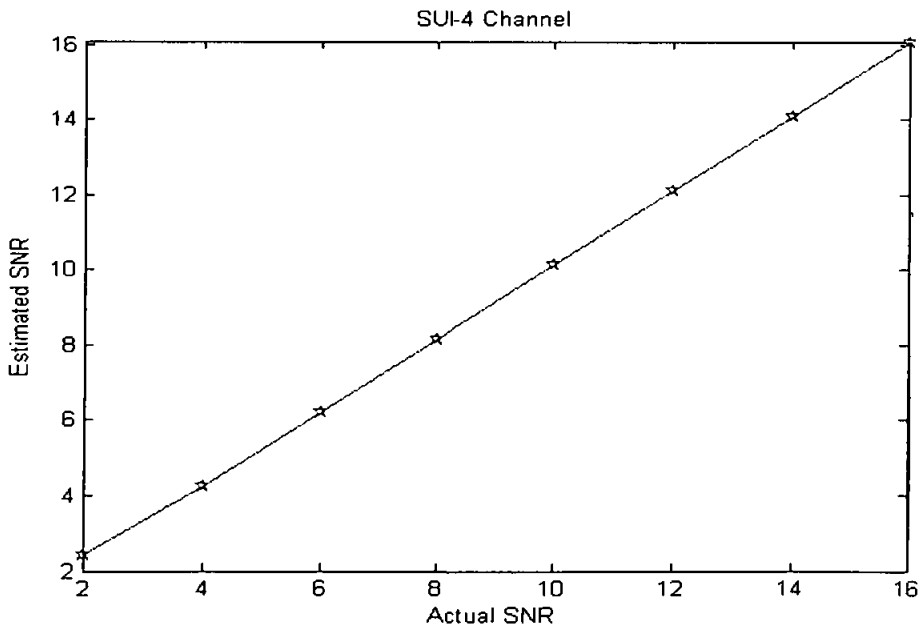


Fig.4.25 Estimated SNR vs. Actual SNR with SUI-4 Channel

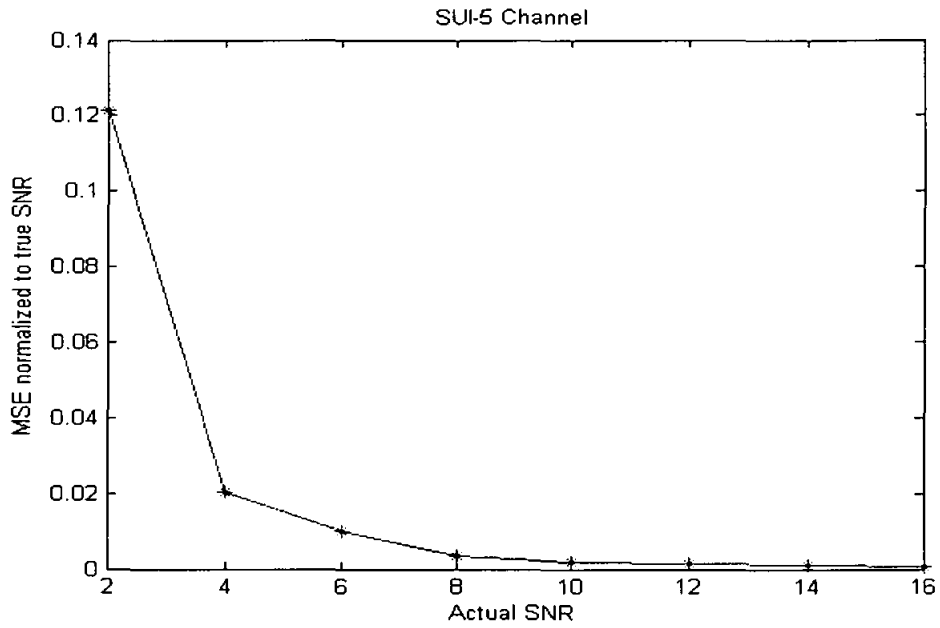


Fig.4.26 SNR NMSE vs. actual SNR with SUI-5 Channel

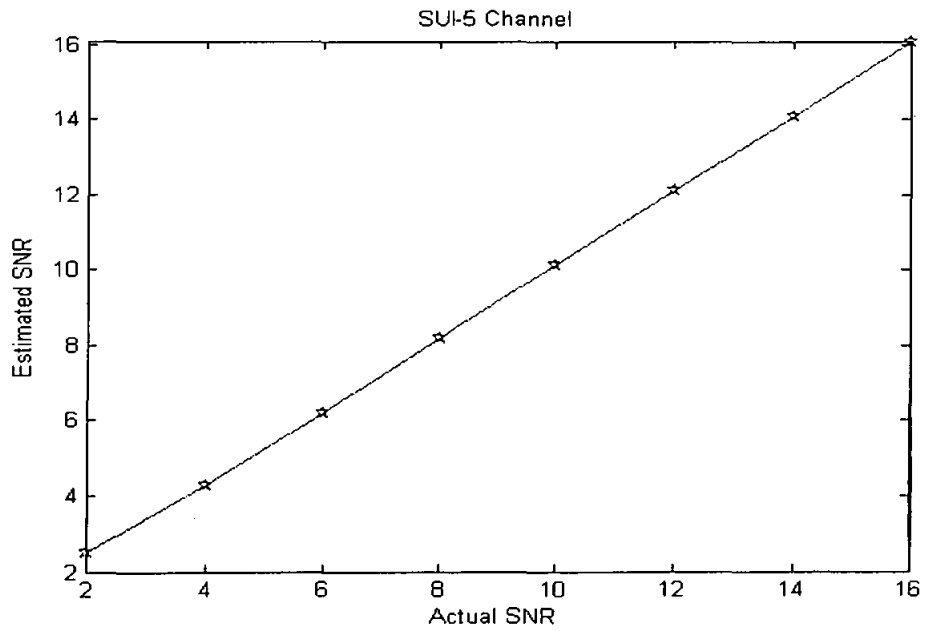


Fig.4.27 Estimated SNR vs. Actual SNR with SUI-5 Channel

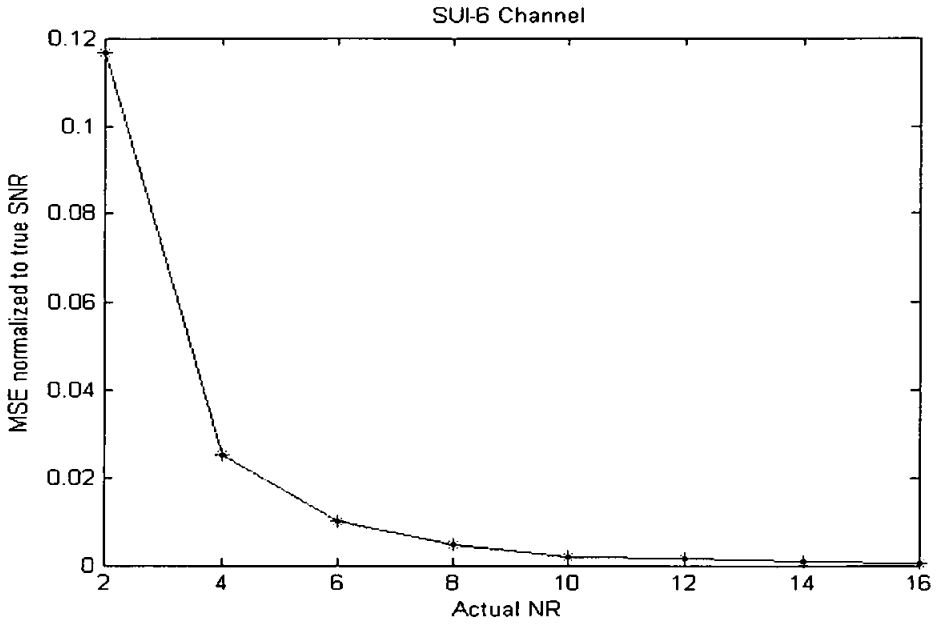


Fig.4.28 SNR NMSE vs. actual SNR with SUI-6 Channel

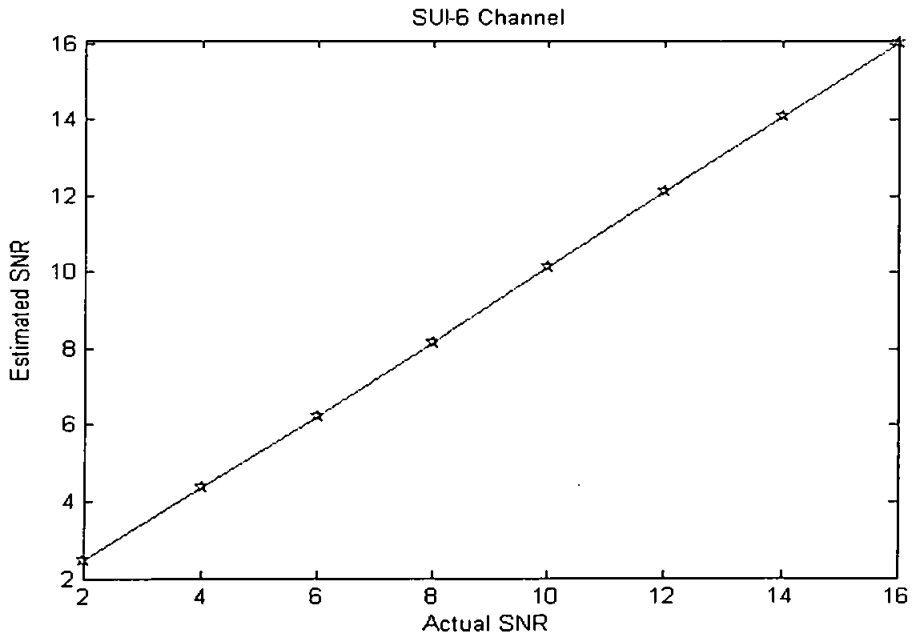


Fig.4.29 Estimated SNR vs. Actual SNR with SUI-6 Channel

4.2.1.4 Performance over Indoor Channel Model for Wi-Fi

In Fig 4.30 is shown the SNR NMSE is plotted against actual SNR using indoor channel models with 10 taps. Description of indoor channel models is shown in Table 4.4.

It can be seen from the Fig.4.30, that the proposed technique has very small NMSE error. It is observed that the rise in NMSE at small SNR is due to window effect of the system.

In Fig 4.31 estimated SNR is plotted against actual SNR. It can be seen that the estimates of SNR have very small bias and are very close to the actual SNR.

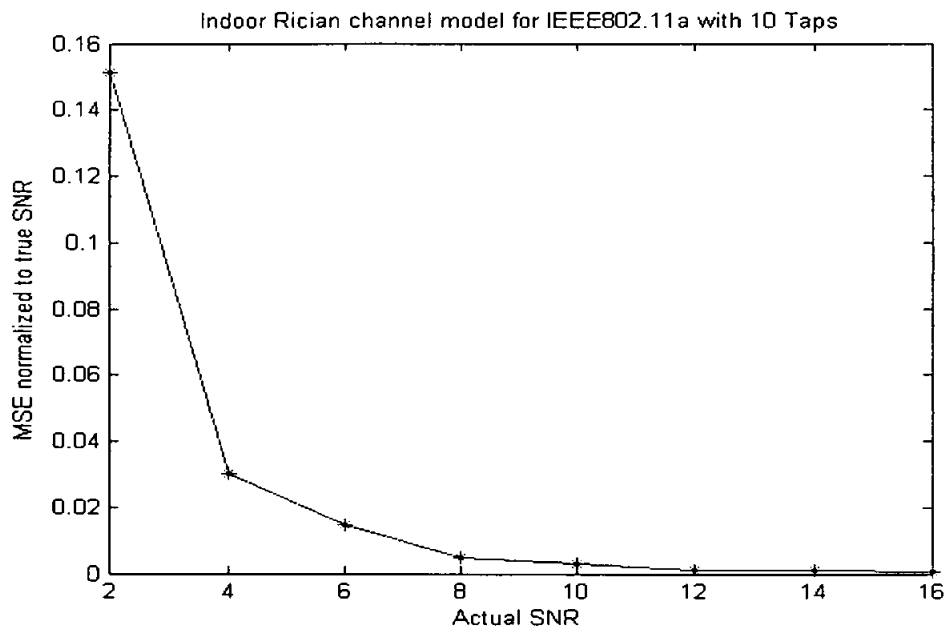


Fig. 4.30 SNR-NMSE vs. Actual SNR for IEEE802.11a

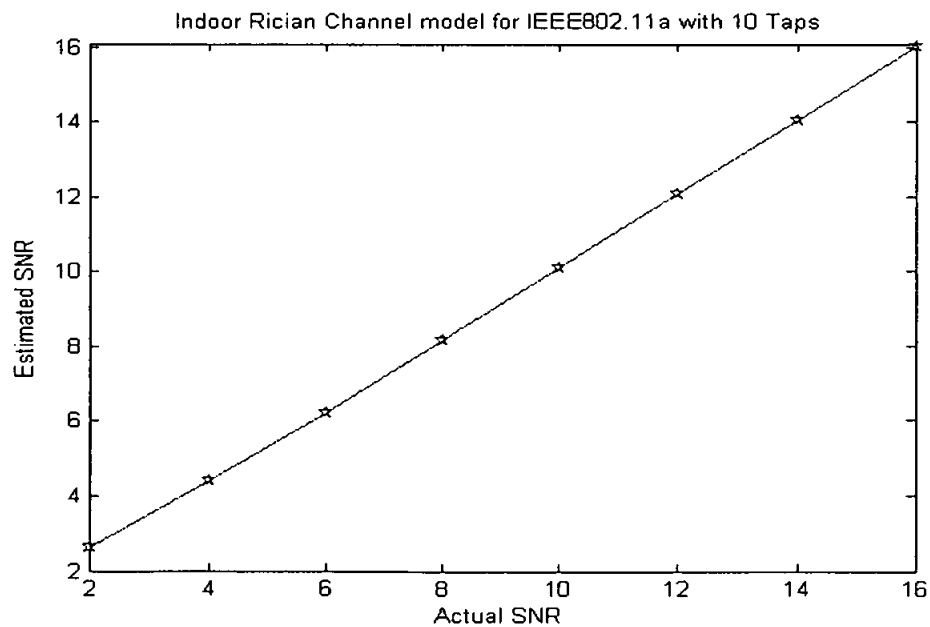


Fig.4.31 Estimated SNR vs. Actual SNR for IEEE802.11a

4.2.2 Computational Complexity

The proposed estimator has relatively low computational complexity because this is unlike other techniques is able to estimate the SNR from only one OFDM preamble signal. Incidentally the preamble used for the proposed technique is of OFDM systems. As we know, in systems which already employ training sequences for equalization or synchronization, there is no additional throughput penalty and those same known sequences could be used to maximize the performance of a DA-SNR estimator.

The proposed technique stipulates autocorrelation to estimate SNR. Autocorrelation on the received preamble at front end of the receiver and gives rise to two peaks because of two identical halves property of preamble. The signal power is obtained first and noise power later by subtracting the signal power from the magnitude of zero-lag peak. As discussed in detail in chapter 3 that at zero-lag, autocorrelation contains the signal power estimate as well as noise power estimate indistinguishable from each other.

Computational load comes primarily from computing autocorrelation. For an N point long preamble, the autocorrelation ($\sum_n x_n x(n+m)$) requires $2N^3$ multiplications and $2N^2$ additions.

Subspace estimator has relatively large complexity as compared to proposed estimator. First and foremost, it performs SNR estimation after 30 OFDM symbols beside FFT unlike proposed technique. FFT is the heart of OFDM systems and very complex due to large amount of multiplications. Subspace estimator gives better SNR estimates only after 20 OFDM symbols. It is based on an eigenvector decomposition of the estimated channel correlation matrix. To track the time variation of the SNR, it forms a moving average of the correlation matrix from the K most recent observation matrix, where K is the observed subspace which contains both the channel power and noise power. Minimum descriptive length (MDL) criteria is used to find the number of multipath (L) which contains signal subspace and the noise subspace. It is observed that subspace method is

quite complex as it makes use of many calculations and many OFDM symbols to give accurate SNR estimates. To perform comparison of this technique with our proposed technique, we used 30 OFDM symbol for subspace method vs. One OFDM preamble for proposed estimator. The comparison results shown that the proposed technique performs better SNR estimation than subspace estimator.

Reddy estimator has also relatively large computational complexity as compared to proposed estimator. Like subspace method it also perform SNR estimation after FFT. It also gives better SNR estimated with more than 30 OFDM symbols. Averaging window is used to perform averaging across several OFDM symbols as well as across OFDM subcarriers. Due to averaging over large number of OFDM symbols it becomes complex as compared to proposed estimator which makes use of only one OFDM symbol to perform SNR estimation.

Complexity of the SNR estimators discussed above is summarized in the Table 4.5 below. It can be seen that the proposed SNR estimator is computationally less complex to perform SNR estimation. The proposed technique needs only one OFDM preamble to find good SNR estimates as compared to Reddy and subspace which uses 30 OFDM symbols to get good SNR estimates. Reddy and subspace estimators has big complexity because of averaging over so many OFDM symbols and also it makes use of many long and complex calculations to reach a better SNR estimate. Unlike Reddy and subspace estimators, the proposed estimator needs no channel frequency response to find noise power and signal power.

Table 4.5 Complexity comparison of SNR estimators

(a) Reddy SNR estimator (Pilot Based), Back-End Estimator	
FFT= $Y_m(k) = DFT\{y_m(n)\} = \sum_n y_m(n) e^{-j2\pi nk/N}$	complexity $\sim N^3$
Channel Frequency Response = $\hat{H}_m(k) = \frac{Y_m(k)}{S_m(k)}$	complexity $\sim N^2$
Instantaneous Noise Power (N) = $\sigma_{N(m)}^2(k) = Y_m(k) - \hat{X}_m(k) \hat{H}_m(k) ^2$	complexity $\sim 2N$
Instantaneous Signal power = $\hat{P}_{(s,j)} = \frac{1}{k} \sum_{l=1}^k Y_m(l) ^2$	complexity $\sim N$
Total complexity of Reddy's Estimator (where 30 shows the number of OFDM symbols used to get better SNR estimates after averaging over these OFDM symbols in both time and frequency domain)	complexity $\sim 30 N^3$
(b) Subspace SNR Estimator (Pilot Based) , Back-End Estimator	
FFT= $Y_m(k) = DFT\{y_m(n)\} = \sum_n y_m(n) e^{-j2\pi nk/N}$	complexity $\sim N^3$
Channel Frequency Response = $H_{i,n} = \sum_{l=1}^L h_i(i, T_s) e^{-j2\pi \frac{nl}{NT}}$	complexity $\sim N$
$\psi = W_p E (h_l \cdot h_l^H) W_p^H$	complexity $\sim N^2$
Compute Moving Average Estimates of Correlation matrix $\hat{R}(m) = \frac{1}{k} \sum_{i=m-K+1}^m H_{i,p} \cdot H_{i,p}^H$	complexity $\sim N^3$
Estimate the Current Dimensions of the subspace using MDL criteria which gives the number of estimated multipath 'L'	

$MDL(k) = -K(M-k) \log \left(\frac{\prod_{i=k+1}^M \hat{\lambda}_i^{1/(M-k)}}{\frac{1}{M-K} \sum_{i=k+1}^M \hat{\lambda}_i} \right) + \frac{1}{2} k(2M-k) \log(K)$	complexity $\sim N^4$
$\hat{L} = \arg \min_k MDL(k) \quad k \in \{0, 1, 2, \dots, M-1\}$	complexity $\sim N$
$\text{Channel Power} = \hat{\sigma}_s^2 = \frac{1}{M} \left(\sum_{i=1}^{\hat{L}} \hat{\lambda}_i - \hat{L} \cdot \hat{\sigma}_N^2 \right)$	complexity $\sim N$
$\text{Noise Power} = \hat{\sigma}_N^2 = \frac{1}{M - \hat{L}} \sum_{i=\hat{L}+1}^M \hat{\lambda}_i$	complexity $\sim N$
<p>Total complexity of subspace estimator complexity $\sim 30 N^4$ (where 30 shows the number of OFDM symbols used to get better SNR estimates after averaging over these OFDM symbols in both time and frequency domain)</p>	
<p>(c) Proposed SNR Estimator (Preamble Based), Front-End Estimator</p>	
$\text{Autocorrelation of received signal} = R_{yy}(m) = R_{xx}(m) + R_{nn}(m)$	complexity $\sim 2 N^3$
$\text{Total complexity of developed estimator} =$	complexity $\sim 2 N^3$

4.2.3 Sensitivity Analysis

To analyze the sensitivity of developed estimator, we derive the estimated SNR with respect to correlation peaks at $(L-N/2, L-N$ and $L)$ that used to estimate the SNR.

As we know, SNR estimated is

$$SNR = \frac{\hat{P}_o}{\hat{\sigma}_N^2} = \frac{2R_{yy}(L - N/2) - R_{yy}(L - N)}{R_{yy}(L) - 2R_{yy}(L - N/2) - R_{yy}(L - N)} \quad (4.2)$$

To perform sensitivity analysis let us suppose that

$$S\hat{N}R = \frac{2x_1 - x_2}{x_3 - (2x_1 - x_2)} \quad (4.3)$$

where,

$$x_1 = R_{yy} (L - N/2)$$

$$x_2 = R_{yy} (L - N)$$

$$x_3 = R_{yy} (L)$$

Any change in the estimated ($S\hat{N}R$) SNR is given by

$$\Delta S\hat{N}R = \frac{\partial S\hat{N}R}{\partial x_1} \cdot \Delta x_1 + \frac{\partial S\hat{N}R}{\partial x_2} \cdot \Delta x_2 + \frac{\partial S\hat{N}R}{\partial x_3} \cdot \Delta x_3 \quad (4.4)$$

where

$$\begin{aligned} \frac{\partial S\hat{N}R}{\partial x_1} &= \frac{2 - x_2/x_3}{x_3 - 2 + x_2/x_1} \\ \frac{\partial S\hat{N}R}{\partial x_2} &= \frac{2x_1/x_2 - 1}{x_3/x_2 - 2x_1/x_2 + 1} \\ \frac{\partial S\hat{N}R}{\partial x_3} &= \frac{2x_1/x_3 - x_2/x_3}{1 - 2x_1/x_3 + x_2/x_3} \end{aligned} \quad (4.5)$$

The parameter of eq. 4.5 describe the sensitivity of estimated SNR as a function of x_1 , x_2 and x_3 . The sensitivity of estimated SNR with respect to $(L-N)$ peak, $(L-N/2)$ peak and (L) peak is plotted against actual SNR value in Fig 4.32, Fig 4.33 and Fig 4.34. The SNR is varied from 1 dB to 16 dB.

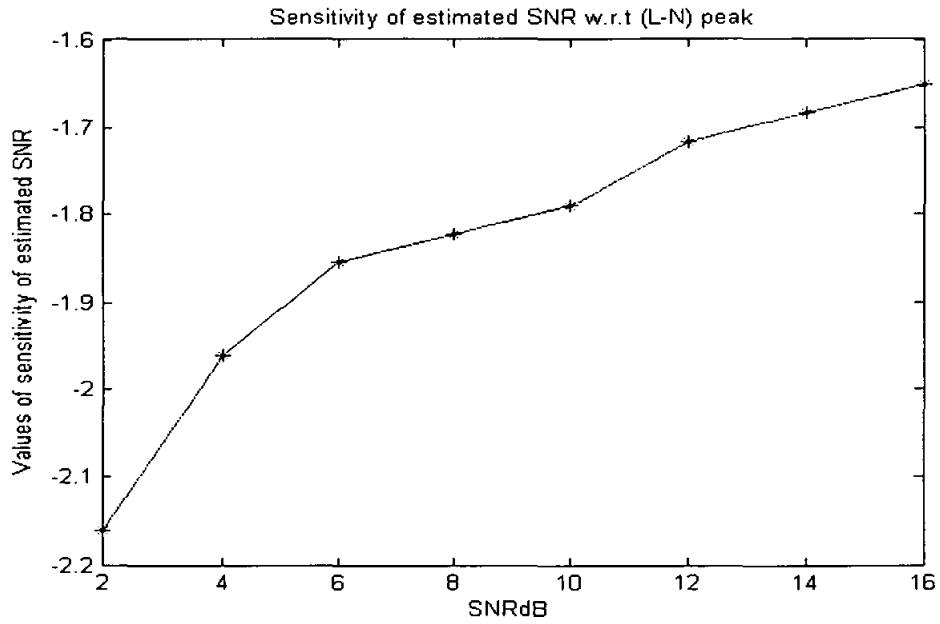


Fig.4.32 : Sensitivity of estimated SNR w.r.t. (L-N) peak

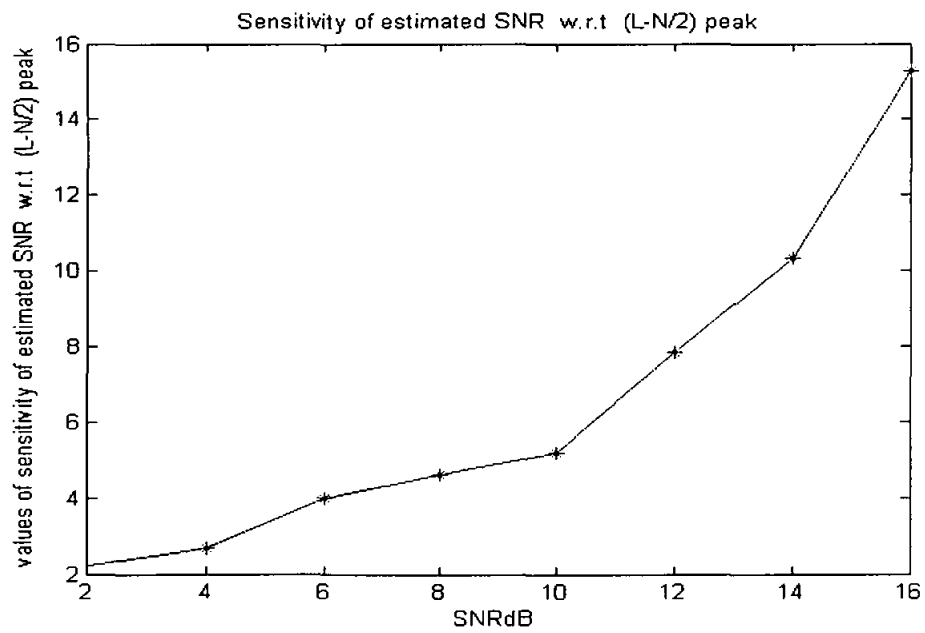


Fig.4.33 : Sensitivity of estimated SNR w.r.t. (L-N/2) peak

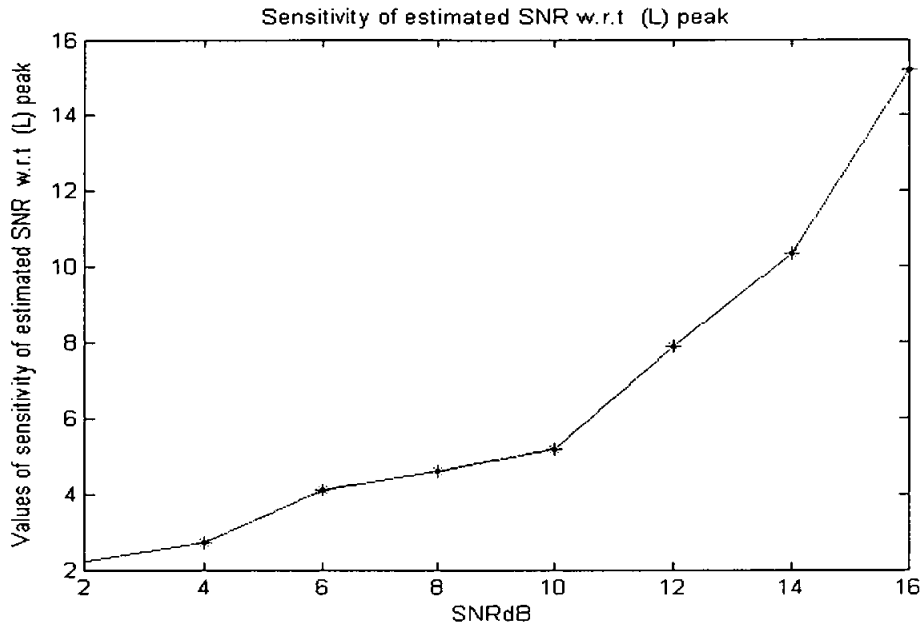


Fig.4.34 : Sensitivity of estimated SNR w.r.t. (L) peak

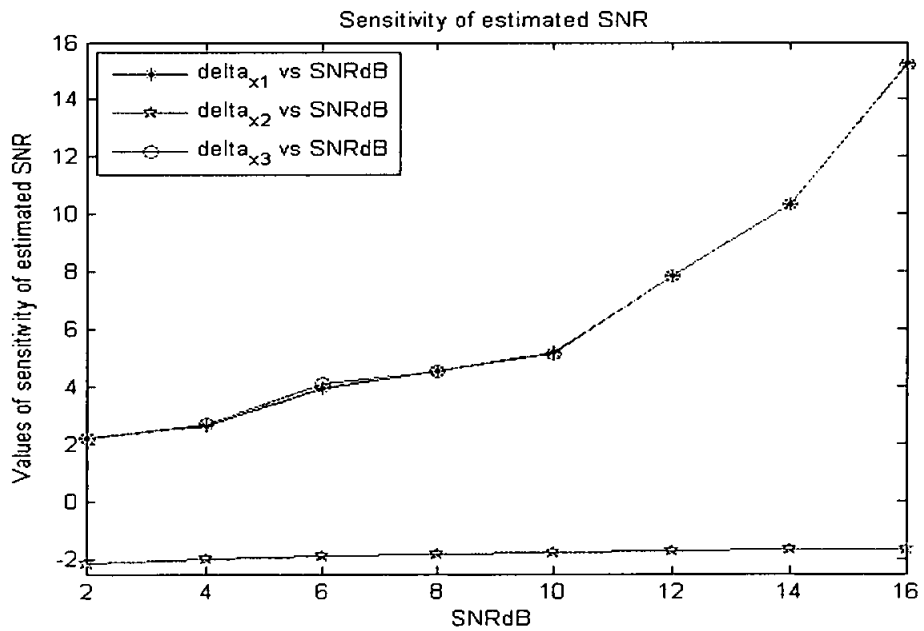


Fig.4.35 : Combined results of sensitivity of estimated SNR

It is observed from the Fig. 4.32, Fig 4.33 and Fig. 4.34, that the estimated SNR is more sensitive to ($L-N$) peak and (L) peak.

In summary, the three criteria used for the search of good SNR estimator are:

- Accuracy of SNR estimates
- Minimum computational complexity
- Easy to implement.

The results show that the proposed estimator fulfill the criteria of good SNR estimator

4.3 Analysis Results of SNR Estimation Technique for Multipath Channel with Colored Noise using Wavelet-Packet Transform in OFDM Systems

The technique describe in section 4.2 is extended to obtaining noise power estimates of colored noise using wavelet-packet based filter bank analysis of the noise. The proposed technique is compared with Reddy's estimator for colored noise in OFDM system with parameters given in Table 3.4 as shown in chapter 3. SNR is varied from 1 dB to 20 dB for each sub-band and the mean-squared error (MSE) is derived for the estimated SNR from 2000 trials according to the following formula

$$MSE = \frac{1}{2000} \sum_{i=1}^{2000} \{ \hat{SNR}(i) - SNR \}^2 \quad (4.6)$$

Figure 4.36 shows the mean-square-error performance of the proposed and conventional algorithms in colored noise. The mean-squared-error between the actual SNR and estimated SNR values in each sub-band are calculated and averaged. As can be seen the proposed algorithm performs much better than Reddy's SNR estimation.

Fig.4.37 shows the plot of actual SNR vs. estimated SNR over all OFDM signal. SNR is estimated in each sub-band first than averaging over all sub-band is performed to get a global (over all sub-carriers) SNR estimates.

Therefore, the proposed approach estimates both local (within smaller sets of subcarriers) and global (over all sub-carriers) SNR values. The short term local estimates calculate the noise power variation across OFDM sub-carriers. These estimates are specifically very useful for adaptive modulation, and optimal soft value calculation for improving channel decoder performance.

The results show that the proposed estimator gives better performance in SNR estimation as compared to Reddy estimator.

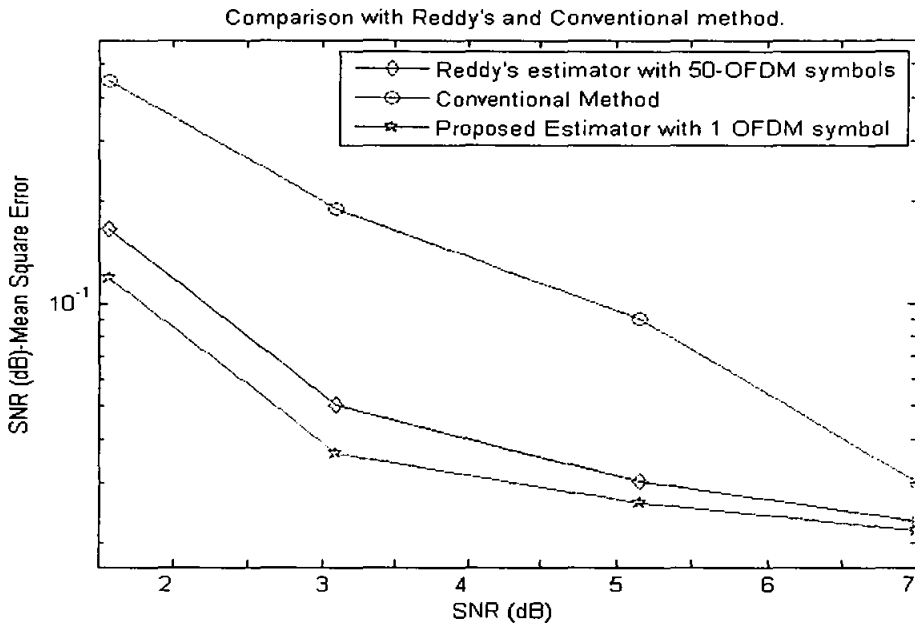


Fig.4.36. Mean-square-error performance of the proposed technique with colored noise

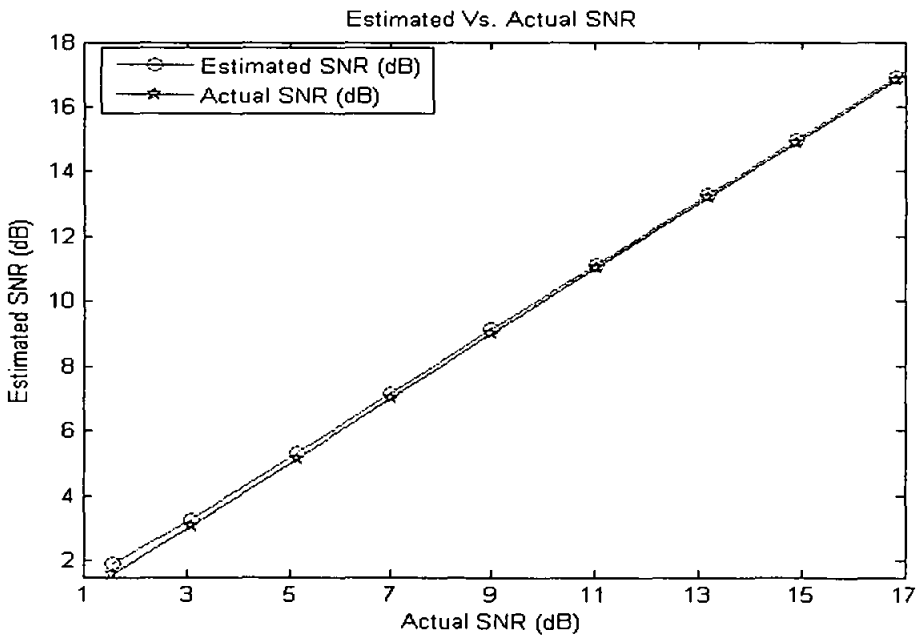


Fig.4.37. Estimated SNR vs. Actual SNR with colored noise

4.3.1 Performance Comparisons of colored noise estimator

Fig.4.36 shows that the proposed technique gives very accurate estimates of colored noise variation which is very useful for adaptive modulation. Proposed technique is compared with Reddy estimator for colored noise. From the results it can be shown that the proposed technique, with only one OFDM symbol, perform better than Reddy estimator which is using 50 OFDM symbols. The mean squared error of proposed technique is much lower than Reddy estimator.

Fig.4.37 shows that the SNR estimates of colored noise using proposed technique is very close to the actual SNR values and has very small bias.

4.4 Summary

In this chapter, the results of proposed front-end noise power and SNR estimation technique for white noise as well as for colored noise are discussed. The simulations are conducted in both frequency non-dispersive and dispersive channels with real additive white Gaussian noise (AWGN) and also colored noise. The results of SNR estimation technique for AWGN in OFDM systems are presented and compared with previously techniques in terms of normalized mean squared error (NMSE) and estimated SNR. The results of SNR estimation technique for colored noise using wavelet-packet in OFDM systems are shown and compared with previous techniques in terms of mean squared error (MSE) and estimated SNR. The results show that the proposed technique gives better performance than previously published SNR estimators. It is observed that the proposed technique can estimate local statistics of the noise power when the noise is colored. The proposed estimator has relatively low computational complexity because it makes use of only one OFDM preamble signal to find the SNR estimates. The proposed estimator is fulfills the criteria of best SNR estimator because it is unbiased (or exhibits the smallest Bias) and has the smallest variance of SNR estimates as shown from results clearly.

5.1 Introduction

In the previous chapters, we have proposed an SNR estimation technique for OFDM systems and evaluated its performance. In this chapter, we conclude the entire work and suggest future work to further the research in this area.

5.2 Conclusion

In this thesis, a novel SNR estimation technique for OFDM is investigated. Most of the SNR estimation techniques discussed in chapter 2 are for single-carrier systems. There is not that much work conducted for OFDM systems. All the estimators discussed in the literature derive the symbol SNR estimates solely from the received signal at the output of the matched filter assuming intersymbol interference (ISI)-free output of the MF (the decision variable). However, in practice, multipath wireless communication gives rise to intersymbol interference, especially in indoor and urban areas. In these ISI dominated scenarios, SNR estimators that do not presume ISI-free reception are highly desirable. Thus, we are able to establish the motivation and build the foundation to the problem of SNR estimation with the aim of providing the most accurate SNR estimates at the front-end of the receiver.

Looking forward to evaluate and test the performance of our proposed SNR estimation, a complete end-to-end OFDM-FBWA system has been developed in Matlab® in both

frequency non-dispersive and dispersive channels with real additive white Gaussian noise (AWGN) and also with colored noise.

To be able to estimate the SNR estimates at front-end of the receiver effectively, we have set ourselves 2 objectives – firstly to select the training signal called preamble which is already in use for OFDM systems, so there will be no extra overhead on the system to perform SNR estimation and secondly, to develop an improved SNR estimation technique with minimal estimation error in mean square error (MSE) and estimated SNR.

We successfully developed an improved SNR estimation technique for OFDM systems. The SNR estimation technique, unlike others, performs noise power and SNR estimation at the front-end of the receiver. We have used the OFDM synchronization preamble for our SNR estimation technique so there would be no additional throughput penalty. The SNR estimation technique developed herein consists of two parts. In the first part, SNR estimation technique for AWGN channel has been developed. In the second part, the SNR estimation technique has been extended to include different noise power levels over the OFDM sub-carriers. The OFDM band has been divided into several sub-bands using wavelet packet and noise in each sub-band has considered white. The second-order statistics of the transmitted OFDM preamble has been calculated in each sub-band and the power of the noise has been estimated. Therefore, the proposed SNR estimation technique estimates both local (within smaller sets of subcarriers) and global (over all sub-carriers) SNR values. The short term local estimates provided the noise power variation across OFDM sub-carriers. When the noise is white, the developed SNR estimation technique works as good as the conventional noise power estimation schemes, showing the generality of the proposed method. We have obtained the simulation results for the proposed technique and compared them with those of previously published estimators for OFDM systems. These results show the superior performance of proposed SNR estimation technique in terms of accuracy of SNR estimates as measured by mean of mean squared error (MSE) and estimated SNR.

We have developed a novel front-end SNR estimation technique in OFDM systems based on one OFDM preamble that shows superior SNR estimation performance. This technique can be employed in practical OFDM systems.

5.3 Suggested Future Works

A possible extension of this work is to undertake the investigation of MIMO technique that enables separate and independent data streams to be transmitted simultaneously from different transmit antennas. This effectively increases the data rates without any expansion in bandwidth.

The front-end based developed technique in this work can be used for efficient inline diversity combining. There are several techniques in wireless communication systems to combat, or even exploit, the detrimental effect of fading channels. The most popular technique is the diversity combining technique, where multiple replicas of the same signal are used to reduce the amount of fading. By coherently combining these multiple copies of the transmitted signal, this technique provides reliability of the communication link and offers a higher dynamic range.

SNR estimation can be used to implement power control algorithms. In wireless communication systems, power control is applied to dynamically adjust the transmitted power according to some chosen criterion to meet the required SINR at the receiver. It represents a flexible tool for exploiting the degrees of freedom offered by the wireless channel. There are a variety of motivations behind the use of power control, including maintaining communication quality in the presence of fading and user mobility.

It is also worthwhile to investigate the problem of adaptive modulation in OFDM systems where an intelligent algorithm controls the modulation and forward error correction code used based on prevailing SNR conditions. The performance of adaptive modulation depends directly on how well the channel SNR is estimated. The more accurate the estimation of the channel SNR is, the better the choice of modulation scheme becomes,

and the better the ability to exploit the variations in the wireless channel is. A higher data rate burst is used when the SNR is high and a more robust but lower data rate burst profile is used when the SNR is low.

As we can see, there are many interesting and ground-breaking research work that can be undertaken as a follow-up to the work that we have done in OFDM systems.

REFERENCES

- [Adachi, 1991]. *BER performance of QDPSK with postdetection diversity reception in mobile radio channels*, IEEE Trans. Veh. Technol., vol. VT-40, pp. 237-219.
- [Adachi, 1993]. *Postdetection optimal diversity combiner for DPSK differential detection*, IEEE Trans. Veh. Technol., vol. VT-42, pp. 326-337.
- [Balaban, 1991]. *Statistical performance estimation of digital radio over fading channels*, in Proc. IEEE Int. Con f. Commun., Denver, CO, vol. 1, pp. 466-472.
- [Bournard, 2003]. *Novel Noise Variance and SNR Estimation Algorithm for Wireless MIMO OFDM Systems*", IEEE GLOBECOM vol., 2003
- [Brennan, 1959]. *Linear diversity combining techniques*, Proc. IRE. vol. 47, pp. 107.5-1102.
- [Chennakeshu, 1993]. *Differential detection of $\pi/4$ -shifted-DQPSK for digital cellular radio*," IEEE Trans. Veh. Technol., vol. VT-42, pp. 46-57.
- [Doukas, 2006]. *SNR Estimation for Low Bit Rate OFDM Systems in AWGN Channel*, Proceedings of ICNICONSMCL'06, IEEE comp., society.
- [Drieberg. 2000]. *MIMO Channel Estimation For Applications in Fixed Broadband Wireless Access Systems*, Master's Thesis, Universiti Teknologi PETRONAS (UTP), Malaysia.
- [Goldsmith, 1999]. *Adaptive Modulation and Coding for fading Channels*, IEEE Proceedings of the Information Theory and Communications Workshop.

REFERENCES

[Hagenauer, 1989]. *A Viterbi algorithm with soft-decision outputs and its applications*, in Proc. IEEE Global Commun. Conf., Dallas, TX, pp. 1650-1686.

[Haykin, 2005]. *Modern Wireless Communicatios*, Ontario, Pearson Education Inc.

[Hladik, 1992]. *Performance of differentially-detected $n/4$ -shifted DQPSK with diversity*, in Proc. 42nd IEEE Veh. Technol. Conf., Denver, CO, vol. 2, pp. 745-751.

[Holtzman, 1992]. *Adaptive measurement intervals for handoffs*, in Proc. IEEE Int. Conf. Commun., Chicago, IL, vol. 2, pp. 1032-1036.

[Hua Xu, 2004]. *A Non-data Aided SNR Estimation Algorithm for QAM Signals*, IEEE conf., pp. 103-107.

[IEEE802.11a, 1999]. *Standard for local and metropolitan area networks: Wireless LAN Medium Access Control (MAC) and Physical Layer (PHY) specifications. High Speed Physical Layer in the 5 GHz Band*. New York: The Institute of Electrical and Electronics Engineers Inc.

[IEEE802.11g, 2003]. *Standard for local and metropolitan area networks: Wireless LAN Medium Access Control (MAC) and Physical Layer (PHY) specifications – Amendment 4: Further Higher Data Rate Extension in the 2.4 GHz Band*. New York: The Institute of Electrical and Electronics Engineers Inc.

[IEEE802.16, 2001]. *Standard for local and metropolitan area networks: Air interface for fixed broadband wireless access systems*. New York: The Institute of Electrical and Electronics Engineers Inc.

[IEEE802.16, 2004]. *Standard for local and metropolitan area networks: Air interface for fixed broadband wireless access systems – Revision of IEEE802.16*. New York: The Institute of Electrical and Electronics Engineers Inc.

REFERENCES

- [IEEE802.16a, 2003]. *Standard for local and metropolitan area networks: Air interface for fixed broadband wireless access systems – Amendment 2: Medium access control modifications and additional physical layer specifications for 2-11 GHz*. New York: The Institute of Electrical and Electronics Engineers Inc.
- [Jakes, 1974]. *Microwave Mobile Communications*. New York: Wiley.
- [Jalali, 1994]. *Effects of diversity, power control, and bandwidth on the capacity of microcellular CDMA systems*, IEEE J. Select. Areas Commun., vol. SAG12, pp. 952-961.
- [Nidal, 2007]. *Linear prediction based approach to SNR estimation in AWGN channel*, 23rd Biennial Symposium on Communications.
- [Lee, 1982] *Mobile Communications Engineering*, New York: Mic-Graw Hill.
- [Matlab®, 7.0.4]. *Digital signal processing toolbox, communication toolbox and wavelet toolbox*.
- [Nahi, 1967]. *Use of limiters for estimating signal to noise ratio*, IEEE Trans. Infom. Theory, vol. IT-13, pp. 127-129.
- [Pauluzzi, 2000]. *A Comparison of SNR Estimation techniques for the AWGN Channel*”, IEEE Transactions on Communications, Vol. 48.
- [Prasad, 2004]. *OFDM for Wireless Communications Systems*, Boston, Artech House Inc.
- [Proakis, 1989] *Digital Communications*, New York: MicGraw-Hill, 2nd ed.
- [Ramesh, 2003]. *SNR Estimation in Nakagami Fading with Diversity for Turbo Decoding*, IEEE conf., Dianat, S.A. Rochester Inst. of Technol., NY.

REFERENCES

[Rana, 2007]. "Front-End estimation of Noise Power and SNR in OFDM Systems", IEEE-ICIAS vol. Malaysia.

[Rana, 2008]. "A Novel Front-End Noise Power and SNR Estimation for OFDM Systems", IEEE-WINSYS, vol., Portugal.

[Rana, 2008]. "Implementation of FFT using Discrete Wavelet Packet Transform (DWPT) and its Application to SNR Estimation in OFDM systems", IEEE-ITSIM-2008, Malaysia

[Rana, 2008]. "Novel Noise power and SNR Estimation in WiMAX systems", IEEE-ITSIM-2008, Malaysia

[Rappaport, 2002]. *Wireless communications: Principles and practice*. New Jersey: Prentice Hall PTR.

[Reddy, 2003]. *Noise Power and SNR Estimation for OFDM Based Wireless Communication Systems*, Wireless Communication and Signal Processing Group.

[Sampath, 2002]. A fourth generation MIMO-OFDM broadband wireless system: Design, performance and field trial results. *IEEE Communications Magazine*, 40, pp.143-149.

[Schmidl, 1997]. *Robust frequency and timing synchronization for OFDM*. *IEEE Trans. Commun*, pp. 1613-1621

[Shousheng, 1998]. Effective SNR Estimation in OFDM Systems Simulations Global Telecom., Conf. Sydney, IEEE (Globecom-98), Australia, vol 2, pp. 945-950.

[Sklar, 1997]. Rayleigh fading channels in mobile digital communication systems part 1: Characterization. *IEEE Communications Magazine*, 35, pp.90-100.

REFERENCES

- [Taesang, 2004]. *Throughput Optimization using Adaptive Techniques*, Technical Report, Wireless Systems Lab, Stanford University.
- [Van Nee, 2000]. *OFDM for wireless multimedia communications*. London: Artech House.
- [Vijayan, 1992]. *Analysis of handoff algorithm using nonstationary signal strength measurements*, in Proc. IEEE Global Commun. Conf., Orlando, FL.
- [Wax, 1985]. *Detection of Signals by Information Theoretic Criteria*, IEEE Transactions on Acoustics, Speech and Signal Processing, Vol. ASSP-33 NO.2.
- [Whitehead, 1993]. *Signal-level-based dynamic power control for cochannel interference management*, in Proc. IEEE Veh. Technol. Conf, Secaucas, NJ, pp. 499-502.
- [Winters, 1984]. *Optimum combining in digital mobile radio with cochannel interference*, IEEE Trans. Veh. Technol., vol. VT-33, pp. 144-155.
- [Winters, 1993]. *Signal acquisition and tracking with adaptive arrays in the digital mobile radio system IS-54 with flat fading*, IEEE Trans. Veh. Technol., vol. VT-42, pp. 377-354.
- [Wintz, 1969]. *Performance of optimum and suboptimum synchronizers*," IEEE Trans. Commun. Technol., vol. COM-17, pp. 380-389.
- [Xiaodong 2005]. *Subspace- Based Noise Variance and SNR Estimation for OFDM Systems*, IEEE Wireless Communications and Networking Conference.
- [Yucek, 2005]. *Noise plus Interference Power Estimation in Adaptive OFDM systems*, IEEE conf.

REFERENCES

[Zander, 1992]. *Performance of optimum transmitter power control in cellular radio systems*, IEEE Trans. Veh. Technol., vol. VT-41, pp. 57-62.

[Zhang, 1994]. *Analysis of handoff algorithms using both absolute and relative measurements*, in Proc. IEEE Veh. Technol. Conf., Stockholm, Sweden, vol. 1, pp. 82-86.

PUBLICATIONS

Conference Papers

Rana Shahid Manzoor, Wabo Majavu, Varun Joeti, Nidal Kamel and Muhammad Asif, "*Front-End estimation of Noise Power and SNR in OFDM Systems*", IEEE-ICIAS vol. , 2007, Malaysia

Rana Shahid Manzoor, Varun Jeoti, Nidal Kamel And M.Asif, "*A Novel Front-End Noise Power and SNR Estimation For OFDM Systems*", IEEE-WINSYS vol., July 2008, Porto, Portugal.

Rana Shahid Manzoor, Regina gani, Varun Jeoti, Nidal Kamel and M.Asif, "*Implementation of FFT using Discrete Wavelet Packet Transform (DWPT) and its Application to SNR Estimation in OFDM systems*", IEEE-ITSIM-2008, Malaysia

Rana Shahid Manzoor, Varun Jeoti, Nidal Kamel And M.Asif, "*Novel Noise power and SNR Estimation in WiMAX systems*", IEEE-ITSIM-2008, Malaysia

Journal Papers

Rana Shahid Manzoor, Varun Jeoti, Nidal Kamel And M.Asif, "*A Novel front-end SNR estimation technique for OFDM Systems*". (Under process)

Rana Shahid Manzoor, Regina gani, Varun Jeoti, Nidal Kamel And M.Asif, "Discrete Wavelet Packet Transform (DWPT) based FFT and its Application to SNR Estimation in OFDM systems". (Under process)

Rana Shahid Manzoor, Varun Jeoti, Nidal Kamel And M.Asif, "*A Novel front-end SNR estimation using wavelet packets in OFDM Systems*". (Under process)

APPENDICES

APPENDIX

A

WAVELET PACKETS
AND WAVELET PACKET
TRANSFORMS

A.1 Introduction

A wavelet decomposition or transform simply re-expresses a function in terms of the wavelet basis $\{\psi_{j,k}(t)\}$. This amounts to decomposing the function space L^2 into a direct sum of orthogonal subspaces $\{W_j\}$ and choosing the combination of the orthonormal bases for W_j s as the orthonormal basis for L^2 . In the case of finite data with information up to a resolution level J , a wavelet transform performs a decomposition of the space V_J into a direct sum of orthogonal subspaces

$$V_J = W_{J-1} \oplus V_{J-1} = W_{J-1} \oplus W_{J-2} \oplus V_{J-2} = \dots = \bigoplus_{j=0}^{J-1} W_j \oplus V_0 \tag{A.1}$$

and the union of the bases of these subspaces forms a basis for the wavelet decomposition. This, of course, is by no means the only way to decompose the space L^2 or V_J . In this section we generalize the wavelet decomposition and introduce a whole family of orthonormal bases for function space.

From multiresolution analysis, we know that given the basis functions $\{\phi_{1,k}(t)\}$ of V_1 , $\{\phi(t-k)\}$ and $\{\psi(t-k)\}$ constitute an orthonormal basis for V_0 and W_0 , respectively, and $V_1 = V_0 \oplus W_0$, where

$$\phi(t) = \sqrt{2} \sum_k h_k \phi(2t-k) \text{ and } \psi(t) = \sqrt{2} \sum_k g_k \phi(2t-k). \tag{A.2}$$

So the V space can be decomposed into a direct sum of the two orthogonal subspaces defined by their basis functions given by the above two equations. This "splitting trick" or splitting algorithm can be used to decompose W spaces as well. For example, if we analogously define

$$w_2(t) = \sqrt{2} \sum_k h_k \psi(2t - k) \text{ and } w_3(t) = \sqrt{2} \sum_k g_k \psi(2t - k), \tag{A.3}$$

then $\{w_2(t - k)\}$ and $\{w_3(t - k)\}$ are orthonormal basis functions for the two subspaces whose direct sum is W_1 . In general, for $n = 0, 1, \dots$, we define a sequence of functions as follows:

$$w_{2^n}(t) = \sqrt{2} \sum_k h_k w_n(2t - k) \tag{A.4}$$

and

$$w_{2^{n+1}}(t) = \sqrt{2} \sum_k g_k w_n(2t - k). \tag{A.5}$$

Clearly, setting $n = 0$, we get $w_0(t) = \phi(t)$, the scaling function, and $n = 1$ yields $w_1(t) = \psi(t)$, the mother wavelet. So far we have been using the combination of $\{\phi(2^j t - k)\}$ and $\{\psi(2^j t - k)\}$ to form a basis for V_j , and now we have a whole sequence of functions $w_n(t)$ at our disposal. Various combinations of these and their dilations and translations can give rise to various bases for the function space. So we have a whole collection of orthonormal bases generated from $\{w_n(t)\}$. We call this collection a "library of wavelet packet bases", and the function of the form $w_{n,j,k} = 2^{j/2} w_n(2^j t - k)$ is called a wavelet packet. Let us call the space formed by the basis $\{w_{n,j,k}(t)\}_k w_{n,j}$; the following diagram illustrates the decomposition of the space $w_{0,3}$ (i.e., V_3) using wavelet packets.

$w_{0,3}$							
$w_{0,2}$				$w_{1,2}$			
$w_{0,1}$		$w_{1,1}$		$w_{2,1}$		$w_{3,1}$	
$w_{0,0}$	$w_{1,0}$	$w_{2,0}$	$w_{3,0}$	$w_{4,0}$	$w_{5,0}$	$w_{6,0}$	$w_{7,0}$

Fig. A.1 Wavelet packet decomposition

Accordingly, a function $x(t)$ expressed in terms of these orthogonal family of wavelet packets is as follows:

$$x(t) = \sum_{i=-\infty}^{\infty} \sum_{j=1}^J a(i, j)\theta(t - i) + \sum_{i=-\infty}^{\infty} \sum_{j=1}^J d(i, j)\theta(t - j) \tag{A.6}$$

Where $a(i,j)$ are scaling coefficients at j scale and i delay and $d(i,j)$ are details.

As an example, we look at the wavelet packets generated from the Haar filter. Since the Haar filter has $h_0 = h_1 = 1/\sqrt{2}$, and, using $g_k = (-1)^k h_{1-k}$, $g_0 = -g_1 = 1/\sqrt{2}$, we have

$$w_{2n}(t) = w_n(2t) + w_n(2t - 1) \tag{A.7}$$

and

$$w_{2n+1}(t) = w_n(2t) - w_n(2t - 1) \tag{A.8}$$

with $w_0(t)$ the characteristic function on the unit interval.

Using a pair of low-pass and high-pass filters to split a space corresponds to splitting the frequency content of a signal into roughly a low-frequency and a high-frequency component. In wavelet decomposition we leave the high-frequency part alone and keep splitting the low-frequency part. In wavelet packet decomposition, we can choose to split

the high-frequency part also into a low-frequency part and a high-frequency part. So in general, wavelet packet decomposition divides the frequency space into various parts and allows better frequency localization of signals.

The transformation of data into wavelet packet basis presents no extra difficulties. We can simply do a convolution using filters h and g on the details $\{d_k^j\}$ as well as on the trend $\{f_k^j\}$. As in the wavelet transform, we can keep doing the decomposition until we cannot go any further. On the other hand, we can also choose not to decompose a particular subspace while decomposing others. So there are many choices for decomposing a signal. We can keep all the coefficients at all decomposition levels and generate a table of coefficients of wavelet packet decomposition.

A.2 Matlab® Wavelet Toolbox

The Wavelet Toolbox contains graphical tools and command line functions that let you examine and explore characteristics of individual wavelet packets. Perform wavelet packet analysis of one- and two-dimensional data. Use wavelet packets to compress and remove noise from signals and images. This chapter takes you step-by-step through examples that teach you how to use the Wavelet Packet 1-D and Wavelet Packet 2-D graphical tools. The last section discusses how to transfer information from the graphical tools into your disk, and back again. Because of the inherent complexity of packing and unpacking complete wavelet packet decomposition tree structures, we recommend using the Wavelet Packet 1-D and Wavelet Packet 2-D graphical tools for performing exploratory analyses. The command line functions are also available and provide the same capabilities. However, it is most efficient to use the command line only for performing batch processing.

A.3 Wavelet Packet

The wavelet packet method is a generalization of wavelet decomposition that offers a richer signal analysis. Wavelet packet atoms are waveforms indexed by three naturally interpreted parameters: position, scale (as in wavelet decomposition), and frequency. For a given orthogonal wavelet function, we generate a library of bases called wavelet packet

bases. Each of these bases offers a particular way of coding signals, preserving global energy, and reconstructing exact features. The wavelet packets can be used for numerous expansions of a given signal. We then select the most suitable decomposition of a given signal with respect to an entropy-based criterion.

There exist simple and efficient algorithms for both wavelet packet decomposition and optimal decomposition selection. We can then produce adaptive filtering algorithms with direct applications in optimal signal coding and data compression.

A.4 from Wavelets to Wavelet Packets: Decomposing the Details

In the orthogonal wavelet decomposition procedure, the generic step splits the approximation coefficients into two parts. After splitting we obtain a vector of approximation coefficients and a vector of detail coefficients, both at a coarser scale. The information lost between two successive approximations is captured in the detail coefficients. Then the next step consists of splitting the new approximations coefficient vector; successive details are never reanalyzed.

In the corresponding wavelet packet situation, each detail coefficient vector is also decomposed into two parts using the same approach as in approximation vector splitting. This offers the richest analysis: the complete binary tree is produced as shown in the following figure.

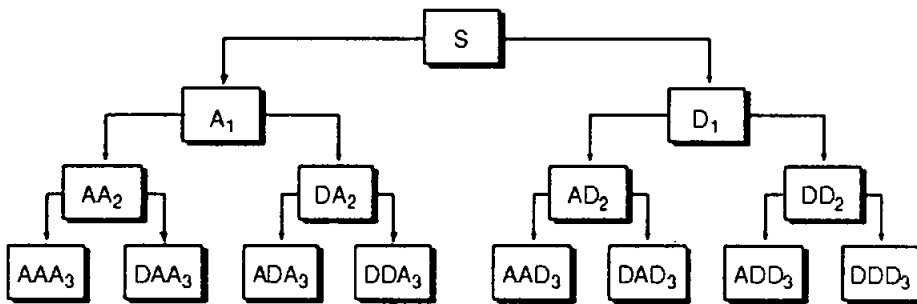


Fig.A.2: Wavelet Packet Decomposition Tree at Level 3

The idea of this decomposition is to start from a scale-oriented decomposition, and then to analyze the obtained signals on frequency sub-bands. The wavelet packet functions and their purpose are shown in the following Tables A.1 - A.4.

Table A.1: Analysis-Decomposition Functions.

Function Name	Purpose
<u>wpccoef</u>	Wavelet packet coefficients
<u>wpdec</u> and <u>wpdec2</u>	Full decomposition
<u>wpsplt</u>	Decompose packet

Table A.2: Synthesis-Reconstruction Functions.

Function Name	Purpose
<u>wprcoef</u>	Reconstruct coefficients
<u>wprec</u> and <u>wprec2</u>	Full reconstruction
<u>wpjoin</u>	Recompose packet

Table A.3: Decomposition Structure Utilities.

Function Name	Purpose
<u>besttree</u>	Find best tree
<u>bestlevt</u>	Find best level tree
<u>entrupd</u>	Update wavelet packets entropy
<u>get</u>	Get WPTREE object fields contents
<u>read</u>	Read values in WPTREE object fields
<u>wenergy</u>	Entropy
<u>wp2wtree</u>	Extract wavelet tree from wavelet packet tree
<u>wpcutree</u>	Cut wavelet packet tree

Table A.4: De-Noising and Compression.

Function Name	Purpose
<code>ddencmp</code>	Default values for de-noising and compression
<code>wbmpen</code>	Penalized threshold for wavelet packet de-noising
<code>wpdencmp</code>	De-noising and compression using wavelet packets
<code>wpthcoef</code>	Wavelet packets coefficients thresholding
<code>wthrmngr</code>	Threshold settings manager

In the wavelet packet framework, compression and de-noising ideas are exactly the same as those developed in the wavelet framework. The only difference is that wavelet packets offer a more complex and flexible analysis, because in wavelet packet analysis, the details as well as the approximations are split as shown in Fig A.2.

Single wavelet packet decomposition gives a lot of bases from which you can look for the best representation with respect to a design objective. This can be done by finding the "best tree" based on an entropy criterion.

De-noising and compression are interesting applications of wavelet packet analysis. The Wavelet packet de-noising or compression procedure involves four steps:

Step1. Decomposition

For a given wavelet, compute the wavelet packet decomposition of signal x at level N .

Step2. Computation of the Best Tree

For given entropy, compute the optimal wavelet packet tree. Of course, this step is optional. The graphical tools provide a Best Tree button for making this computation quick and easy.

Step3. Thresholding of Wavelet Packet Coefficients

For each packet (except for the approximation), select a threshold and apply thresholding to coefficients. The graphical tools automatically provide an initial threshold based on balancing the amount of compression and retained energy. This threshold is a reasonable first approximation for most cases. However, in general you will have to refine your threshold by trial and error so as to optimize the results to fit your particular analysis and design criteria. The tools facilitate experimentation with different thresholds, and make it easy to alter the tradeoff between amount of compression and retained signal energy.

Step4. Reconstruction

Compute wavelet packet reconstruction based on the original approximation coefficients at level N and the modified coefficients.

References

- [1]. Matlab® 7, “Wavelet Packet Toolbox” , 2007.
- [2]. Olivier R. et,al. “Wavelet and signal processing” , IEEE signal processing magazine, 1991.
- [3]. [http:// www.dsprelated.com](http://www.dsprelated.com)

APPENDIX

B**IMPLEMENTATION OF FFT USING
DISCRETE WAVELET PACKET
TRANSFORM (DWPT) AND IT'S
APPLICATION TO SNR ESTIMATION
IN OFDM SYSTEMS****B.1 Introduction**

In this chapter, wavelet packet based FFT and its application to SNR estimation is reported. OFDM systems demodulate data using FFT. The proposed solution computes the exact result, and its computational complexity is same order of FFT, i.e. $O(N \log_2 N)$. SNR estimation is done inside wavelet packet based FFT block unlike previous SNR estimations techniques which perform SNR estimation after FFT. Wavelet packet analyzed data is used to perform SNR estimation. The proposed estimator takes into consideration the different noise power levels over the OFDM sub-carriers. The OFDM band is divided into several sub-bands using wavelet packet and noise in each sub-band is considered white. The second-order statistics of the transmitted OFDM preamble are calculated in each sub-band and the power noise is estimated. The proposed estimator is compared with Reddy's estimator for colored noise in terms of mean squared error (MSE).

Signal-to-noise ratio (SNR) is defined as the ratio of the desired signal power to the noise power. Noise variance and hence SNR estimates of the received signal are very important parameters for the channel quality control in communication systems. The search for a good SNR estimation technique is motivated by the fact that various algorithms require knowledge of the SNR for optimal performance [1, 2, 3, 4, 5]. For instance, in OFDM

systems, SNR estimation is used for power control, adaptive coding and modulation, turbo decoding etc.

SNR estimation indicates the reliability of the link between the transmitter and receiver. In adaptive system, SNR estimation is commonly used for measuring the quality of the channel and accordingly changing the system parameters [6]. For example, if the measured channel quality is low, the transmitter may add some redundancy or complexity to the information bits (more powerful coding), or reduce the modulation level (better Euclidean distance), or increase the spreading rate (longer spreading code) for lower data rate transmission. Therefore, instead of implementing fixed information rate for all levels of channel quality, variable rates of information transfer can be used to maximize system resource utilization with high quality of user experience.

Many SNR estimation algorithms have been suggested in the last ten years as discussed in chapter two of this thesis and successfully implemented in OFDM systems using the system pilot symbols. The essential requirement for an SNR estimator in OFDM system is of low computational load. This is in order to minimize hardware complexity as well as the computational time.

In many SNR estimation techniques, noise is assumed to be uncorrelated or white. But, in wireless communication systems, where noise is mainly caused by a strong interferer, noise is colored in nature.

OFDM demodulation uses discrete Fourier transform (DFT). An FFT (fast Fourier transform) is used to demodulate data. In this appendix, wavelet packet based FFT and its application to SNR estimation is presented. The proposed solution computes the exact result, and its computational complexity is same order of FFT, i.e. $O(N \log_2 N)$.

The proposed SNR technique performs SNR estimation inside FFT unlike previous SNR estimators. SNR estimator for the colored noise in OFDM system is proposed. The algorithm is based on the two identical halves property of time synchronization preamble used in some OFDM systems. The OFDM band is divided into several sub-bands using

wavelet packet and noise in each sub-band is considered white. The second-order statistics of the transmitted OFDM preamble are calculated in each sub-band and the power noise is estimated. Therefore, the proposed approach estimates both local (within smaller sets of subcarriers) and global (over all sub-carriers) SNR values. The short term local estimates calculate the noise power variation across OFDM sub-carriers. When the noise is white, the proposed algorithm works as good as the conventional noise power estimation schemes, showing the generality of the proposed method.

The remainder of the appendix is organized as follows. In Section B.2, the proposed FFT technique is presented. Section B.3 provides the proposed SNR estimation. Section B.4 presents simulation results and discussion. Section B.5 concludes the appendix.

B.2. Proposed Wavelet Packet Based FFT (DWPT-FFT)

The fundamental principle that the FFT is based upon is that of decomposing the computation of the discrete Fourier transform of a sequence of length N into successively smaller discrete Fourier transforms of the even and odd parts. In the proposed method the even – odd separation is replaced by wavelet packet decomposition.

The block diagram of proposed DWPT-FFT is shown in Fig.1. The idea borrowed from Guo [7]. Wavelet packet based FFT first performs Wavelet Packet decomposition, followed by reduced size FFT and butterfly operation as shown in Fig.B.1. This can be extended so that WP analysis is 3 to 4 level analysis and FFT is $N/4$, $N/8$ or $N/16$ size FFT. Butterfly is appropriately designed.

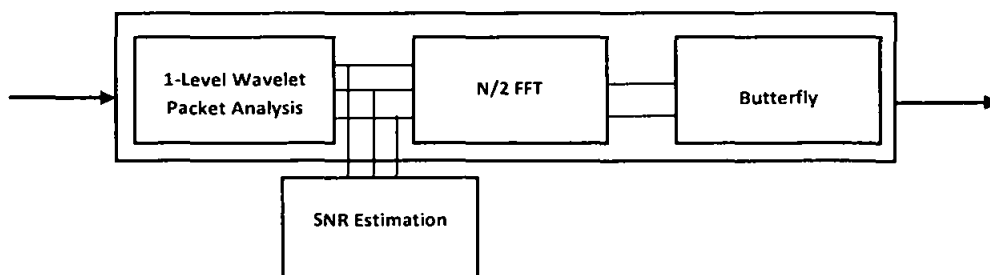
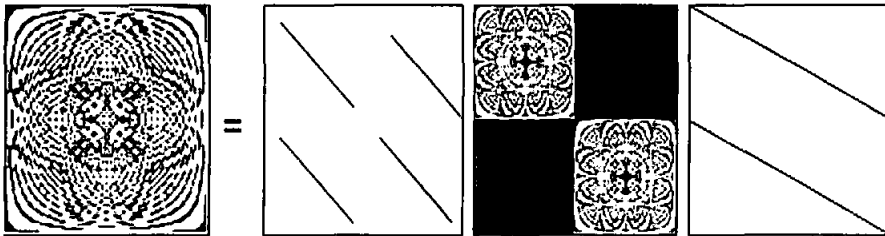


Fig.B.1 Block Diagram of DWPT-FFT

The wavelet packet based FFT (DWPT-FFT) shown in Fig B.1 is represented by eq. B.1.

$$F_N = \begin{bmatrix} A_{N/2} & B_{N/2} \\ C_{N/2} & D_{N/2} \end{bmatrix} \begin{bmatrix} F_{N/2} & 0 \\ 0 & F_{N/2} \end{bmatrix} [WP_N] \tag{B.1}$$

where $A_{N/2}, B_{N/2}, C_{N/2}$ and $D_{N/2}$ are all diagonal matrices. In eq. B.1, the values on the diagonal of $A_{N/2}$ and $C_{N/2}$ are the length-N DFT of 'h, ' and the values on the diagonal of $B_{N/2}$ and $D_{N/2}$ are the length-N DFT of 'g. The factorization can be visualized as



where we image the real part of DFT matrices, and the magnitude of the matrices for butterfly operations and the one-scale DWPT using Db3 wavelets. Clearly we can see that the twiddle factors have non-unit magnitude.

The above factorization suggests a DWPT-FFT algorithm. The block Diagram of length 8 algorithm is shown in Fig.B.2. Following this, the high pass and the low pass DWPT outputs go through separate length-4 DFT, then they are combined with butterfly operations.

Same procedure in Fig.B.2 is iteratively applied to short length DFTs to get the full DWPT based FFT algorithm where the twiddle factors are the frequency wavelet filters. The detail of butterfly operations is shown in Fig.B.3 where 'i' belongs to $\{0,1,\dots,N/2-1\}$.

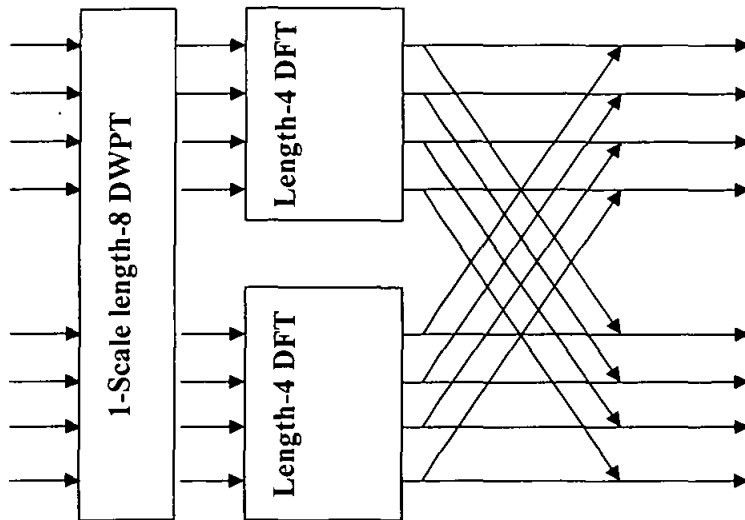


Fig.B.2. Last stage of length 8 DWPT-FFT

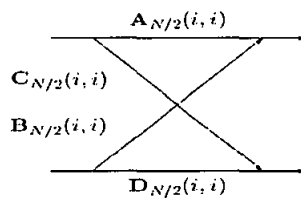
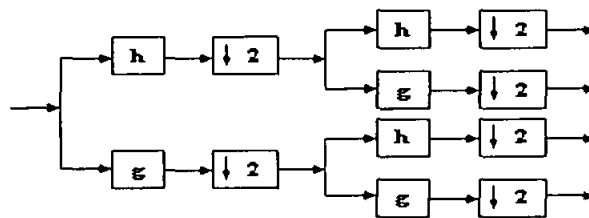


Fig.B.3. Butterfly operation in DWPT-FFT

Wavelet packet allows a finer and adjustable resolution of frequencies at high frequency. Input data are first filtered by pair of filters h and g (low pass and high pass respectively) and then down sampled. The same analysis is further iterated on both low and high frequency bands as shown in Fig.B.4.



FigB.4. Two-scale discrete wavelet packet transforms

For the DWPT based FFT algorithm, the computational complexity is also $O(N \log, N)$. However, the constant appears before $N \log_2 N$ depends on the wavelet filters used.

B.3. SNR Estimation inside FFT Block

As discussed in chapter 3, the preamble used for timing synchronization is derived from alternate loading of subcarriers with PN-sequence modulated constellation as follows:

$$P_{even}(k) = \begin{cases} \sqrt{2} \cdot P(m) & k = 2m & m = 1, 2, 3, \dots, N/2 \\ 0 & otherwise \end{cases} \tag{B.2}$$

Here, $P(m)$ is the PN sequence loaded onto even subcarriers taken from IEEE802.16d. The factor $\sqrt{2}$ is related to the 3 dB boost and k shows the sub-carriers index.

In actual practice, an OFDM signal is provided with a guard band on either side of its spectrum. Accordingly the data are not loaded on the sides. For example, for a typical IEEE802.16d signal of length 256 subcarriers wide, 28 carriers on either side are null carriers as shown in Fig.B.5.

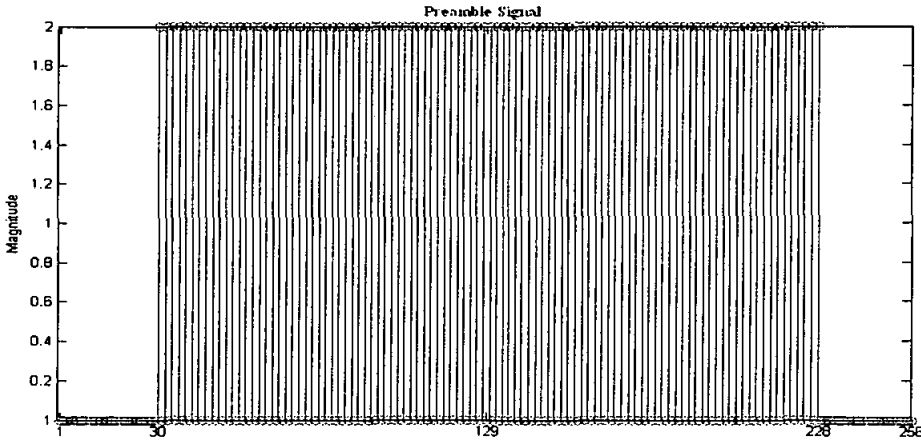


Fig.B.5 Preamble signal loaded on even subcarriers using PN sequence

Therefore for our purposes, eq.B.2 is rewritten as

$$P_{even}(k) = \begin{cases} \sqrt{2} \cdot P(m) & k=2m & m=1,5,6,7,\dots,(N/2-1) \\ 0 & & m=1,2,3,\dots,14 \\ 0 & & m=N/2-1,3,N/2-2,\dots,N/2 \end{cases} \quad (B.3)$$

The corresponding time-domain preamble $P(n)$, is obtained by Inverse discrete Fourier transform (IDFT) of $P_{even}(k)$ as follows.

$$\begin{aligned} p(n) &= IDFT\{P_{even}(k)\} \\ &= \sum_{k=0}^{N-1} P_{even}(k) \cdot e^{j2\pi nk/N} \quad 0 \leq n \leq N-1 \end{aligned} \quad (B.4)$$

Since $P_{even}(k)$ has values only at even subcarriers, this can be seen from the properties of $e^{j2\pi nm/N}$ (also written as $W_{N/2}^{-nm}$, where W_N is the N -th root of unity).

For $k = 2m$,

$$e^{j2\pi n2m/N} = e^{j2\pi nm/N} \quad (B.5)$$

So, for $n = n + N/2$,

$$\begin{aligned} e^{j2\pi(n+N/2)m/N} &= e^{j2\pi nm/N} \cdot e^{j2\pi m \cdot N/2/N} \\ &= e^{j2\pi nm/N} \end{aligned} \quad (B.6)$$

In other words

$$p(n) = p(n + N/2) \quad (B.7)$$

To avoid intersymbol interference (ISI) caused by multipath fading channels, cyclic prefix (CP) of length l_{CP} is added so that the total length of OFDM data becomes $N_{total} = N + l_{CP}$. It is assumed that the signal is transmitted over Rayleigh multipath fading channel characterized by

$$h(t, \tau) = \sum_{l=1}^L h_l(t) \delta(t - \tau_l) \quad (B.8)$$

where $h_l(t)$ are the different path complex gains, τ_l are different path time delays, and L is the number of paths. $h_l(t)$ are wide-sense stationary (WSS) narrow-band complex Gaussian processes. At the receiver side, with the assumption that the guard interval duration is longer than the channel maximum excess delay, the received OFDM data can be represented by

$$y(n) = x(n) + n(n) \quad (B.9)$$

where

$$x(n) = s(n) * h(n)$$

* = Linear convolution

$s(n) = IDFT \{S(K)\}$, $S(K)$ are the constellation symbols, and $S(n)$ is the transmitted signal in time-domain.

$n(n) =$ white Gaussian noise with variance σ^2 .

$h(n) =$ discretized version of impulse response of the system.

B.3.1 Autocorrelation based SNR Estimator

Wavelet Packet analyzed data becomes available for SNR estimation inside FFT block as shown in Fig.1. After removing cyclic prefix at receiver, OFDM data is divided into 2^n

sub-bands using periodic wavelet packets where ‘ n ’ shows the number of levels. The length of each sub-band is $N_{sub}=N/2^n$. It inherits the two identical halves property of synchronization preamble. The noise in each sub-band is considered white. The system’s parameters and the structure of wavelet packet used for the simulations are shown in table B.1. It makes use of two identical halves property of time synchronization preamble and relies on the autocorrelation of the same. From eq. B.10, it can be shown that the autocorrelation function of the received signal, $R_{yy}(m)$, has the following relationship to the autocorrelation of the data signal, $R_{xx}(m)$ and the noise, $R_{nn}(m)$:

$$R_{yy}(m) = R_{xx}(m) + R_{nn}(m) \quad (B.10)$$

where

$$R_{yy}(m) = \sum_n y(n) y^*(n+m)$$

$$R_{xx}(m) = \sum_n x(n) x^*(n+m)$$

$$R_{nn}(m) = \sum_n n(n) n^*(n+m)$$

The noise in the channel is modeled as additive white Gaussian noise and its autocorrelation function only has a value at a delay of $m = 0$, with magnitude given by the noise variance (σ^2), expressed as

$$R_{nn}(m) = \sigma^2 \delta(m) \quad (B.11)$$

where $\delta(m)$ is the discrete delta sequence.

B.3.2 Signal Power and Noise Power Estimation

We undertake the study of OFDM signal statistics, and observe, as shown in Fig. B.6, that its power spectrum is nearly white. Hence its autocorrelation is generally given by:

$$R_{ss}(m) = P_o \delta(m) \quad (\text{B.12})$$

where P_o is signal power.

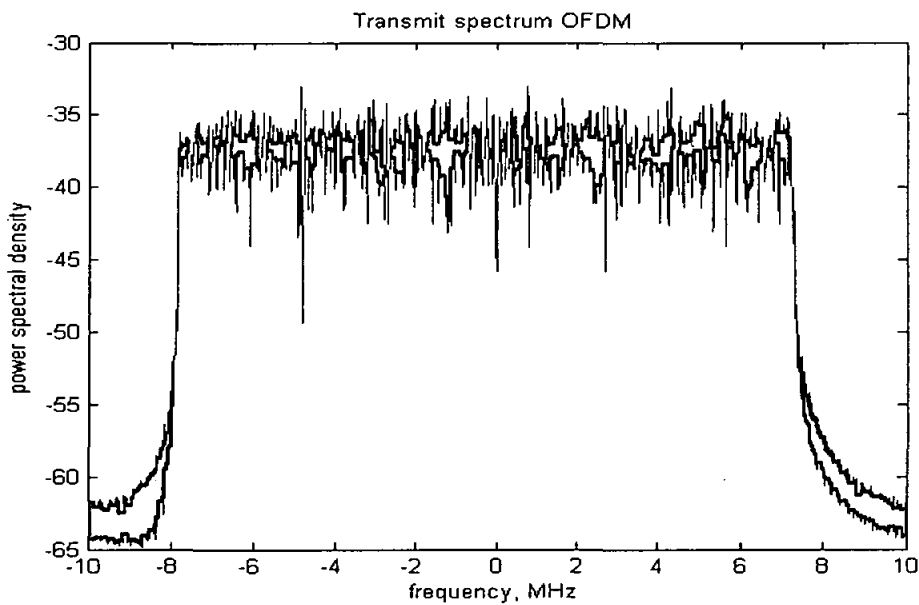


Fig.B.6 Power spectrum of an OFDM signal

Hence, at zero lag (shown at ' L ' in Fig.B.8) the autocorrelation $R_{xx}(0)$ contains both the signal power estimate and noise power estimate indistinguishable from each other as shown in eq. B.10 and eq. B.11 before. However, because of the identical halves nature of the preamble, the received signal power can be estimated from auto correlation peak at $N/2$ or at $-N/2$ as shown in Fig.B.7a. In Fig.B.7, $R_{xx}(m)$ has been sketched for $N=256$.

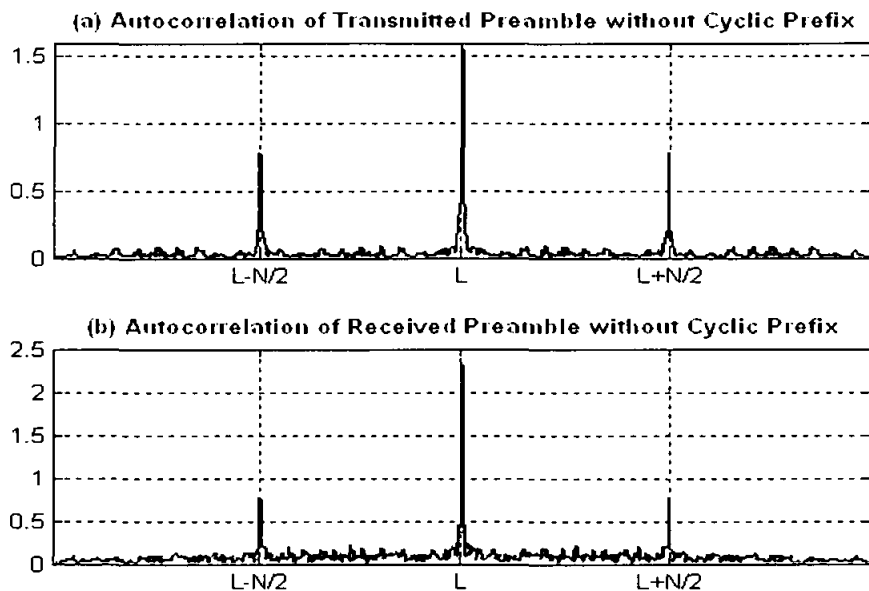


Fig.B.7 (a): Transmitted Preamble (b): Received Preamble after coming through a channel (Plots show two identical halves with no cyclic prefix).

It is clear that the autocorrelation values apart from the zero-offset are unaffected by the channel effects, so one can find the signal power from the $N/2$ or $-N/2$ lag autocorrelation value.

B.3.2.1 Signal Power Estimation in each Sub-band

Sub-bands inherit the two identical halves property of synchronization preamble as shown in Fig B.8. After removing CP, WP data is available inside FFT for SNR estimation; the length of data is changed. So after correlation of each sub-band, first peak rises at at $L_{sub}-N_{sub}/2$ when one half of sub-band matches with itself with energy of $\rho \cdot (N_{sub}/2)$ and main peak at zero-lag (L_{sub}) rises when full sub-band matches with itself with energy of $\rho \cdot (N_{sub})$

Taking into consideration the autocorrelation values for $L_{sub}-N_{sub}/2$ lag or $L_{sub}+N_{sub}/2$ as shown in Fig.B.8 , signal power is given as

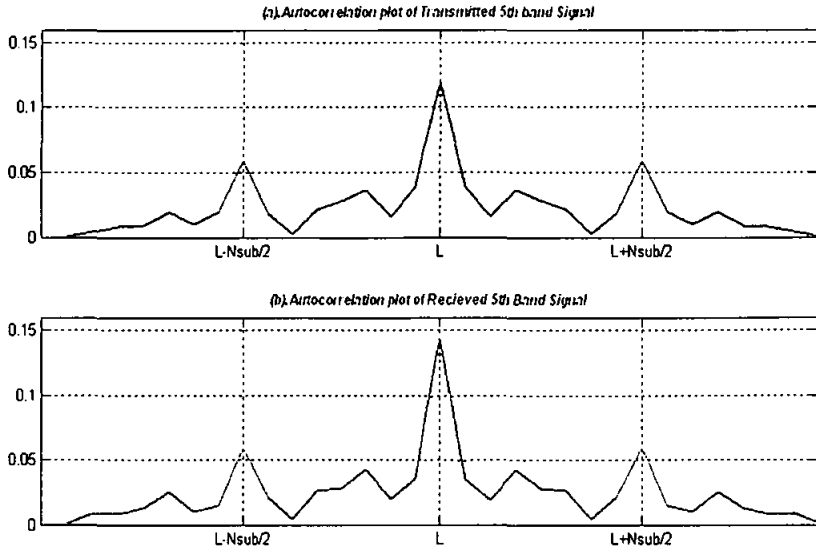


Fig.B.8. Autocorrelation plot of Transmitted (a) and Received (b) 5th band signal

$$\hat{P}_{ss} = 2R_{yy}((L - N_{sub} / 2)) \quad (B.21)$$

Or

$$\hat{P}_{ss} = 2R_{yy}((L + N_{sub} / 2)) \quad (B.22)$$

B.3.2.2 Noise Power Estimation in each Sub-band

Having obtained the power of signal in certain sub-band, noise power can be calculated using eq.B.23.

$$\hat{\sigma}^2 = R_{yy}(L_{sub}) - \hat{P}_{ss} \quad (B.23)$$

Where $\hat{\sigma}^2$ is the estimated value of noise power in each sub-band.

B.3.2.3 SNR Estimation in Each Sub-band

Finally we can find the SNR estimates in the sub-band by using equation (B.21 or B.22) and equation (B.23).

$$\hat{SNR} = \frac{\hat{P}_{SS}}{\hat{\sigma}^2} \tag{B.24}$$

Where \hat{SNR} is the estimated value for SNR in each sub-band.

B.4. Results and Discussions

For the DWPT based FFT algorithm, the computational complexity is also $O(N \log, N)$. However, the constant appears before $N \log_2 N$ depends on the wavelet filters used. The proposed DWPT-FFT computes the exact result, for example, for $x(n) = e^{j\pi n^2} / N$, chirp signal $X(k) = \sum_n x(n)e^{-j2\pi nk} / N$ as shown in Fig.B.9.

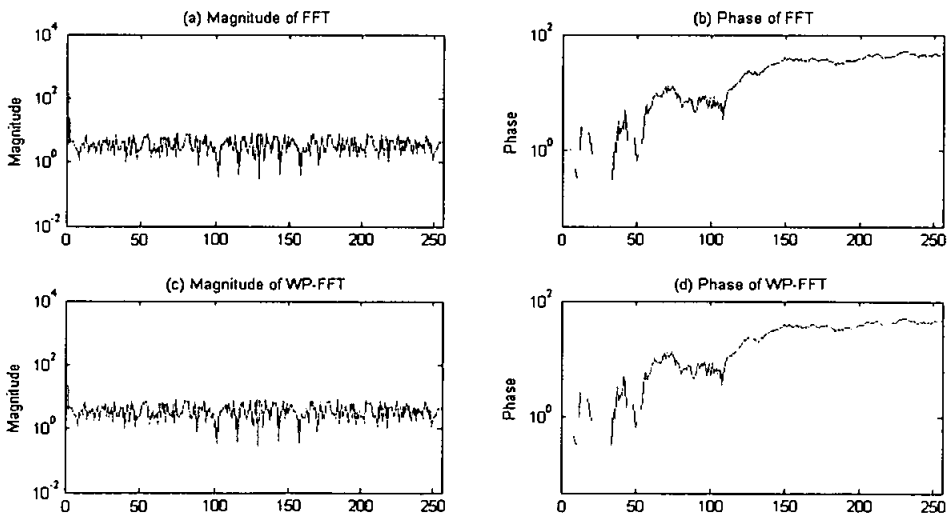


Fig.B.9. FFT result with and without wavelet packet

The proposed SNR estimator is compared with Reddy’s estimator for colored noise in OFDM systems with parameters given in Table B.1. SNR is varied from 1 dB to 14 dB for each sub-band and to measure statistically accurate SNR, the mean-squared error (MSE) is obtained over 2000 samples according to the following formula

$$MSE = \frac{1}{2000} \sum_{i=1}^{2000} (\hat{SNR}(i) - SNR)^2 \tag{B.25}$$

B.4.1 Performance Comparison

From Fig.B.10 and Fig.B.11 it is clear that the proposed estimator gives better performance in SNR estimation as compared to Reddy estimator. It is observed that the proposed technique can estimate local statistics of the noise power when the noise is colored. The proposed estimator has relatively low computational complexity because it makes use of only one OFDM preamble signal to find the SNR estimates. The proposed estimator is fulfills the criteria of best SNR estimator because it is unbiased (or exhibits the smallest Bias) and has the smallest variance of SNR estimates as shown from results clearly.

Table B.1: Parameters for the simulation [9]

<i>Ifft size</i>	256
<i>Sampling Frequency = F_s</i>	20MHz.
<i>Sub Carrier Spacing= Δf = F_s/Ifft</i>	1×10 ⁵
<i>Useful Symbol Time = T_b = 1/Δf</i>	1×10 ⁻⁵
<i>CP Time = T_g = G * T_b where G=1/4</i>	2.5×10 ⁻⁶
<i>OFDM Symbol Time = T_s=T_b+T_g</i>	1.25×10 ⁻⁵
<i>T_s = 5/4 * T_s (Because 1/4 CP makes the sampling faster by 5/4 times)</i>	1.56×10 ⁻⁵
<i>T_{sub} = T_s/16</i>	9.8×10 ⁻⁷

```

Wavelet Packet Object Structure
Wavelet Decomposition Command : wpdec
Size of initial data : [1 320]
Order= 2
Depth=: 4
Terminal nodes : [15 16 17 18 19 20 21 22 23 24 25 26
27 28 29 30]
Wavelet Name : Daubechies (db3) ,
Entropy Name : Shannon
    
```

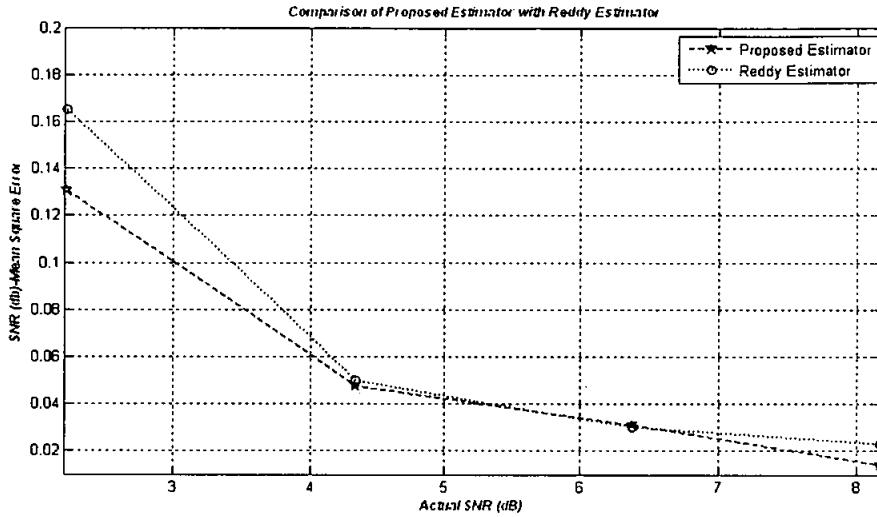


Fig.B.10. MSE performance of the proposed technique

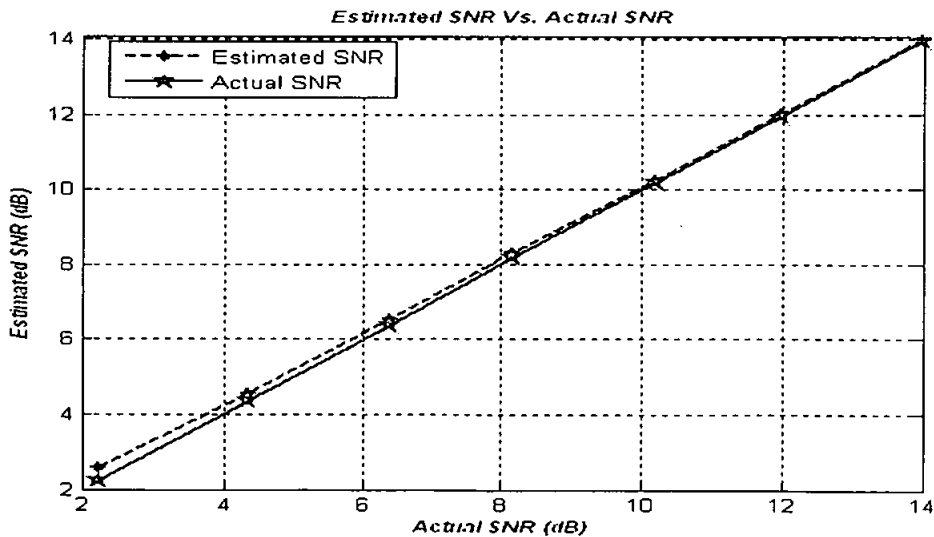


Fig.B.11. Actual SNR vs. Estimated SNR of colored noise

B.5. Summary

In this appendix, discrete wavelet packet based FFT and its application to SNR estimation inside FFT is presented. Also, variation of the noise power across OFDM sub-carriers is allowed. The second-order statistics of the transmitted OFDM preamble are calculated in each sub-band and the power noise is estimated. Therefore, the proposed approach estimates both local (within smaller sets of subcarriers) and global (over all sub-carriers) SNR values. The short term local estimates calculate the noise power variation across OFDM sub - carriers. These estimates are specifically very useful for diversity combining, adaptive modulation, and optimal soft value calculation for improving channel decoder performance. Its performance has been evaluated via computer simulations using AWGN and multipath fading channels and implemented in OFDM systems. The results show that the current estimator performs better than other conventional methods. Complexity to find SNR estimates is much lower because the current estimator makes use of only one OFDM preamble signal. The current estimator fulfills the criteria of best SNR estimator as it is unbiased and has the smallest variance of SNR estimates.

REFERENCES

- [1] Xiaodong X., Ya Jing. and Xiaohu Y.,2005 “*Subspace- Based Noise Variance and SNR Estimation for OFDM Systems*”, IEEE Wireless Communications and Networking Conference.
- [2] Reddy, S. and Arslan H., 2003 “*Noise Power and SNR Estimation for OFDM Based Wireless Communication Systems*”, Wireless Communication and Signal Processing Group.
- [3] Kamel N.S. and Joeti V., 2006 “*Linear prediction based approach to SNR estimation in AWGN channel*”, 23rd Biennial Symposium on Communications.
- [4] Pauluzzi D.R. and Norman C.B., 2000 “*A Comparison of SNR Estimation techniques for the AWGN Channel*”, IEEE Transactions on Communications, Vol. 48.

- [5] Bournard, S., 2003 "*Novel Noise Variance and SNR Estimation Algorithm for Wireless MIMO OFDM Systems*", IEEE GLOBECOM.
- [6] Oppenheim, A. V.; Schafer, R. W.: "Discrete-Time Signal Processing", Prentice-Hall, 1989.
- [7] Guo, H.; Burrus, C. S.: "Wavelet Transform Based Fast Approximate Fourier Transform", Proc. of ICAASP-1997, Munich, Germany
- [8] Prasad, R., 2004, *OFDM for Wireless Communications Systems*, Boston, Artech House Inc.
- [9] IEEE 802.16-2004., 2004 "*IEEE Standard for Local and Metropolitan Area Networks Part 16: Air Interface for Fixed Broadband Wireless Access Systems*".
- [10] H. Van Trees., 1968 "*Detection, Estimation, and Modulation Theory*", vol.1, New York, Wiley.
- [11] H. Hayes, 1996, *Statistical Digital Signal Processing and Modeling*, John Wiley,.